

**University of São Paulo  
“Luiz de Queiroz” College of Agriculture**

**First investigation of genetic control of meiosis in sugarcane**

**Nina Reis Soares**

Thesis presented to obtain the degree of Doctor in  
Science. Area: Genetics and Plant Breeding

**Piracicaba  
2023**

**Nina Reis Soares**  
**Bachelor's Degree in Biological Sciences**

**First investigation of genetic control of meiosis in sugarcane**

Advisor:  
Profa. Dra. **MARIA LUCIA CARNEIRO VIEIRA**

Thesis presented to obtain the degree of Doctor in  
Science. Area: Genetics and Plant Breeding

**Piracicaba**  
**2023**

**Dados Internacionais de Catalogação na Publicação**  
**DIVISÃO DE BIBLIOTECA – DIBD/ESALQ/USP**

Soares, Nina Reis

First investigation of genetic control of meiosis in sugarcane / Nina Reis Soares. - -  
Piracicaba, 2023.

120 p.

Tese (Doutorado) - - USP / Escola Superior de Agricultura “Luiz de Queiroz”.

1. *Saccharum* 2. Meiose 3. ZIP4 4. Sinapse I. Título

**DEDICATORY**

*Aos meus pais, Adriana e Cassio.*

## ACKNOWLEDGEMENTS

À Escola Superior de Agricultura "Luiz de Queiroz" (ESALQ/USP), e ao Programa de Pós-Graduação em Genética e Melhoramento de Plantas.

Gostaria de agradecer o apoio financeiro da Fundação de Amparo à Pesquisa do Estado de São Paulo ao projeto (FAPESP, Projeto número. 2020/07741-0); do Conselho Nacional de Desenvolvimento Científico e Tecnológico pela bolsa de estudo (CNPq, bolsa nº 140163/2020-4) e da Coordenação de Aperfeiçoamento de Pessoal de Nível Superior – CAPES pela bolsa de estudos (88887.695456/2022-00).

Em especial, à Professora Maria Lucia Carneiro Vieira, pelas oportunidades oferecidas e pela confiança em mim depositada. Agradeço imensamente sua orientação, supervisão e apoio científico neste trabalho.

À Dra. Mathilde Grelon e a toda equipe do IJPB (Institut Jean-Pierre Bourgin) do INRA, Versailles (France), por toda a colaboração e auxílio no desenvolvimento deste trabalho.

À Dra. Angélique D'Hont e a toda equipe do AGAP (Amélioration Génétique et Adaptation des Plantes Méditerranéennes et Tropicales) do CIRAD, Montpellier pela sua contribuição e por todos os conhecimentos partilhados durante o desenvolvimento deste trabalho.

À Professora Claudia Barros Monteiro Vitorello e ao seu grupo de pesquisa pela colaboração nos experimentos.

A todos os docentes do Programa de Pós-Graduação em Genética e Melhoramento de Plantas da ESALQ, pela atenção, dedicação e disposição em compartilharem seus conhecimentos.

Ao Carlos Alberto de Oliveira, pela amizade e pelo suporte técnico durante a realização deste trabalho.

Aos colaboradores Monalisa Sampaio Carneiro, UFSCar, Silvana A. Creste dias de Souza, IAC/ Centro de Cana e ao Mauro Alexandre Xavier, IAC/ Centro de Cana.

Aos amigos do laboratório de Genética Molecular de Plantas Cultivadas da ESALQ pelo ensinamento e paciência.

Por fim, a todos aqueles que de alguma forma contribuíram para a minha formação e com o desenvolvimento deste trabalho deixo os meus sinceros agradecimentos.

**EPIGRAPH**

*“O espírito sem limites é o maior tesouro do homem.”*

(J.K. Rowling)

## SUMMARY

<b>RESUMO</b> .....	<b>8</b>
<b>ABSTRACT</b> .....	<b>9</b>
<b>FIGURE LIST</b> .....	<b>10</b>
<b>TABLE LIST</b> .....	<b>12</b>
<b>1. INTRODUCTION</b> .....	<b>13</b>
<b>2. MEIOSIS IN POLYPLOIDS AND IMPLICATIONS FOR GENETIC MAPPING: A REVIEW</b> .....	<b>22</b>
<b>ABSTRACT</b> .....	<b>22</b>
2.1. OVERVIEW .....	22
2.2. REVISITING EARLY MEIOSIS .....	23
2.3. MEIOSIS IN AUTOPOLYPLOIDS .....	24
2.4. FREQUENCY OF CROSSOVERS .....	26
2.5. MULTIVALENTS AND CYTOLOGICAL DIPLOIDIZATION .....	26
2.6. GENETIC CONTROL OF MEIOSIS IN AUTOPOLYPLOIDS .....	27
2.7. MEIOSIS IN ALLOPOLYPLOIDS .....	29
2.8. CHROMOSOME PAIRING, RECOMBINATION, AND SEGREGATION IN ALLOPOLYPLOIDS .....	29
2.9. HOMOELOGOUS EXCHANGES .....	31
2.10. NEOALLOPOLYPLOIDS .....	32
2.11. GENETIC REGULATORY SYSTEMS IN ALLOPOLYPLOIDS .....	33
2.12. WHEAT .....	33
2.12.1. <i>The Ph1 locus</i> .....	34
2.12.2. <i>The ZIP4 gene</i> .....	35
2.12.3. <i>Ph2</i> .....	37
2.13. BRASSICA AND THE PREVALENCE OF BIVALENT PAIRING .....	39
2.13.1. <i>PrBn molecular characterization and function</i> .....	40
2.13.2. <i>BnaPh1</i> .....	41
2.14. MEIOTIC PROTEINS AND CROSSOVER FORMATION .....	43
2.15. THE CONSEQUENCES OF MEIOSIS FOR GENETIC MAPPING IN AUTO- AND ALLOPOLYPLOIDS .....	44
2.16. CASE STUDIES .....	47
<b>REFERENCES</b> .....	<b>49</b>
<b>3. IN SITU EVIDENCE OF GENOMIC RELATIONSHIPS AMONG THE FOUNDING ANCESTRAL GENOMES OF SACCHARUM SPP.</b> .....	<b>70</b>
<b>ABSTRACT</b> .....	<b>70</b>
3.1. INTRODUCTION .....	70
3.2. MATERIAL AND METHODS .....	71
3.2.1. <i>Microsporogenesis and chromosome association analysis in S. robustum</i> .....	71
3.2.2. <i>Mitotic chromosome preparation and genomic in situ hybridization (GISH)</i> .....	72
3.3. RESULTS AND DISCUSSION .....	72
3.3.1. <i>Microsporogenesis and chromosome association in Saccharum robustum</i> .....	72
3.3.2. <i>Genomic relationships among the founding ancestral genomes using GISH</i> .....	73
<b>REFERENCES</b> .....	<b>75</b>
<b>4. FIRST INVESTIGATION OF GENETIC CONTROL OF MEIOSIS IN SUGARCANE</b> .....	<b>77</b>
<b>ABSTRACT</b> .....	<b>77</b>
4.1. INTRODUCTION .....	77
4.2. EXPERIMENTAL PROCEDURES .....	79
4.2.1. <i>Plant material</i> .....	79
4.2.2. <i>ZIP4 candidates</i> .....	80
4.2.3. <i>ZIP4 protein analyses</i> .....	80
4.2.4. <i>RNA isolation and Real Time quantitative PCR (RT-qPCR)</i> .....	80
4.2.5. <i>Antibodies</i> .....	81
4.2.6. <i>Immunocytology</i> .....	81

4.3. RESULTS .....	82
4.3.1. <i>ZIP4</i> gene characterization in <i>Saccharum</i> .....	82
4.3.2. Comparison between <i>Saccharum ZIP4</i> and <i>TaZIP4</i> from wheat.....	84
4.3.3. 3D protein structure prediction .....	85
4.3.4. <i>ZIP4</i> gene expression.....	85
4.3.5. Immunolocalization of the SC proteins, <i>ZYP1</i> and <i>ASY1</i> .....	86
4.4. DISCUSSION .....	87
4.4.1. The sugarcane <i>ZIP4</i> gene and protein prediction.....	88
4.4.2. Expression profile of the <i>ZIP4</i> gene.....	89
4.4.3. Immunolocalization of SC proteins.....	89
<b>REFERENCES .....</b>	<b>91</b>
<b>APPENDIX .....</b>	<b>99</b>



## RESUMO

### Primeira investigação do controle genético da meiose em cana-de-açúcar

A cana-de-açúcar (*Saccharum spp.*) é a espécie cultivada com um dos genomas mais complexos. As variedades modernas são altamente poliplóides e aneuploides, resultantes da hibridização interespecífica entre *Saccharum officinarum* e *S. spontaneum*. A pesquisa sobre o controle meiótico em espécies poliplóides é limitada, com exceção do locus *Ph1* do trigo, que carrega o gene meiótico *ZIP4* (*TaZIP4-B2*) que promove o pareamento e a sinapse entre homólogos, enquanto suprime o CO entre os cromossomos homoeólogos. Na cana-de-açúcar, apesar de sua origem interespecífica, a associação bivalente é favorecida, e os multivalentes, caso ocorram, são resolvidas ao final da meiose I. Nosso objetivo aqui foi investigar o suposto controle da sinapse na cana-de-açúcar. Investigamos o gene *ZIP4* e realizamos a imunolocalização de proteínas meióticas, especificamente as proteínas do complexo sinaptonêmico ZYP1 e ASY1. O gene *ZIP4* da cana-de-açúcar está localizado no cromossomo 3 e é expresso mais abundantemente nas flores, apresentando perfil semelhante ao do *TaZIP4-B2*. O nível de expressão de *ZIP4* é maior em *S. spontaneum*, um autopoliplóide em evolução, e menos expresso em *S. officinarum*, uma espécie octaplóide legítima. A proteína *ZIP4* contém um domínio TPR, essencial para a sua função de scaffold, e a predição da estrutura 3D é altamente semelhante à do *TaZIP4-B2*. A imunolocalização das proteínas ASY1 e ZYP1 revelou que *S. officinarum* completa a sinapse. Porém, em *S. spontaneum* e SP80-3280, uma variedade moderna, não foram observados núcleos com sinapse completa. Nossos resultados terão implicações para o mapeamento genético e a genômica da cana-de-açúcar, cuja compreensão da herança e da organização do genoma permanece um tanto obscura.

Palavras-chave: *Saccharum*, Meiose, *ZIP4*, Sinapse

## ABSTRACT

### First investigation of genetic control of meiosis in sugarcane

Sugarcane (*Saccharum* spp.) has one of the most complex crop genomes. Modern varieties are highly polyploids and aneuploids, resulting from interspecific hybridization between *Saccharum officinarum* and *S. spontaneum*. Research on the meiotic control in polyploid species is limited, with the exception of wheat *Ph1* locus, carrying the meiotic gene *ZIP4* (Ta*ZIP4*-B2) that promotes pairing and synapsis between homologues, whilst suppressing CO between homoeologous chromosomes. In sugarcane, despite its interspecific origin, bivalent association is favored, and multivalents, if they occur, are resolved at the end of meiosis I. Our aim here was to investigate the supposedly control of synapsis in sugarcane. We have investigated the *ZIP4* gene and performed the immunolocalization of meiotic proteins, namely the synaptonemal complex proteins ZYP1 and ASY1. The sugarcane *ZIP4* gene is located on chromosome 3 and it is expressed more abundantly in flowers, showing a similar profile to that of Ta*ZIP4*-B2. The expression level of *ZIP4* is higher in *S. spontaneum*, an evolving autopolyploid, and less expressed in *S. officinarum*, a legitimate octaploid species. The *ZIP4* protein contains a TPR domain, essential to its scaffolding function, and the 3D structure prediction is highly similar to that of Ta*ZIP4*-B2. The immunolocalization of the ASY1 and ZYP1 proteins revealed that *S. officinarum* completes synapsis. However, in *S. spontaneum* and SP80-3280, a modern variety, no nuclei with complete synapsis were observed. Our results will have implications for sugarcane genetic mapping and genomics, whose understanding of inheritance and genome organization remain somewhat obscure.

Keywords: *Saccharum*, Meiosis, *ZIP4*, Synapsis

## FIGURE LIST

Figure 1. Pre-meiotic and early meiotic events in auto- and allotetraploid species illustrating regular meiotic behavior during Prophase I. Meiosis is preceded by one round of DNA replication during which sister chromatids are duplicated. During leptotene, genetic recombination is initiated, and double-strand breaks (DSBs) catalyzed by the protein Spo11 and repaired through homologous recombination. This process leads to DSB invasion into the non-sister chromatid by the RAD51 protein, initiating physical interactions and driving chromosome sorting. Homologous recognition may be facilitated by the clustering of telomeres at one pole of the cell forming the telomere bouquet. During zygotene, chromosomes begin synapsis via the formation of the synaptonemal complex (SC), which consists of axial and central elements. The SC is formed between pairs of homologous chromosomes, but it can also be formed between more than two homologs in autotetraploids and between homoeologous chromosomes in allotetraploids, resulting in synaptic partner switches (PPS) at pachytene. As recombination proceeds, in some species multiple/homoeologous associations are corrected by the MLH1 protein, a DNA mismatch repair that is required to resolve DHJ into COs. By contrast, in other species, specific localization of crossovers between pairs of homologous chromosomes resolves multiple/homoeologous associations at diplotene, when the SC is disassembled. Irrespective of when the corrections occur, only bivalents are visualized at diakinesis when chromosomes recondense in established polyploid lineages. Modified from Cifuentes et al. On the left, prophase I images depict a commercial variety of sugarcane. Photo credit: Oliveira, G.K., Universidade de São Paulo, Brazil..... 25

Figure 2. Thirty-six possible genotypes in an autotetraploid cross. A) Completely informative multiallelic scenario, in which all the genotypes formed by the combination of 6 gametes can be differentiated and segregated with equal probability. B) Biallelic scenario, in which both parents have two doses (duplex marker), in which case the genotypes collapse into five different classes segregating in a 1:8:18:8:1 ratio..... 46

Figure 3. Fluorescent *in situ* hybridization with centromeric probes on *Saccharum robustum* cells at diakinesis. (a) Chromosomes stained with DAPI (blue); (b) Centromeric sites hybridized with the CENT probe detected with anti-DIG-rhodamine (red); (c) Merged images (a/b) showing 50 bivalents. The scheme represents a bivalent with the 2 centromeres in red. The inset shows a typical bivalent. Genomic *in situ* hybridization of *Saccharum officinarum* and *Saccharum spontaneum* mitotic chromosome preparations using labeled genomic DNA of *S. robustum*. (d) Mitotic metaphase of *S. officinarum* counterstained with DAPI; (e) red fluorescence (TRITC) indicates full hybridization with *S. robustum* DNA; (f) Merged images (d/e). The scheme represents. The inset shows the chromosome fully hybridized. (g) Mitotic metaphase of *S. spontaneum* counterstained with DAPI; (h) red fluorescence (TRITC) indicates localized hybridization with *S. robustum* DNA; (i) Merged images (g/h). The inset shows typical hybridized telomeric/centromeric regions. Bar, 10  $\mu$ m ..... 74

Figure 4. Structure of the *ZIP4* gene in *Saccharum*. a) *ZIP4* genomic sequence structure consisting of 5 exons (thick lines) and 4 introns (narrow lines). b) Aligned CDS sequences of the *ZIP4* gene copies in *S. officinarum*, *S. spontaneum*, R570 and SP80-3280 modern varieties. Polymorphisms are shown as vertical yellow lines at the identity bar (green). ..... 83

Figure 5. ZIP4 protein alignment in *Saccharum*. a) ZIP4 multiple amino acid sequence alignment. Regions with identical amino acid sequences across the proteins are in black, and polymorphism sites are in white vertical lines. b) Predicted functional domains (SPORULATION-SPECIFIC PROTEIN 22/ZIP4, TPR-like and Meiosis protein SPO22/ZIP4 like). c) Predicted TPRs. d) Graphical representation of the conserved residues in the aligned TPR sequences: A is the only conserved amino acid. Predicted secondary structure of the TPRs copies (1–5). ‘Alpha Helix’ is represented by a pink cylindrical shape, ‘Beta Strand’ by the yellow arrow, ‘Coil’ is shown as a white wave and ‘Turn’ is represented by a blue arrow. .... 84

Figure 6. ZIP4 sequence alignment in *Saccharum* and wheat (Ta). a) Alignment of the *Saccharum* CDS nucleotide consensus sequence and the corresponding *TaZIP4* CDSs. b) Alignment of the *Saccharum* aminoacid consensus sequence and *TaZIP4* proteins. Identity bar with green, yellow, and red colors, representing high, medium and low identity among sequences. White spaces represent gaps created during the sequences alignments. .... 85

Figure 7. ZIP4 3D protein prediction and structure alignments. a) *Saccharum*. b) *TaZIP4* 3A. c) *TaZIP4* B2. Merged alignments: d) *Saccharum* ZIP4 and *TaZIP4* 3A. e) *Saccharum* ZIP4 and *TaZIP4* B2. *Saccharum* ZIP4 structure is in red and *TaZIP4* 3A and *TaZIP4* B2 are in blue. Protein prediction was done using AlphaFold2 and structure alignments with iCn3D... 85

Figure 8. Relative expression of the *ZIP4* gene in *S. officinarum*, *S. spontaneum* and SP80-3280 according to the Real Time-quantitative PCR results. The relative gene expression in flower, roots and leaves are shown as blue, gray, and green bars, respectively. Graphing data expressed as fold changes between the *ZIP4* expression level with respect to that of reference genes. Different letters above the bars indicate expression levels significantly different ( $p < 0.05$ ) by one-way analysis of variance and Tukey’s test. Black letters indicate comparisons across tissues from the same species, and red letters comparisons across species from the same tissue. Error bars correspond to the standard deviations of measurements performed in triplicate. .... 86

Figure 9. Immunolocalization of synaptonemal complex proteins. Immunolocalization of the ZYP1 and ASY1 proteins in *S. officinarum* (Caiana-Fita) (a), *S. spontaneum* (SES205) (b) and SP80-3280 (c), in late pachytene. Bar 5  $\mu$ m. .... 87

Figure 10. Percentage of ZYP1 and ASY1 in sugarcane cells. In red and green are the percentages of the ZYP1 and ASY1 proteins, respectively, in *S. officinarum*, *S. spontaneum* and SP80-3280. .... 87

**TABLE LIST**

Table 1. Number of possible gametes for one locus with no double-reduction, and number of possible genotypes generated by their combination given even ploidy levels. ....	45
--	----

## 1. INTRODUCTION

The sugarcane (*Saccharum* spp.) crop is of considerable industrial importance, accounting for nearly 80% of global sugar production (see <https://www.isosugar.org/sugarsector/sugar>). Sugarcane is generally regarded as the most sustainable source of biomass for producing biofuels, with high potential for mitigating the effects of climate change without affecting food security (Kline et al., 2017; Long et al., 2015). Crops and by-products can be developed for producing bioelectricity, bioplastics, and fertilizers, in addition to cellulosic ethanol.

Species originated in New Guinea, where sugar canes have been grown for millions of years. The earliest record of domestication dates to around 8,000 BCE, and cultivation gradually spread across human migration routes to Southeast Asia, India, and China. This long history of cultivation has facilitated the generation of a diversified germplasm which includes species of the *Saccharum* complex (two wild species, *S. spontaneum* ( $2n = 8x = 40-128$ ,  $x = 8$ ) and *S. robustum* ( $2n = 60, 80$  to  $200$ ), and four cultivated species, *S. officinarum* ( $2n = 8x = 80$ ,  $x = 10$ ), *S. sinense*, *S. barberi*, and *S. edule*) and four interbreeding genera (*Erianthus*, *Miscanthus*, *Narenga*, and *Sclerostachya* (Barreto et al., 2021; Cursi et al., 2021). Selection practices in former times resulted in *S. officinarum* clones with a higher sugar content and fewer fibers, known as ‘noble canes’ (Simmonds, 1975). Subsequently, in the late 19th century, new varieties emerged from interspecific hybridization of the formerly cultivated species (*S. barberi* and *S. officinarum*) and wild *S. spontaneum*, the latter one chosen due to its peculiar attributes, including hardiness, ratooning capability, and resistance to diseases (Barreto et al., 2021; Cheavegatti-Gianotto et al., 2011; Grivet et al., 2004). These hybrids were then successively crossed with *S. officinarum* to recover the sucrose content. The peculiarity in this process is that the hybrid progenies receive  $2n$  gametes from *S. officinarum* (when it was used as the female parent) and  $n$  gametes from *S. spontaneum* (Bremer, 1961; Price, 1961), which accounts for the overrepresentation of the *S. officinarum* genome in subsequent generations. As a result of all these processes, sugarcane has an ‘artificial’ genome of interspecific constitution (polyploid and aneuploid), produced by human intervention, and a complexity that exceeds that of most crops (Gouy et al., 2013). Despite its redundant origin (all modern varieties have primarily the same origin) and genome complexity, including a variable number of chromosomes ( $2n = 110$  to  $130$ ). According to pioneering molecular cytogenetic analysis, *S. officinarum* and *S. spontaneum* account respectively for 75 to 85% and 15 to 25% of sugarcane chromosomes. The remaining

chromosomes are recombinant from both origins (Cuadrado, 2004; D'Hont et al., 1996; G. Piperidis et al., 2010; N. Piperidis & D'Hont, 2020), due to pairing and recombination between homoeologous chromosomes.

From a meiotic point of view several classic analyses have suggested that both parental species and interspecific hybrids predominantly form bivalents (Bielig et al., 2003; Burner, 1991; Nair, 1975; Pagliarini et al., 1990; Price, 1963a, 1963b; Suzuki, 1941). Recently, our group performed a comparative analysis of the meiotic behavior in representatives of *S. officinarum* and *S. spontaneum* and the Brazilian variety SP80-3280 (Oliveira et al., 2023). The two latter exhibited several abnormalities, including delayed chromosomes, from metaphase I to the end of the division, while the *S. officinarum* clone showed regular behavior. Centromeric probes FISH (fluorescent in situ hybridization) at diakinesis allowed us to enumerate the centromeres, 40, 32 and 56 bivalents for *S. officinarum* and *S. spontaneum* and SP80-3280, respectively, although in some cells for *S. spontaneum* and SP80-3280, 1 or 2 univalents were also found. Furthermore, we also visualized the presence of dicentric chromosomes, and a pericentric inversion that was evidenced by a detailed pachytene analysis. In this study, we determined, for the first time, with the use of genomic in situ hybridization (GISH) the origin of univalents and lagging chromosomes during the first and second divisions (Oliveira et al., 2023). These are extremely important data, as they suggest that there is a coordinated segregation of chromosomes during meiosis, regardless of their origin, whether from *S. officinarum*, *S. spontaneum* or recombinant. In this scenario, the existence of mechanisms that regulate sugarcane meiosis is suggested and needs to be investigated.

The multivalent or bivalent formation, in natural polyploids, depends on the species evolutionary history and reproductive system, resulting in a meiotic progression different from diploid organisms (Zielinski & Mittelsten Scheid, 2012). The formation of non-reduced cells is the main mechanism that leads to the occurrence of polyploids (Pelé et al., 2018). Thus, one of the biggest challenges faced by a polyploid, is how to manage the correct recognition, synapsis, recombination, and segregation of its multiple related chromosomes during meiosis, to produce balanced gametes.

The particular case of cultivated wheat (*Triticum aestivum*,  $2n = 6 \times = 42$ , AABBDD) is noteworthy: wheat is a relatively recent allopolyploid (7,000 BC), whose ancestral genomes are syntenic and collinear, with highly complex coding sequences and large proportion of repetitive DNA (>85%) (International Wheat Genome Sequencing Consortium (IWGSC), 2018). Sears (1977) identified that hexaploid wheat lines lacking the chromosome 5B, were

used to generate haploids and wheat-wild relative hybrids, both of which exhibited crossover (CO) between homoeologous chromosomes at metaphase I (Riley & Chapman, 1958; Sears & Okamoto, 1958). The 5B deletion mutant (now known to be 59.3 Mb in size (Martín et al., 2018)) termed *ph1b*, has been used over the last 60 years for the introgression of desirable chromosome segments during breeding. However, this line also showed meiotic abnormalities and reduced fertility, leading Riley and others (Riley & Chapman, 1958) to propose that the suppression of homoeologous CO between wheat chromosomes observed in wheat haploids (where only homoeologous chromosomes are present), was important for stabilizing the wheat genome and preserving its fertility. Thus, the term ‘pairing homoeologous’ (*Ph1*) became the accepted term for the chromosome 5B associated ‘suppression of homoeologous CO’ phenotype observed in haploids and wheat-wild relative hybrids (Wall et al., 1971). In wild type wheat, telomeres cluster as a bouquet at one nuclear pole during early meiosis, and homologous chromosomes pair and synapse from these telomere regions. In wild type wheat-rye hybrids (where no homologues are present), homoeologous chromosomes can also synapse; however, synapsis only occurs after the telomere bouquet stage, when telomeres have dispersed (Martín et al., 2017). Synaptonemal complex studies also revealed that a ‘promotion of homologous synapsis’ phenotype was also associated with *Ph1* on chromosome 5B (Holm & Wang, 1988; Martín et al., 2017; Martinez-Perez et al., 2001). Homologous chromosome sites were pairing early at the telomere bouquet stage in wild type wheat, which led to the promotion of homologous synapsis, reducing the chances of homoeologous synapsis occurring after the telomere bouquet stage (Martín et al., 2017). Therefore, although *Ph1* was originally defined as a ‘suppressing homoeologous CO’ phenotype, a ‘promotion of pairing-synapsis’ phenotype was also associated with *ph1b*. Both the ‘homoeologous CO suppression’ and the ‘promotion of homologous pairing-synapsis’ phenotypes were defined to the same region of chromosome 5B, possessing a copy of the major meiotic gene *ZIP4* (Ta*ZIP4*-B2) that duplicated and diverged from chromosome 3B (Griffiths et al., 2006; M. D. Rey et al., 2017). Thus, hexaploid wheat carries four copies of *ZIP4*, one copy on each of the group 3 chromosomes and a fourth copy, the duplicated and diverged Ta*ZIP4*-B2 on chromosome 5B. *ZIP4* has previously been shown to be required for 85% of homologous COs in yeast, *Sordaria*, mammals, rice, and *Arabidopsis*, and for the initial pairing and synapsis in yeast and *Sordaria* (Chelysheva et al., 2007; Dubois et al., 2019; Shen et al., 2012; Tsubouchi et al., 2006). Thus, although in *Arabidopsis* and rice, *ZIP4* has only been shown to be required for homologous CO and not synapsis, in yeast, *ZIP4* is required for both CO and synapsis. The analysis of a CRISPR deletion mutant of Ta*ZIP4*-B2, revealed the presence of major



meiotic abnormalities including a similar level of CO between homoeologous chromosomes when crossed with the same wild relative (M.-D. Rey et al., 2018). This confirms that the duplicated and diverged TaZIP4-B2 copy is responsible for both the ‘suppression of homoeologous CO’ and the ‘promotion of homologous pairing-synapsis’ phenotypes defined on chromosome 5B. ZIP4 belongs to the ZMM (an acronym for Zip1–4, Msh4–5, Mer3, Spo16) group of proteins that bind to and stabilize meiotic recombination intermediates (Chelysheva et al., 2007; Lynn et al., 2007; Tsubouchi et al., 2006). It acts as a scaffold (via tetratricopeptide repeats - TPR) for the formation of multi-protein complexes and couples meiotic CO formation to the assembly of the synaptonemal complex (De Muyt et al., 2018; Pyatnitskaya et al., 2022).

During meiosis, homologous chromosomes are synapsed along their length by the loading of a proteinaceous structure, the synaptonemal complex (SC), between them (Zickler, 2006). This elaborate structure assembles onto the chromosomes to stabilize the pairing interactions between the homologues (synapsis), promote CO formation, regulate cessation of DNA double-strand break (DSB) and ensure accurate meiotic chromosome segregation (Lenormand et al., 2016). The SC has been observed in a wide range of sexually reproductive organisms, from yeast to human (Lenormand et al., 2016). In all cases, it adopts a remarkably conserved tripartite ribbon-like organization, consisting of lateral elements (LEs) that holds the sister chromatids of the homologues together, a central element (CE) along the midline and an array of transverse filaments (TFs) that interconnect the LEs generating a zipper-like structure (Gao & Colaiácovo, 2018). In higher plants, ASY1 temporally associates with the meiotic chromosome axis, forming the LE and possess distinct functions (S. J. Armstrong et al., 2002a; Cuacos et al., 2021). For instance, in *Arabidopsis* and *Brassica*, ASY1 proteins stabilize the axial core and ensure obligate CO, while in rice, the orthologous PAIR2 does not play a role in axial element formation, sister chromatid cohesion at centromeres or kinetochore assembly in meiosis I (Nonomura et al., 2006). ZYP1, on the other hand, form parallel homodimers, which subsequently overlap in the central space of the SC, where they associate with the LE via their amino-termini, ensuring alignment and synapsis between homologous chromosomes. Observations on centromere and chromosome pairing revealed that centromere clustering coincides with the initial formation of SC axial elements during meiotic leptotene and is temporally tightly followed by the formation of the telomere bouquet (Maestra et al., 2002; Sepsi et al., 2017). In accordance with other studies, the location of synapsis (initiation and elongation) is spatiotemporally separated (J. D. Higgins et al., 2012): sub-telomeric synapsis occurs at the leptotene-zygotene transition, while elongation of

interstitial synapsis emerged at mid-zygotene at multiple points of the chromosome arms (Sepsi et al., 2017).

Returning to sugarcane, it is suggested that bivalent association is favored, and that multivalents, if they occur, are resolved at the end of meiosis I, forming bivalents due to suppression of COs between homeologous (Vieira et al., 2018). Therefore, the hypothesis underlying the idea of this project is that a similar mechanism of genetic meiosis control, such as the one present in Wheat, is put into action in the generations that follow interspecific hybridizations (*S. officinarum* × *S. spontaneum*) and 'nobilization', when the genotypes begin to transmit  $n + n$  chromosomes (Vieira et al., 2018).

Herein, our aim was to investigate the genetic control of synapsis during meiosis in sugarcane. Through a bioinformatics approach we examined the presence of the *ZIP4* gene in both parental species (*S. officinarum* and *S. spontaneum*) and in two modern varieties (R570 and SP80-3280), we analyzed both gene and protein's identity, protein domains, TPR distribution and 3D protein structure. We also investigated *ZIP4* gene expression in different tissues. Using immunocytology for the first time in sugarcane, we were able to determine the SC polymerization during prophase, using ASY1 and ZYP1 sugarcane specific antibodies, revealing irregularities in synapsis for all genotypes, except for *S. officinarum*. Our findings, in addition to being original, will have implications for studies of genetic mapping, genomics and molecular cytogenetics, since this is a species of extreme commercial relevance, whose understanding of the inheritance of traits of agronomic interest (Mendelian and quantitative) and the organization of the genome still remains somewhat obscure.

## References

- Armstrong SJ, Caryl AP, Jones GH, Franklin FCH (2002) Asy1, a protein required for meiotic chromosome synapsis, localizes to axis-associated chromatin in Arabidopsis and Brassica. *J Cell Sci* 115:3645–3655. <https://doi.org/10.1242/jcs.00048>
- Barreto FZ, Balsalobre TWA, Chapola RG, et al (2021) Genetic Variability, Correlation among Agronomic Traits, and Genetic Progress in a Sugarcane Diversity Panel. *Agriculture* 11:533. <https://doi.org/10.3390/agriculture11060533>
- Bielig LM, Mariani A, Berding & N (2003) Cytological studies of 2n male gamete formation in sugarcane, *Saccharum L*
- Bremer G (1961) Problems in breeding and cytology of sugar cane - II. The sugar cane breeding from a cytological view-point. *Euphytica* 10:121–133. <https://doi.org/10.1007/BF00022203>
- Burner DM (1991) Cytogenetic analyses of sugarcane relatives (Andropogoneae: Saccharinae). *Euphytica* 54:125–133. <https://doi.org/10.1007/BF00145639>
- Cheavegatti-Gianotto A, de Abreu HMC, Arruda P, et al (2011) Sugarcane (*Saccharum X officinarum*): A Reference Study for the Regulation of Genetically Modified Cultivars in Brazil. *Trop Plant Biol* 4:62–89. <https://doi.org/10.1007/s12042-011-9068-3>
- Chelysheva L, Gendrot G, Vezon D, et al (2007) Zip4/Spo22 Is Required for Class I CO Formation but Not for Synapsis Completion in Arabidopsis thaliana. *PLoS Genet* 3:e83. <https://doi.org/10.1371/journal.pgen.0030083>
- Cuacos M, Lambing C, Pachon-Penalba M, et al (2021) Meiotic chromosome axis remodelling is critical for meiotic recombination in Brassica rapa. *J Exp Bot* 72:3012–3027. <https://doi.org/10.1093/jxb/erab035>
- Cuadrado A (2004) Genome remodeling in three modern *S. officinarum* x *S. spontaneum* sugarcane cultivars. *J Exp Bot* 55:847–854. <https://doi.org/10.1093/jxb/erh093>
- Cursi DE, Hoffmann HP, Barbosa GVS, et al (2021) History and Current Status of Sugarcane Breeding, Germplasm Development and Molecular Genetics in Brazil. *Sugar Tech*. <https://doi.org/10.1007/s12355-021-00951-1>
- D'Hont A, Grivet L, Feldmann P, et al (1996) Characterisation of the double genome structure of modern sugarcane cultivars (*Saccharum* spp.) by molecular cytogenetics. *Mol Gen Genet* 250:405–413. <https://doi.org/10.1007/BF02174028>
- De Muyt A, Pyatnitskaya A, Andréani J, et al (2018) A meiotic XPF–ERCC1-like complex recognizes joint molecule recombination intermediates to promote crossover formation. *Genes Dev* 32:283–296. <https://doi.org/10.1101/GAD.308510.117>
- Dubois E, De Muyt A, Soyer JL, et al (2019) Building bridges to move recombination complexes. *Proc Natl Acad Sci U S A* 116:12400–12409. <https://doi.org/10.1073/pnas.1901237116>
- Gao J, Colaiácovo MP (2018) Zipping and Unzipping: Protein Modifications Regulating Synaptonemal Complex Dynamics. *Trends in Genetics* 34:232–245. <https://doi.org/10.1016/J.TIG.2017.12.001>
- Gouy M, Nibouche S, Hoarau JY, Costet L (2013) Improvement of Yield per se in Sugarcane. In: *Translational Genomics for Crop Breeding*. John Wiley & Sons Ltd, Chichester, UK, pp 211–237

- Griffiths S, Sharp R, Foote TN, et al (2006) Molecular characterization of Ph1 as a major chromosome pairing locus in polyploid wheat. *Nature* 439:749–752. <https://doi.org/10.1038/nature04434>
- Grivet L, Daniels C, Glaszmann JC, D’Hont A (2004) A review of recent molecular genetics evidence for sugarcane evolution and domestication. *Ethnobotany Research and Applications* 2:009. <https://doi.org/10.17348/era.2.0.9-17>
- Higgins JD, Perry RM, Barakate A, et al (2012) Spatiotemporal Asymmetry of the Meiotic Program Underlies the Predominantly Distal Distribution of Meiotic Crossovers in Barley. *Plant Cell* 24:4096–4109. <https://doi.org/10.1105/tpc.112.102483>
- Holm PB, Wang X (1988) The effect of chromosome 5B on synapsis and chiasma formation in wheat, *triticum aestivum* cv. Chinese Spring. *Carlsberg Res Commun* 53:191–208. <https://doi.org/10.1007/BF02907179>
- Kline KL, Msangi S, Dale VH, et al (2017) Reconciling food security and bioenergy: priorities for action. *GCB Bioenergy* 9:557–576. <https://doi.org/10.1111/gcbb.12366>
- Lenormand T, Engelstädter J, Johnston SE, et al (2016) Evolutionary mysteries in meiosis. *Philosophical Transactions of the Royal Society B: Biological Sciences* 371:1–27. <https://doi.org/10.1098/rstb.2016.0001>
- Long SP, Karp A, Buckeridge MS, et al (2015) Chapter 10: Feedstocks for Biofuels and Bioenergy. *Bioenergy & Sustainability: Bridging the gaps* 302–346
- Lynn A, Soucek R, Börner GV (2007) ZMM proteins during meiosis: Crossover artists at work. *Chromosome Research* 15:591–605. <https://doi.org/10.1007/s10577-007-1150-1>
- Maestra B, De Jong JH, Shepherd K, Naranjo T (2002) Chromosome arrangement and behaviour of two rye homologous telomers at the onset of meiosis in disomic wheat-5RL addition lines with and without the Ph1 locus. *Chromosome Research* 10:655–667. <https://doi.org/10.1023/A:1021564327226>
- Martín AC, Borrill P, Higgins J, et al (2018) Genome-Wide Transcription During Early Wheat Meiosis Is Independent of Synapsis , Ploidy Level , and the Ph1 Locus. *Front Plant Sci* 9:1–19. <https://doi.org/10.3389/fpls.2018.01791>
- Martín AC, Rey MD, Shaw P, et al (2017) Dual effect of the wheat Ph1 locus on chromosome synapsis and crossover. *Chromosoma* 126:669–680. <https://doi.org/10.1007/s00412-017-0630-0>
- Martinez-Perez E, Shaw P, Moore G (2001) The Ph1 locus is needed to ensure specific somatic and meiotic centromere association. *Nature* 411:204–207. <https://doi.org/10.1038/35075597>
- Nair MK (1975) Cytogenetics of *Saccharum officinarum* L. And 5. *Spontaneum* L.IV. Chromosome number and meiosis in *S. officinarum* X *S. spontaneum* hybrids. *Caryologia* 28:1–14. <https://doi.org/10.1080/00087114.1975.10796591>
- Nonomura KI, Nakano M, Eiguchi M, et al (2006) PAIR2 is essential for homologous chromosome synapsis in rice meiosis I. *J Cell Sci* 119:217–225. <https://doi.org/10.1242/jcs.02736>
- Oliveira GK, Soares NR, Costa ZP, et al (2023) Meiotic abnormalities in sugarcane (*Saccharum* spp.) and parental species: Evidence for peri- and paracentric inversions. *Annals of Applied Biology*. <https://doi.org/10.1111/aab.12855>
- Pagliarini MS, Sila SP, Mollinari R (1990) Análise meiótica em cultivares de cana-de-açúcar. *Archives of Biology and Technology* 33:283–293
- Pelé A, Rousseau-Gueutin M, Chèvre A-M (2018) Speciation Success of Polyploid Plants Closely Relates to the Regulation of Meiotic Recombination. *Front Plant Sci* 9:1–9. <https://doi.org/10.3389/fpls.2018.00907>

- Piperidis G, Piperidis N, D'Hont A (2010) Molecular cytogenetic investigation of chromosome composition and transmission in sugarcane. *Molecular Genetics and Genomics* 284:65–73. <https://doi.org/10.1007/s00438-010-0546-3>
- Piperidis N, D'Hont A (2020) Sugarcane genome architecture decrypted with chromosome-specific oligo probes. *The Plant Journal* 103:2039–2051. <https://doi.org/10.1111/tpj.14881>
- Price S (1961) Cytological Studies in *Saccharum* and Allied Genera VII. Maternal Chromosome Transmission by *S. officinarum* in Intra- and Interspecific Crosses. <https://doi.org/10.1086/336118> 122:298–305. <https://doi.org/10.1086/336118>
- Price S (1963a) Cytogenetics of Modern Sugar Canes. *Econ Bot* 17:97–103
- Price S (1963b) Cytological Studies in *Saccharum* and Allied Genera. VIII. F2 and BC1 Progenies from 112- and 136-chromosome *S. officinarum* x *S. spontaneum* Hybrids. *Botanical Gazette* 124:186–190. <https://doi.org/10.1086/336190>
- Pyatnitskaya A, Andreani J, Guérois R, et al (2022) The Zip4 protein directly couples meiotic crossover formation to synaptonemal complex assembly. *Genes Dev* 36:53–69. <https://doi.org/10.1101/GAD.348973.121>
- Rey MD, Martín AC, Higgins J, et al (2017) Exploiting the ZIP4 homologue within the wheat Ph1 locus has identified two lines exhibiting homoeologous crossover in wheat-wild relative hybrids. *Molecular Breeding* 37:. <https://doi.org/10.1007/s11032-017-0700-2>
- Rey M-D, Martín AC, Smedley M, et al (2018) Magnesium Increases Homoeologous Crossover Frequency During Meiosis in ZIP4 (Ph1 Gene) Mutant Wheat-Wild Relative Hybrids. *Front Plant Sci* 9:1–12. <https://doi.org/10.3389/fpls.2018.00509>
- Riley R, Chapman V (1958) Genetic Control of the Cytologically Diploid Behaviour of Hexaploid Wheat. *Nature* 182:713–715. <https://doi.org/10.1038/182713a0>
- Sears ER (1977) An induced mutant with homoeologous pairing in common wheat. *Canadian Journal of Genetics and Cytology* 19:585–593. <https://doi.org/10.1139/g77-063>
- Sears ER, Okamoto M (1958) Intergenomic chromosome pairing in hexploid wheat. *Proc 10th Intern Congr Genet* 2:258–259
- Sepsi A, Higgins JD, Heslop-Harrison JS (Pat), Schwarzacher T (2017) CENH3 morphogenesis reveals dynamic centromere associations during synaptonemal complex formation and the progression through male meiosis in hexaploid wheat. *The Plant Journal* 89:235–249. <https://doi.org/10.1111/tpj.13379>
- Shen Y, Tang D, Wang K, et al (2012) ZIP4 in homologous chromosome synapsis and crossover formation in rice meiosis. *J Cell Sci* 125:2581–2591. <https://doi.org/10.1242/jcs.090993>
- Simmonds NW (1975) Sugar canes. In: *Evolution of Crop Plants*. Longman, London, pp 104–108
- Suzuki E (1941) Cytological Studies of Sugar Cane. Observations on some POJ varieties. *Cytologia (Tokyo)*
- Tsubouchi T, Zhao H, Roeder GS (2006) The Meiosis-Specific Zip4 Protein Regulates Crossover Distribution by Promoting Synaptonemal Complex Formation Together with Zip2. *Dev Cell* 10:809–819. <https://doi.org/10.1016/j.devcel.2006.04.003>
- Vieira MLC, Almeida CB, Oliveira CA, et al (2018) Revisiting meiosis in sugarcane: chromosomal irregularities and the prevalence of bivalent configurations. *Front Genet* 9:1–12. <https://doi.org/10.3389/fgene.2018.00213>

- Wall AM, Riley R, Chapman V (1971) Wheat mutants permitting homoeologous meiotic chromosome pairing. *Genet Res* 18:311–328. <https://doi.org/10.1017/S0016672300012714>
- Zickler D (2006) From early homologue recognition to synaptonemal complex formation. *Chromosoma* 115:158–174. <https://doi.org/10.1007/s00412-006-0048-6>
- Zielinski M-L, Mittelsten Scheid O (2012) Meiosis in Polyploid Plants. In: *Polyploidy and Genome Evolution*. Springer Berlin Heidelberg, Berlin, Heidelberg, pp 33–55

## 2. MEIOSIS IN POLYPLOIDS AND IMPLICATIONS FOR GENETIC MAPPING: A REVIEW<sup>1</sup>

### Abstract

Plant cytogenetic studies have provided essential knowledge on chromosome behavior during meiosis, contributing to our understanding of this complex process. In this review, we describe in detail the meiotic process in auto- and allopolyploids from the onset of prophase I through pairing, recombination and bivalent formation, highlighting recent findings on the genetic control and mode of action of specific proteins that lead to diploid-like meiosis behavior in polyploid species. During the meiosis of newly formed polyploids, related chromosomes (homologous in autopolyploids; homologous and homoeologous in allopolyploids) can combine in complex structures called multivalents. These structures occur when multiple chromosomes simultaneously pair, synapse and recombine. We discuss the effectiveness of crossover frequency in preventing multivalent formation and favoring regular meiosis. Homoeologous recombination in particular can generate new gene (locus) combinations and phenotypes, but may destabilize the karyotype and lead to aberrant meiotic behavior, reducing fertility. In crop species, understanding the factors that control pairing and recombination has the potential to provide plant breeders with resources to make fuller use of available chromosome variations in number and structure. We focused on wheat and oilseed rape, since there is an abundance of elucidating studies on this subject, including the molecular characterization of the Ph1 (wheat) and PrBn (oilseed rape) loci which are known to play a crucial role in regulating meiosis. Finally, we exploited the consequences of chromosome pairing and recombination for genetic map construction in polyploids, highlighting two case studies of complex genomes: (i) modern sugarcane, which has a man-made genome harboring two sub-genomes with some recombinant chromosomes; and (ii) hexaploid sweet potato, a naturally occurring polyploid. The recent inclusion of allelic dosage information has improved linkage estimation in polyploids, allowing multilocus genetic maps to be constructed.

Keywords: auto- and allopolyploids; meiosis; early meiosis; genetic control; homoeologous recombination; genetic maps; allelic dosage; multilocus linkage

### 2.1. Overview

The study of meiosis in polyploid species began in 1920s with the classic report of Newton and Darlington (1929) who studied triploid and pentaploid tulips. A number of important studies on meiotic variations in polyploids have been published over the past century, particularly in the last few decades (Bombliés et al., 2015, 2016; Cifuentes, Grandont, et al., 2010; Gillies, 1989; Grandont et al., 2013; Jenkins, 1989; A. Lloyd & Bombliés, 2016; Pelé et al., 2018; Zickler & Kleckner, 1999). There are two classes of naturally occurring polyploids: autopolyploids, which have three or more copies of the same genome (e.g., the autotetraploid *Solanum tuberosum*,  $2n=4x=48$ ); and allopolyploids, the result of interspecific hybridization between related progenitors and genome doubling (e.g., the allotetraploid *Nicotiana tabacum*,  $2n=4x=24$ , whose genome composition is AABB).

---

<sup>1</sup> The text corresponds to that of the article published by Soares et al. (2021) in *Genes*, 12 (10), 1517.

However, this classification is relatively flexible. For example, chromosome sets in allopolyploids differ in proportion to the divergence level between the parental genomes: the closer the parents, the more similar the resulting allopolyploid is to an autopolyploid (Comai, 2005). During the meiosis of newly formed polyploids, related chromosomes (homologous in autopolyploids; homologous and homeologous in allopolyploids) may pair and combine in complex structures called multivalents (autopolyploids) or form illegitimate homeologous pairing (allopolyploids) (E. E. Higgins et al., 2021; McCollum, 1957; Szadkowski et al., 2010; Yant et al., 2013). These structures occur when multiple chromosomes simultaneously pair, synapse and recombine. Multivalent or homeologous pairing, that reach metaphase I (MI) are related to segregation issues, leading to aneuploid gametes, compromised fertility and low-fitness of offspring (Zamariola et al., 2014).

## 2.2. Revisiting early meiosis

The premeiotic organization of homologous chromosomes in polyploid and diploid species is very similar. Homologous chromosomes are nonrandomly distributed and organized in the nucleus (Figure 1) (Avivi & Feldman, 1980; Schubert & Shaw, 2011). In many eukaryotes, telomeres and centromeres cluster at opposite poles of the nucleus during prophase I (PI) (Cowan et al., 2001), forming the Rabl-configuration, first described by the pioneering studies of Rabl in 1885 and Boveri in 1909 [see 20]. In *Arabidopsis*, in which a non-Rabl pattern of chromosome organization occurs, dominant ‘chromosome territories’ arise, consisting of heterochromatic centromeric regions at the nuclear periphery, from which chromosome arms emanate (Fransz et al., 2002). In this case, the chromosome position is also associated with the gene expression level (Cremer & Cremer, 2010; Dixon et al., 2016).

Then, chromosomes must move at the beginning of meiosis to find the correspondent homolog. This movement can be telomere oriented to form the bouquet, or involve chromatin unfolding (Bass et al., 1997; Tiang et al., 2012). Once the chromosomes are close enough to interact, potential partners must be chosen. This process is mediated by homology. A certain degree of sequence identity is required, and pairing depends on the type of polyploidy level, species, individual chromosomes and chromosome segments (Figure 1) (Clancy, 2008; Sybenga, 1996).

Early stages of recognition and pairing can be more complex in polyploids than in diploids, this is caused by the high number of potential homologous partners that can delay the progression of meiosis (Zielinski & Mittelsten Scheid, 2012). During the telomere bouquet phase in early meiosis, centromere associations begin the process of sorting chromosomes. When more than one complement of chromosomes is present, early association of the centromeres is triggered in auto- and allopolyploids (Martinez-Perez et al., 2000) leading to the formation of multicentromeric clusters, which help resolve nonhomologous centromere associations, thereby contributing to homologous chromosome sorting (Figure 1)(Martinez-Perez et al., 2000).

After chromosomes are associated by their centromeres, the process of homologous chromosome alignment begins. First, the programmed double-strand DNA breaks (DSBs) produced in early leptotene are catalyzed by the topoisomerase-like protein, Spo11, causing physical interactions which lead to chromosome sorting (Keeney et al., 1997; Neale & Keeney, 2006). After a DSBs occurs, each chromosome has two or more potential partners to interact with in order to repair the DSBs by homologous recombination using a non-sister chromatid as a template. Fragments of DNA around the 5'-end of the break are nicked during



resection, and the overhanging 3'-end of the broken DNA molecule associates with recombinase RAD51 and/or the meiosis-specific recombinase DMC1, which invades a similar or identical DNA molecule a nucleoprotein filament (Hunter & Kleckner, 2001). Shortly after the chromosomes align, they are united by the synaptonemal complex (SC), a stable proteinaceous structure (Zielinski & Mittelsten Scheid, 2012). The SC is formed by three elements: axial element (AE), central element (CE), and recombination nodules (RNs) (Figure 1) (Lohmiller et al., 2008). The RNs are complexes of several proteins involved in synapsis and recombination (Anderson & Stack, 2005). After the assembly of the SC in zygotene, homologous chromosomes become fully synapsed at pachytene (Page & Hawley, 2004; Roeder, 1997). Homologous chromosomes are kept together along their length by the SC, which also serves as a scaffold to recruit factors of the recombinational repairing machinery (Zickler & Kleckner, 2015).

Interestingly, during PI, a range of SC assembly variations may occur, including multiple SCs and synaptic multivalents exhibiting pairing partner switches (PPS). The most frequent meiotic variation in polyploids is the occurrence of complex synaptic interactions, when the progressive pairing of three or more chromosomes starts simultaneously at different points along their lengths, producing PPS (Gillies, 1989). PPS distribution is irregular but not accidental (Figure 1). The existence of more than one switch per chromosome imply the presence of additional autonomous pairing sites (APS) along the chromosomes, each with a low probability of generating a PPS (Vincent & Jones, 1993). Pairing with one chromosome at one APS promotes the continuation of pairing in a zipper-like manner (Zielinski & Mittelsten Scheid, 2012). Variations in meiosis are mainly due to the type of presynaptic alignment, either distal or complete; the number and distribution of synapsis initiation points; the number of partner exchanges and progress through zygotene and pachytene; and whether or not there are preferences in partner selection (Prieto & Naranjo, 2020). These synaptic multivalents can be observed in auto- and allopolyploid plants, with PPS occurring more often in triploids than in tetraploids (Grandont et al., 2013; Loidl, 1986; Loidl & Jones, 1986; Vincent & Jones, 1993).

### **2.3. Meiosis in autopolyploids**

Autopolyploidy occurs in individuals or species that have undergone a whole genome duplication (WGD) event, due to non-disjunction of the gametes during meiosis, resulting in  $2n$  gametes rather than haploid ( $n$ ) gametes. When these gametes are fertilized, they can produce triploid ( $2n + n$ ) or tetraploid ( $2n + 2n$ ) individuals. Therefore, an autopolyploid has more than two copies of homologous chromosomes that are equally capable of randomly pairing, synapsing and recombining (crossing over) during PI. When these events are observed in more than two homologous chromosomes, a multivalent can be formed at MI and chromosome missegregation can occur at anaphase I (AI) [27] (Figure 1). On the one hand, most of these multivalents are dissolved prior to MI in established autopolyploids, which primarily form bivalents. On the other hand, multivalents are frequently retained in resynthesized autopolyploids, mainly as tri- and/or tetravalents (or quadrivalents). The occurrence of multivalents depends on the ploidy level and homology between chromosomes (John & Henderson, 1962), and is known to be controlled by genetic factors (Bomblies et al., 2016; A. Lloyd & Bomblies, 2016). Metaphase I multivalents are related with an increased risk of homologous missegregation at AI. However, molecular mechanisms evolved to reduce the meiotic challenges faced by polyploids, generating fertile autopolyploids (Bomblies et al., 2015, 2016; A. Lloyd & Bomblies, 2016)

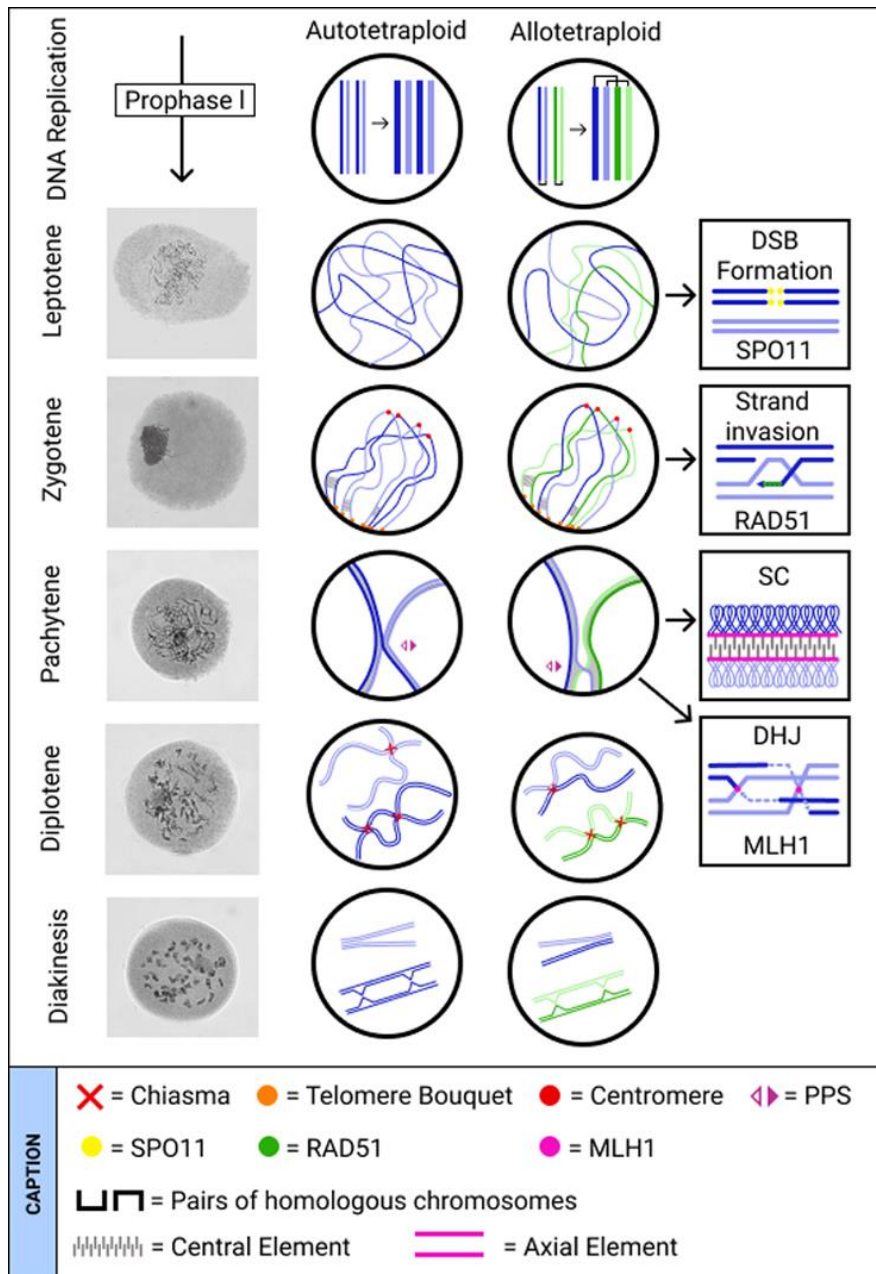


**Figure 1. Pre-meiotic and early meiotic events in auto- and allotetraploid species illustrating regular meiotic behavior during Prophase I.** Meiosis is preceded by one round of DNA replication during which sister chromatids are duplicated. During leptotene, genetic recombination is initiated, and double-strand breaks (DSBs) catalyzed by the protein Spo11 and repaired through homologous recombination. This process leads to DSB invasion into the non-sister chromatid by the RAD51 protein, initiating physical interactions and driving chromosome sorting. Homologous recognition may be facilitated by the clustering of telomeres at one pole of the cell forming the telomere bouquet. During zygotene, chromosomes begin synapsis via the formation of the synaptonemal complex (SC), which consists of axial and central elements. The SC is formed between pairs of homologous chromosomes, but it can also be formed between more than two homologs in autotetraploids and between homoeologous chromosomes in allotetraploids, resulting in synaptic partner switches (PPS) at pachytene. As recombination proceeds, in some species multiple/homoeologous associations are corrected by the MLH1 protein, a DNA mismatch repair that is required to resolve DHJ into COs. By contrast, in other species, specific localization of crossovers between pairs of homologous chromosomes resolves multiple/homoeologous associations at diplotene, when the SC is disassembled. Irrespective of when the corrections occur, only bivalents are visualized at diakinesis when chromosomes recondense in established polyploid lineages. Modified from Cifuentes et al. On the left, prophase I images depict a commercial variety of sugarcane. Photo credit: Oliveira, G.K., Universidade de São Paulo, Brazil.

## 2.4. Frequency of crossovers

In contrast to populations of natural, well-established autopolyploids, natural neo-autopolyploids often have a high number of COs and multivalents at MI, resulting in high levels of aneuploidy and consequently in low fertility (Pecinka et al., 2011; Ramsey & Schemske, 2002). When an autopolyploid is resynthesized and selected for meiotic stabilization resulting and therefore successful chromosome transmission, fewer multivalents are observed, followed by the reduction in the number of crossovers (CO) (A. Lloyd & Bomblies, 2016). In plants, as the number of initial DSBs exceeds the number of COs, the majority of DSBs are resolved, but a minority fraction (~5%) result in CO (de Muyt et al., 2009; Edlinger & Schlögelhofer, 2011; Hamant et al., 2006; Mercier & Grelon, 2008; Sanchez-Moran et al., 2008). When chromosomes form COs with more than one partner, multivalents are observed at MI. Therefore, ensuring one CO per chromosome prevents the formation of multivalents. In many natural species, decreased CO frequencies have been observed in evolved tetraploids in comparison to their diploid precursor (Carvalho et al., 2010; Lavania, 1986, 1991; Yant et al., 2013).

Notably, there are no correlations between chromosome length and the number of COs (Brubaker et al., 1999; Mézard, 2006). In fact, genomes consist of ‘hot and cold spots’, with respective high and low rates of meiotic recombination (Drouaud et al., 2006; Kim et al., 2007; Mézard, 2006), suggesting that reduced CO frequency is an effective path toward meiotic adaptation. Results reported in *Arabidopsis* support the idea that one CO per chromosome is associated with low frequency of multivalents in the natural autotetraploid *A. arenosa*, evidencing the effect of genes on CO rates (Carvalho et al., 2010; Yant et al., 2013). In *A. thaliana*, the CO number increases in newly formed polyploids (Pecinka et al., 2011), with fewer multivalents seen after a few generations (Santos et al., 2003; Weiss & Maluszynska, 2001). Thus, while there may be a temporary increase in COs, it seems that evolution favors reductions in CO rates in the longer term, at least in autotetraploids.

The ability of CO positioning ensures that every chromosome copy has at least one CO, thus excluding ‘zero-CO’ univalents and trivalent-plus-univalent configurations (Bomblies et al., 2016). Some insights into which genes might be involved in this process emerged from a comparison between diploid and tetraploid *A. arenosa* genomes, identifying several meiotic genes as targets for selection in the tetraploid lineage, where most of these genes encode chromosome axis components such as *Asy1*, *Asy3* and *Syn1/ Rec8*, or their direct interactors *Zip1a/Zip1b* and *Pds5* (Hollister et al., 2012; Yant et al., 2013).

## 2.5. Multivalents and cytological diploidization

Polyploid meiotic configurations during MI may comprise the presence of univalents, bivalents, and multivalents. In 1947 Stebbins has already pointed out that multivalents are disadvantageous due to their negative impact on fertility and karyotype stability. Several subsequent studies support this view, determining that selection for fertility results in fewer multivalents and produces a cytological diploidization, in which chromosomes predominantly (or exclusively) pair as bivalents in MI (Ramsey & Schemske, 2002; Santos et al., 2003).

Studies on autotetraploids, nevertheless, shows that high fertility correlates with increased quadrivalents at MI (Abraham et al., 2013; Crowley & Rees, 1968), suggesting that univalents and trivalents are the main cause of reduced fertility, probably because they are less likely to segregate appropriately. In established autotetraploid lines of *A. thaliana* (ecotype Columbia)

fewer multivalents were observed than in newly synthesized lines, suggesting that partial cytological diploidization occurred over 13 generations (Santos et al., 2003).

A reduction in the number of multivalents has been observed through PI and from PI to MI in polyploids, regardless the presence of univalents (Cifuentes, Grandont, et al., 2010). Some multivalents formed during zygotene are resolved into bivalents in pachytene, either due to the removal of SC sections or due to the suppression of recombination so that only bivalent associations are retained [37,62]. The correction of multivalent associations proceeds during late zygotene. However, a proportion of multivalents persists in most cases. Overall, the process of diploidization in meiotic behavior is a common strategy throughout the evolution of autopolyploid species [49,62–65].

Autopolyploids also exhibit idiosyncrasies in allelic segregation. While both diploids and allopolyploids display disomic inheritance, autopolyploids exhibit polysomic inheritance. Polysomic inheritance is generated by (i) the random assortment of multiple homologous chromosomes; (ii) a series of dosage allelic combinations (AAAA, AAAa, AAaa, Aaaa, and aaaa for an autotetraploid, for instance); and (iii) the presence of more than two alleles at a locus. Such polysomic inheritance occurs in autopolyploids irrespective of the presence of multivalents or bivalents at MI, a point that will be addressed later. Disomic and polysomic inheritance are only extreme cases on a gradient, with intermediate inheritance patterns taking place when every chromosome has a preferential, but not exclusive, partner (Jannoo et al., 2004). In contrast, multivalent formation is often associated with ‘double reduction’, when distal segments of sister chromatids end up in the same gamete, i.e. in one gamete two copies of the same gene sequence (allele) will be derived from the same parental chromosome [27]. All these attributes directly impact population genetic parameters with possible consequences for evolution (Parisod et al., 2010). In addition, such attributes might significantly influence genetic mapping, which is especially relevant for crop species.

## 2.6. Genetic control of meiosis in autopolyploids

In autopolyploids, only few studies have identified genes regulating chromosomal pairing, synapsis and CO occurrence. In the autotetraploid *A. arenosa*, some meiotic genes (Asy1, Asy3, Pds5b, Prd3, Rec8, Smc3, Zyp1a, Zyp1b) encode proteins that coordinate early meiotic functions (Yant et al., 2013). In early PI, the chromosomal axis present in each of the sister chromatids are transformed into two SC lateral elements which are composed of a scaffold of cohesin proteins (SMC1, SMC3, PDS5, REC8, and SCC3) (Bhatt et al., 1999; Cai et al., 2003; Chelysheva et al., 2005; Lam et al., 2005; Pradillo et al., 2015), these proteins arrange the two sister chromatids into loops that are turned away from the axis (Figure 1) (Lambing, Tock, et al., 2020). The binded-loop axis model proposes that meiotic DSBs are generated on the chromatin loops that become connected to the axis during inter-homolog repair (Kleckner, 2006; Zickler & Kleckner, 1999). ASY1, ASY3 and ASY4 are meiosis-specific proteins that land into the cohesin scaffold, increasing inter-homolog recombination (S. J. Armstrong et al., 2002b; Chambon et al., 2018; Ferdous et al., 2012). Furthermore, ASY1 and ASY3 are essential for establishing precise chromosomal pairing and synapsis (Caryl et al., 2000; Ferdous et al., 2012; West et al., 2019).

Morgan et al. (2020) have investigated the effects of the previously described genes Asy1 and Asy3 on the autotetraploid *A. arenosa*, focusing on the derived (autotetraploid, T) and ancestral (diploid, D) alleles. The ASY1 and ASY3 proteins constitute the chromosome axis, this protein structures are formed along the replicated chromosomes during PI and are

necessary for chromosome pairing, synapsis and homologous recombination (Zickler & Kleckner, 1999). As a result, mutants for *Asy1* or *Asy3* are found to be deficient in synapsis, have low levels of COs and possess high levels of univalents (Ferdous et al., 2012; Sanchez-Moran et al., 2007). The presence of "rod-shaped" bivalents and chromosome axis with reduced length besides a reduction of multivalent association are all associated with the derived alleles *Asy1* and *Asy3* (Morgan et al., 2020).

Derived alleles of *Asy1* and, to a lesser extent, *Asy3*, are linked to a higher frequency of bivalents at MI with "rod-like" forms, which are thought to indicate more distant CO locations (Moran et al., 2001). *Asy1* and *asy3* mutants in *A. thaliana* contain relatively few COs, but those that do exist are mostly subtelomeric (Caryl et al., 2000; Moran et al., 2001). Centromeres and surrounding repetitive sequences (pericentromeric heterochromatin) are frequently suppressed for meiotic recombination; therefore, high CO levels are typically observed at distal subtelomeric regions that also tend to have higher gene density (Choi et al., 2018; He et al., 2017; Underwood et al., 2018).

The derived alleles (T or D) of *Asy1* and *Asy3* may be responsible for the reduced CO number in autotetraploid *A. arenosa*, preventing multivalent formation, by reducing the CO number to one per bivalent, ensuring that only bivalents are formed (Bomblies et al., 2016). Plants homozygous for *Asy1*-T alleles exhibited less multivalent cells at MI than *Asy1*-D homozygotes, suggesting that *Asy1*-T are important for meiotic stability. This is supported by the fact that *Asy1*-TTTT plants exhibit less synaptic partner switches and multivalent formation in PI. In the presence of the *Asy1*-T allele, the reduction in multivalent formation may be determined, at least in part, to a higher propensity for COs to be positioned on the same side relative to partner switch sites (Bomblies et al., 2016). The fact that the *Asy1* allele status may affect the axis length supports the concept that allelic variation at *Asy1* might change axis organization in some way, and it's possible that this encourages the "safer" placement of CO sites on the same side as partner switch sites.

However, the factors and mechanisms that shape the meiotic recombination landscape along chromosomes remain understood. This could be related to the fact that telomeres cluster in PI and this clustering is largely preserved in *A. thaliana asy1* mutant, possibly allowing interhomolog recombination events to proceed in these regions due to close proximity of the chromosomes (S. J. Armstrong et al., 2001; Carvalho et al., 2010). Lambing et al. (2020a) using chromatin immunoprecipitation reported an ascending gradient of the protein ASY1 from telomeres to centromeres, and this differential distribution along the arms is required for more equally distributing recombination. However, despite high amounts of ASY1 in centromeric areas, meiotic DSBs and COs are repressed due to high concentration of heterochromatin in these areas (Choi et al., 2018; Underwood et al., 2018; Yelina et al., 2015).

In order to further study the *Asy3* gene influence in autopolyploids, Seear et al. (2020) traced the evolutionary origins of the autotetraploid lines of *A. lyrata* and *A. lyrata* x *A. arenosa* hybrid populations, demonstrating that *Asy3* stabilizes the autotetraploid male meiosis. A novel allele was discovered, harboring a tandem duplication (TD) in a serine-rich region of the ASY3 protein, which is correlated with stable meiotic phenotypes in tetraploids.

In comparison to diploid *A. lyrata*, the number of CO in autotetraploid individuals was decreased, with a reduction of CO in proximal and interstitial areas, thus indicating a basic procedure for meiotic adaptation to autopolyploidy (Hazarika & Rees, 1967; Seear et al., 2020). Therefore, the ASY3 TD protein, present in autopolyploids may be hypomorphic and act in distancing CO (Chambon et al., 2018; Ferdous et al., 2012; Hazarika & Rees, 1967).

The *Asy3* TD allele possibly arose from diploid *A. lyrata*, according to a phylogenetic study of the *Asy3* alleles (Marburger et al., 2019). The bidirectional gene flow among *A. arenosa* and *A. lyrata* tetraploids has increased the gene pool from which favorable alleles may be acquired and chosen, and new gene conversion chimeric alleles can accurately combine favorable sequences from different origins for adaptation. The adaptive *Asy3* TD allele's genesis in tetraploid populations appears to be recent, although it has disseminated widely and introgressed within strict bounds in the *A. lyrata* x *A. arenosa* hybrid genomes studied (Marburger et al., 2019). Gene flow of adaptive alleles (*Asy1*, *Prd3*, *Rec8*, *Smc3*, *Zyp1a* and *Zyp1b*) from *A. arenosa* may have been required to establish meiotic stability in recent *A. lyrata* tetraploids prior to the origin of the *Asy3* TD allele, but this requirement has since been relaxed due to the presence of the dominant *Asy3* TD allele. Additionally, gene flow has introduced *Asy1*, *Prd3*, *Rec8*, *Smc3*, *Zyp1a*, and *Zyp1b* alleles from *A. arenosa* into tetraploid *A. lyrata* (Seear et al., 2020).

## 2.7. Meiosis in allopolyploids

Allopolyploids are formed by the fusion of unreduced gametes followed by genome doubling in  $F_1$  hybrids, or interspecific or intergeneric hybridization (Comai, 2005; Pelé et al., 2018) (Figure 2). Therefore, allopolyploids carry two (or more) full complements of chromosomes, each from a distinct progenitor genome, thus forming homoeologous subgenomes, which are differentiated by differences in chromosome architecture, DNA sequences and gene order. Nevertheless, chromosomes retain some degree of genetic affinity and thus share genomic synteny. This genetic affinity allows homoeologous to compete with homologous chromosomes during interactions such as recognition, alignment, SC assembly, and CO (Prieto & Naranjo, 2020). However, exclusive bivalent pairing at MI is essential to ensure regular homologous segregation at AI and consequently reproductive stability. Such diploid-like behavior is a result of genetic regulatory systems, as evidenced in wheat, *Avena sativa*, *Festuca arundinacea*, cotton and *Brassica napus* (reviewed in 93).

## 2.8. Chromosome pairing, recombination, and segregation in allopolyploids

During allopolyploid meiosis, chromosomes recombine with their closest related homolog, forming bivalents at diakinesis (Grandont et al., 2014; Pecinka et al., 2011; Sears, 1976). Bivalent formation is accomplished by two complementary systems: in one system, differences between homoeologues lead to preferential pairing between homologues; in the other, a genetic control can differentiate sets of chromosomes and prevent pairing between homoeologues (Mason & Wendel, 2020).

The classic explanation for complete cytogenetic diploidization holds that the absence of homology between chromosomes from different subgenomes prevents their association during the early stages of meiosis, resulting in homologous pairing (Figure 2) (see 98). These chromosomes are then associated as bivalents by chiasma formation prior to MI. In addition, the preference of homologues over homoeologues in allopolyploids also seems to be under genetic control. The most important studied example is the *Pairing homoeologous 1 (Ph1)* locus in wheat (Sears, 1976).

In allopolyploids, diploidization can be accomplished by combining different processes during the interphase and early stages of meiosis (Cuñaado et al., 1996; Jenkins & Rees, 1991).

It has been proposed that polyploid chromosome ordering starts with centromere association (Martinez-Perez et al., 2000). Followed by the restriction of synapsis initiation between homoeologues, so that most of the pairing at zygotene is between homologous chromosomes. In a third stage, the dissolution of SCs in homoeologues occurs before COs at pachytene, decreasing the frequency of multivalents. However, in most species, such a correction is insufficient and some multivalents persist. Finally, multivalents are fully resolved in the last recombination stages, when the prevention of COs between synapsed homoeologous segments results exclusively in homologous bivalents (Figure 1) (Jenczewski & Alix, 2004).

The visualization of chromosomes during interphase allows chromosome pairing to be examined before the first division. The initial reports on this subject indicated that centromeres associate in hexaploid wheat (Bennett, 1979) and that a high level of homologous pairing is achieved upon entry into meiosis (Moore, 2002). During early meiotic PI, telomeres aggregate on the nuclear envelope forming a cluster or bouquet (Chikashige et al., 1997; Niwa et al., 2000; Trelles-Sticken et al., 1999), facilitating homologous chromosome sorting. The timing of telomere bouquet formation differs across species, appearing earlier at PI in wheat and rye, and later in maize (Bass et al., 1997; Martinez-Perez et al., 1999; Mikhailova et al., 2001). After the formation of the telomere bouquet, SC formation is initiated near the telomeres during early PI, progressing lengthwise pairing as PI proceeds (Figure 1) (Bass et al., 2000; Gillies, 1975, 1985).

As in autopolyploids, multiple homologues and homoeologues in allopolyploids align in early PI, forming multivalents at zygotene (Gillies, 1985; Grandont et al., 2014; Loidl et al., 1990). This results in pairing configurations such as cross-structures, rings, and chains during metaphase (Grant, 1978; Sybenga, 1975). However, such pairing configurations occur less often in allopolyploids and are frequently restricted to smaller chromosome regions. During zygotene, these pre-synaptic associations may progress into synaptic partner switches (Cuñado et al., 1996; Grandont et al., 2014; Hobolth, 1981), although to a lesser extent than in autopolyploids (Figure 1).

In allopolyploids, recombination nodules are found in homoeologous synapsis regions (Hobolth, 1981), indicating that strand invasion and CO formation occur between homoeologous chromosomes. However, they do not progress as true COs (Jenkins & Rees, 1991). At the time cells enter pachytene, the number of synaptic partner switches declines and almost all chromosomes show homologous synapsis by the end of pachytene (Grandont et al., 2014; Holm, 1986). However, when compared to diploids, the number of COs per chromosome can be higher in allopolyploids, which present multiple sets of homoeologous chromosomes, as demonstrated in *Arabidopsis* (Pecinka et al., 2011), *Gossypium* (Desai et al., 2006), *Zea* (Bingham et al., 1968) and *Brassica* (Leflon et al., 2010; Pelé et al., 2017). For example, the genetic mapping of *Brassica napus* allotetraploids (AACC,  $2n = 4x = 38$ ), generated from the natural hybridization between *B. rapa* (AA,  $2n = 2x = 20$ ) and *B. oleracea* (CC,  $2n = 2x = 18$ ) (Jenczewski et al., 2013), revealed around twice as many COs between the homologous A07 chromosomes than in the diploid AA hybrids (Leflon et al., 2010). A rise in the number of COs was also linked with a decrease in the CO interference strength (Suay et al., 2014). The molecular mechanisms underlying this increase are unknown, but they appear to be dependent on the addition of specific C chromosomes, as demonstrated by Suay *et al.* (Suay et al., 2014), who demonstrated a non-additive dosage effect. Nevertheless, in allotriploids AAC *Brassica* hybrids was observed a higher number of CO and the reshaping of the recombination landscapes, when compared to diploid AA (Pelé et al., 2017). In allotriploids, the presence of the 9 additional C chromosome leads to an increase of COs between all homologous A chromosomes, especially in the centromeres proximity,

with a strong decrease of interference of Class I COs compared to the case of diploid AA (Pelé et al., 2017).

In naturally occurring allopolyploids, homoeologous pairing is corrected by diplotene. Consequently, allopolyploids show homologous bivalent formations at MI and disomic inheritance (Comai et al., 2003; Pecinka et al., 2011). The dissociation of chromosomes from multivalent configurations often leads to deficient gametes, with duplication and aneuploidy, ultimately leading to reduced fertility (Gillies, 1989). Recombination between homoeologous chromosomes can be problematic: it contributes to homogenize the subgenomes, promoting further recombination between homoeologues, and can eliminate the contribution of one parent in a genomic region, leading to gene dosage imbalance and other problems related to aneuploidy (Gaeta & Chris Pires, 2010; Xiong et al., 2011).

Importantly, recombination between homoeologues in established allopolyploids appears to be an uncommon phenomenon. Therefore, fertile allopolyploids either had some level of pre-existing control over pairing or must have acquired such genetic control during their evolution. It is also possible that structural changes occurring in newly formed polyploids (e.g. expansion or contraction of repeat elements or other genomic rearrangements) contribute to divergence among homoeologues and facilitate correct homolog pairing (Gaeta & Chris Pires, 2010).

## 2.9. Homoeologous exchanges

In many allopolyploid species, mispairing between homoeologous chromosomes leads to exchanges. HEs can generate homoeologous reciprocal translocations (HRT) or homoeologous non-reciprocal translocations (HNRT), leading to deletions, duplications, and translocations, even when including small regions of duplicated DNA (Mason & Wendel, 2020). Recurrent polyploidy events have originated primary and secondary homoeology: homoeology between subgenomes (primary, resulting from a recent event) and homoeology within each subgenome (secondary, arising from older events). A good example of this are the genomes A, B and C in *Brassica* (I. A. P. Parkin et al., 2003).

Duplications, deletions, and rearrangements can be caused by non-homologous recombination events. Although these abnormalities supposedly occur in almost all evolutionary lineages, a rearrangement is more likely to be fatal in a diploid lineage if a large deletion or duplication is involved (Schuermann et al., 2005). Nonetheless, in polyploids, an extra set of chromosomes facilitates chromosome change because when two or more copies of a gene (or genomic region) is present, this allows rearrangements to occur without affecting gamete viability and fertility. In fact, the success of polyploidy in many lineages is partially due to genomic redundancy (Leitch & Leitch, 2008), although it can slow down the loss or fixation of deleterious and beneficial alleles, respectively (Otto & Whitton, 2000; Stebbins, 1971).

HEs and other karyotypic variations have been associated with phenotypic changes in many polyploids (Schiessl et al., 2019). HNRTs and deletions were correlated with qualitative changes in the expression of specific homoeologous genes and anonymous cDNA amplified fragment length polymorphisms and with phenotypic variation among polyploids. Indicating that exchanges among homoeologous chromosomes are a major mechanism for creating novel allele combinations and phenotypic variation in newly formed polyploids, generating extensive genetic diversity in a short period of time (Gaeta et al., 2007; Gaeta & Chris Pires, 2010; K. Song et al., 1995; Szadkowski et al., 2010). HEs,



duplications/deletions and chromosome rearrangements may therefore provide an important evolutionary substrate in neoallopolyploids for divergence, speciation and adaptation (Mason & Wendel, 2020).

## 2.10. Neoallopolyploids

In contrast to established allopolyploids, neoallopolyploids have a higher number of synaptic multivalents persisting to MI, resulting in high rates of homoeologous recombination, chromosomal rearrangements and aneuploidy (Henry et al., 2014; Szadkowski et al., 2010; Xiong et al., 2011). In neoallopolyploids, rearrangements are often accumulated and passed on to subsequent generations. However, since fertility is usually lower, they are selected against during the establishment of a new polyploid species (Gaeta & Chris Pires, 2010; Xiong et al., 2011).

Progenies of hybridization events have variable chromosome constitutions, and this may expand genetic variation and contribute to the success of neoallopolyploids. Variations in chromosome constitution in neoallopolyploids are not random: they are usually genetically balanced, i.e., the lack of one or a chromosome pair is compensated by an increased dose of its homoeologue, or, in case of translocations incidence, by equivalent segments of homoeologues. According to (Oleszczuk & Lukaszewski, 2014) these changes do not alter gene dosages; in other words, new allopolyploids do not suffer any immediate impairment due to random numerical aneuploidy and may benefit from altered dosages of homoeoalleles.

When homoeologous pair, the pattern of chromosome segregation is usually altered: univalents deliver one sister chromatid and paired homoeologues deliver both sister chromatids to each pole. This behavior results in nullisomic gametes for one homoeologue and disomic for the other. Then, during fertilization, when these gametes fuse, either a nullitetrasonic or a monotrisonic will be formed, both with compensating chromosome constitutions (Ramanna & Jacobsen, 2003). On the other hand, the segregation of a bivalent delivers both sister chromatids from a homoeologue to the same pole. Since the formation of bivalents depends on homoeologous CO and chiasmata, at least one of the two sister chromatids is recombined in each chromosome consisting of segments from both homoeologues, thus, the gametes should be genetically complete, hence viable (Chester et al., 2012).

Meiotic restitution is another event that often occurs in neoallopolyploids, which is genetically controlled, at least in wheat (L. Q. Zhang et al., 2007). In wide hybrids, for instance, when specific homologous pair were present, restitution occurred in meiocytes where homologous chromosomes failed to pair (Silkova et al., 2013). Deviations from chromosome behavior during meiotic restitution, such as infrequent homoeologous pairing or early migration of univalents to the poles, are capable of generating unusual chromosome constitutions (Chester et al., 2012; H. Zhang et al., 2013), and may explain some patterns of loss of linked loci (Buggs et al., 2012; Tate et al., 2009).

Patterns of chromosome segregation may create diverse chromosome constitutions, including deviations in chromosome numbers among the progeny than implied by unreduced gametes. These deviations boost genetic variation among newly-created genotypes, allowing natural selection to select the best fit combinations. Slight alterations in the patterns of truncated meiosis common of hybrids expand the dimension of available chromosome compositions amid progeny, and usually in a genetically balanced way, which can contribute

considerably to the fitness of spontaneously generated allopolyploids (Oleszczuk & Lukaszewski, 2014).

### 2.11. Genetic regulatory systems in allopolyploids

Over 70% of angiosperms are polyploids, mostly allopolyploids, including wheat, canola, oats, cotton, tobacco and oilseed rape, some of the world's most important crops. The significant levels of allopolyploidy suggest that species already had mechanisms for sorting homologous and homoeologous chromosomes, leading to allopolyploid fertility (Martín et al., 2017). Mechanisms regulating chromosomal pairing were identified in several allopolyploid species. A key study by (Sears, 1976)Sears (1976) pointed out that homoeologous pairing at MI is suppressed by the *Ph1* locus, increasing karyotypic stability and acting as a pairing regulator in wheat. Similar evidence has been reported for *Avena sativa* (Gauthier & McGinnis, 1968), *Festuca arundinacea* (Jauhar, 1975), *B. napus* (Jenczewski et al., 2003), and *Oryza sativa* (Nonomura et al., 2006). Moreover, a relevant indicator for the presence of pairing control genes (PCG) is the mendelian segregation of polymorphic meiotic behaviors, e.g., in *B. napus* (Jenczewski et al., 2003), *Lolium perenne* (Armstead et al., 1999; Evans & Davies, 1985), and *Festuca apennina* (Thomas, 1987).

When PCGs are present in wheat (Holm, 1986; Holm & Wang, 1988) and *Lolium* hybrids (Jenkins, 1985), the proportion of multivalents at zygotene is lower indicating that the PCGs affect the assembly of initial synapsis and correct SCs among homoeologues and that more than one gene contributes to allopolyploids' diploidization. Indeed, some chromosomes implicated in the homoeologous pairing regulation have been identified in *Avena*, *Lolium*, *Festuca*, and *Brassica* (Mason & Wendel, 2020).

Two important hypotheses have been put forward regarding the origin and evolution of pairing regulators in allopolyploids: (i) alleles suppressing homoeologous recombination already existed in diploid progenitors at low frequencies. These pairing control alleles could be transmitted to the new allopolyploid, enhancing homologous bivalent pairing and fertility [153], (ii) at the time of allopolyploid formation, mutations suppressing homoeologous pairing could have arisen (Jenczewski & Alix, 2004). So far, none of these hypotheses has been supported by direct evidence, and we may also hypothesize that pairing control systems evolved from a combination of evolutionary scenarios, leading to cumulative suppression of homoeologous pairing (Grusz et al., 2017). Herein we will discuss genetic meiotic control in two allopolyploid species in which it has been thoroughly described.

### 2.12. Wheat

The domesticated wheat (*Triticum aestivum*) is an allohexaploid, originated 500,000 years ago from the hybridization of two diploid species, *T. urartu* (AA) and an unknown *Aegilops* species (BB), generating a tetraploid wheat (*T. dicoccoides*;  $2n = 4x = 24$ ; AABB), followed by domestication into *T. dicoccum* and *T. turgidum*. Later on, 10,000 years ago, *T. turgidum* hybridized with *A. tauschii* (DD) forming the allohexaploid wheat ( $2n = 6x = 42$ ; AABBDD; see (Matsuoka, 2011). Each of the seven homologous chromosome pairs has a corresponding homoeologue within the other two genomes with similar gene order and content (Martín et al., 2017). Wheat behaves as a diploid with every chromosome synapsing and recombining only with its true homolog (for example, 1A pairs only with 1A, but not with 1B or 1 D). *Pairing*

*homoeologous 1 (Ph1)*, a dominant locus on the long arm of chromosome 5B identified by (Riley & Chapman, 1958; Sears & Okamoto, 1958) is primarily responsible for this phenotypic behavior. Rather than being passed down from a diploid ancestor, the *Ph1* locus is most likely to have originated during the polyploidization process. It was first discovered by scoring the MI phenotype of hexaploid wheat hybrids lacking the 5B whole chromosome, and this kind deletion mutant was found to control correct pairing in wheat and its hybrids (Holm & Wang, 1988; Prieto et al., 2004) and is assumed to inhibit homoeologous recombination (Dhaliwal et al., 1977).

Wheat and rye interspecific hybridization produce a hybrid consisted of haploid complements from both species. In the cultivar Chinese Spring (CS *ph1b*, Sears, 1976), a *Ph1* deletion mutant has been largely used in breeding programs. *Ph1* inhibits introgression by suppressing COs between homoeologous chromosomes. Nonetheless, the number of COs rises in *Ph1* mutant wheat-rye hybrids (Martín et al., 2014). Following that, further deletion mutants of the *Ph1* locus were created and studied (Al-Kaff et al., 2008; King et al., 2017; Roberts et al., 1999).

### 2.12.1. The *Ph1* locus

Combined cereal synteny and wheat BAC (Bacterial Artificial Chromosome) contigging, with MI analysis of mutants carrying deletions of chromosome 5B have been used for molecular characterizing the *Ph1* locus (Al-Kaff et al., 2008; Griffiths et al., 2006; Roberts et al., 1999). However, smaller deletions on 5B were characterized later, and the locus was found to be located in a 2.5 Mb region containing two *Ph1* candidate genes, namely *cdc2* (Griffiths et al., 2006) and *C-Ph1* (Bhullar et al., 2014).

According to (Griffiths et al., 2006)Griffiths et al. (2006), the *Ph1* locus is a region containing a cluster of *Cdk2-like* and *S-adenosyl methionine-dependent methyltransferase* (SAM-MTases) genes and a duplicated segment of heterochromatin from chromosome 3B. Within this heterochromatin segment, a gene formerly designated as *hypothetical 3 (Hyp3, UniProtKBQ2L3T5)*, which has been reannotated as *TaZIP4-B2 (UniProtKBQ2L3T5)* (Al-Kaff et al., 2008; Griffiths et al., 2006; Martín et al., 2017). Although the *ZIP4* copy on the 5B locus is dominant, the ancestral homoeologous *ZIP4* copies on 3A, 3B, and 3D are still expressed (Alabdullah et al., 2019; Griffiths et al., 2006).

A more detailed BAC library analysis by (Al-Kaff et al., 2008) al-kaff showed that the *Cdk-like* locus on chromosome 5 differs from the locus on chromosome 3 insofar as it harbors a segment of sub-telomeric heterochromatin. Furthermore, the Cdk-like cluster on 5B is different than the clusters on 5A and 5D, and sequencing analysis revealed tandem duplication events gave origin to these loci. Expression studies showed that the Cdk-like locus on chromosome 5B is dominant in transcription control over the analogous Cdk-like loci on chromosomes 5A and 5D, rendering the *Ph1* phenotype specific to 5B. Nonetheless, the overall transcription levels are not affected by the deletion of the Cdk-like locus on 5B, since the genes located on chromosome 5A and 5D can compensate the transcription levels.

The *Ph1* locus stabilizes polyploidy in wheat by controlling the accuracy of homologous synapsis and regulating CO formation (Martín et al., 2014). Early in meiosis, *Ph1* promotes synapsis between homologous chromosomes. In wheat, chromosomes assume a telomere bouquet arrangement where homologous and homoeologous are sorted, independently of *Ph1* (Martín et al., 2014). During the telomere bouquet only synapsis between homologous chromosomes can occur in hexaploid wheat. However, in the absence of

*Ph1*, homologous synapsis is less efficient, with more overall synapsis occurring after the telomere bouquet has dispersed, when homoeologous synapsis can occur. This non-specific synapsis between homoeologs leads to the low level of multivalents and univalents observed at MI in wheat lacking *Ph1*, indicating that, during the telomere bouquet stage, meiocytes from wheat and wheat-rye hybrids, with and without *Ph1*, exhibit significant differences in the level of synapsis and chromatin structure, implying that homoeologous synapsis is independent of *Ph1* (Martín et al., 2014, 2017, 2018). Importantly, this observation led to the idea that *Ph1* may promote homologous synapsis rather than prevent homoeologous synapsis.

*Ph1*'s influence on synapsis is mostly likely due to a change in chromatin structure produced by the Cdk-like and SAM-MTase cluster (M. D. Rey et al., 2017). Cdk2 has been found to have a role in histone H1 phosphorylation, replication, chromatin condensation and homoeologues' synapsis (Krasinska et al., 2008; Viera et al., 2009). The Cdk2 kinase is essential for meiosis and phosphorylates a variety of targets (Cohen et al., 2006; Marston & Amon, 2004); during early meiosis, it co-localizes with mismatch repair proteins to form recombination nodules and telomere regions (Knight et al., 2010). Through histone phosphorylation and chromatin remodeling Cdk2 has been implicated in licensing replication origins (Alexandrow & Hamlin, 2005). Additionally, in both the presence and absence of *Ph1*, increased histone H1 CDK2-dependent phosphorylation is related to the effect of *Ph1* on synapsis during CO (Greer et al., 2012). Altered phosphorylation affects chromatin structure and delay pre-meiotic replication, affecting homologous synapsis and thus allowing homoeologous synapsis to occur (Greer et al., 2012; Martín et al., 2017). In *Arabidopsis* lines carrying mutations in the *Ph1CDK2*-like homologs also show reduced synapsis under particular circumstances, implicating these genes in efficient synapsis (Zheng et al., 2014). Also, the treatment with okadaic acid, an inhibitor of phosphatase activity, enhances Cdk2-type phosphorylation and phenocopies the *ph1b* allele by inducing COs (Knight et al., 2010).

The second effect of *Ph1* occurs later in meiosis, affecting CO formation levels and the progression of MLH1 sites to Cos, according to immunolocalization analysis using the MLH1 DNA mismatch repair protein (Martín et al., 2014). MLH1 is necessary to resolve DHJ into COs and is part of the primary class I CO route in plants (Mézarad et al., 2007) and is required to resolve DHJ as COs. All MLH1 sites on synapsed chromosomes become COs in plants (Ashley et al., 2001; Lhuissier et al., 2007). However, whether *Ph1* is present or not, similar numbers of MLH1 sites are detected in wheat-rye hybrids. The presence of *Ph1* inhibits MLH1 sites from progressing to COs by inhibiting recombination (Martín et al., 2014). On the other hand, its absence allows one-third of MLH1 sites to proceed to COs, indicating that it plays a role in homoeologous MLH1 site resolution. Irrespective of *Ph1*, in hexaploid wheat, similar numbers of MLH1 sites are found on synapsed chromosomes at diplotene, but only when *Ph1* is present the number of COs matches the number of MLH1 sites. As a result, the CO level in *Ph1*-deficient wheat and its hybrids is lower than expected.

### 2.12.2. The *ZIP4* gene

In both *Arabidopsis* and rice, *ZIP4* has been shown to have a major effect on homologous COs, but not on synapsis, in contrast to *Ph1* (Chelysheva et al., 2007; Shen et al., 2012). Knockouts of this gene in diploids usually result in sterility, as the elimination of homologous COs leads to pairing failure and incorrect segregation at late MI. Thus, it seems more likely that *ZIP4* is involved in the *Ph1* influence on CO formation. Increased *ZIP4* gene dosage may bias recombination toward homologues rather than homoeologues (M. D. Rey et al., 2017).

According to bioinformatics studies, in certain polyploid plant lineages, meiotic recombination genes are the fastest to return to a single copy state, which is thought to be a rapid response for adapting meiotic recombination post whole-genome duplication (Blanc & Wolfe, 2004; A. H. Lloyd et al., 2014; Sidhu et al., 2017). This is the opposite effect of *ZIP4*, which has a novel dominant copy. Therefore, the stabilization process upon the polyploidization of wheat is assumed to be involved in rapid changes in the content and expression of the genes on homoeologues. This process would facilitate the correct pairing and synapsis of homoeologues.

The evolution of *Ph1* during *Triticum* polyploidization likely explains why wheat has maintained a similar gene content and balanced expression of its homoeologous groups. It's until unclear how meiosis has adapted to cope with allopolyploidy in other plants. However, it has been hypothesized that a reduction in the copy number of meiotic genes (MG) may stabilize the meiotic process after polyploidization (Gonzalo et al., 2019; A. H. Lloyd et al., 2014). Though, in wheat, the presence of *Ph1* is more likely to have enabled the retention of multiple copies of MGs as a strategy to ensure correct chromosome segregation (Alabdullah et al., 2019). The discovery of the *TaZIP4* gene as a candidate for the effect of the *Ph1* locus on recombination implicates more *TaZIP4* in meiosis than originally suspected from studies with model systems (Chelysheva et al., 2007; Shen et al., 2012).

Finally, *ZIP4* has been proposed to act as a scaffold protein containing tetratricopeptide repeats (TPRs), facilitating the assembly of protein complexes and promoting homologous COs (Chelysheva et al., 2007; de Muyt et al., 2018; Shen et al., 2012).

A co-expression gene network comparative analysis of meiosis-specific genes has shown that the three *TaZIP4* homoeologues 3A, 3B, and 3D (*TaZIP4-A1*, *TaZIP4-B1* and *TaZIP4-D1*) formed a cluster and were connected to many orthologs of MGs with different functions (Alabdullah et al., 2019). The *TaZIP4* copy on 5B (*TaZIP4-B2*), responsible for the *Ph1* phenotype, did not cluster with the *ZIP4* from the group 3 chromosome, given its different expression profile compared to the other homoeologues and its expression in most tissues (Martín et al., 2017, 2018; M.-D. Rey et al., 2018).

The stabilizing effects of the meiotic gene *TaZIP4-B2* were explored by alabduala (Alabdullah et al., 2021). The removal of *TaZIP4-B2* via CRISPR resulted in 56% of meiocytes exhibiting meiotic irregularities at MI, chromosome mis-segregation at AI, and 50% of tetrads with micronuclei. A hexaploid wheat mutant (*ph1b*) with a 59.3 Mb deletion covering *TaZIP4-B2* shows a comparable amount of disruption, with 56% of meiocytes displaying meiotic irregularities. Given the existence of three additional *ZIP4* copies in the wheat genome, the emergence of a meiotic pairing and CO phenotype resulting in decreased fertility with loss of a single copy of *ZIP4* was unexpected. The *TaZIP4-B2* copy enhances homologous pairing, synapsis, and CO whilst repressing homoeologous COs. Because of the TPR difference between *TaZIP4-B2* and *TaZIP4-B1*, the hexaploid wheat *TaZIP4-B2* phenotypes are most likely the effect of a reduction in the normal functions of group 3 *ZIP4*s (*TaZIP4-A1*, *TaZIP4-B1* and *TaZIP4-D1*). *TaZIP4-B2* is expected to compete with group 3 *ZIP4*s, for loading into meiotic chromosomes due to its early and 3-fold higher expression relative to group 3 (M. D. Rey et al., 2017).

The elongation of the chromosomal axis during meiosis (Prieto et al., 2004) and the interaction of *ZIP4* protein on these axes producing "pairing bridges" between homologues are believed to be involved in *TaZIP4-B2*'s facilitation of homologous pairing. Homologue alignment and pairing are delayed during early meiosis if the degree of homologue elongation differs (Colas et al., 2008). The cohesion protein REC8 is needed for proper meiotic chromosome conformation as well as chromosomal axis elongation via ASY1 assembly (Ding

et al., 2016; Golubovskaya et al., 2006). ZIP4 is found near the end of chromatin regions linked with REC8 (Shen et al., 2012). The simplest explanation for TaZIP4-B2's capacity to promote homologous pairing is that it reduces homologue elongation, resulting in more comparable conformations and permitting fast attachment of ZIP4 foci, thereby lowering the likelihood of homoeologous pairing later in meiosis (Martín et al., 2014, 2017; Prieto et al., 2004).

The interaction between ZIP4 copies on chromosome 5B and on chromosomal group 3 is believed to be the cause of TaZIP4-B2's inhibition of homoeologous COs. As in other species, group 3 ZIP4s are predicted to handle 85% of homologous COs (Chelysheva et al., 2007; Shen et al., 2012). Given the number of COs found in wheat haploids missing TaZIP4-B2 (Jauhar, 1999), they are also expected to process homoeologous CO activity. The divergent TaZIP4-B2 copy, on the other hand, exhibits some homologous CO activity but no homoeologous CO activity (M.-D. Rey et al., 2018). As a result, the presence of TaZIP4-B2 with wheat group 3 ZIP4s in chromosomal foci that assemble CO proteins, including MLH1, indicates that only homologous CO, not homoeologous CO, is effectively processed (Martín et al., 2014, 2018; M. D. Rey et al., 2017).

The TaZIP4-B2 deletion decreases homologous CO, which leads to an increase in meiotic irregularities at MI (M.-D. Rey et al., 2018). This shows that TaZIP4-B2 enhances homologous Cos and implies that the ZIP4 impact on homologous CO might be dose-dependent.

### 2.12.3. Ph2

Ph2 located on the short arm of chromosome 3D (3DS) (Mello-Sampayo, 1971; Mello-Sampayo and Lorente, 1968; Upadhyya and Swaminathan, 1967) and another suppressor of smaller magnitude located on the short arm of chromosome 3A (3AS) (Driscoll, 1972; Mello-Sampayo and Canas, 1973). The Ph2 gene is more Ph2 located on the short arm of chromosome 3D (3DS) (Mello-Sampayo, 1971; Mello-Sampayo and Lorente, 1968; Upadhyya and Swaminathan, 1967) and another suppressor of smaller magnitude located on the short arm of chromosome 3A (3AS) (Driscoll, 1972; Mello-Sampayo and Canas, 1973). The Ph2 gene is more Ph2 located on the short arm of chromosome 3D (3DS) (Mello-Sampayo, 1971; Mello-Sampayo and Lorente, 1968; Upadhyya and Swaminathan, 1967) and another suppressor of smaller magnitude located on the short arm of chromosome 3A (3AS) (Driscoll, 1972; Mello-Sampayo and Canas, 1973). The Ph2 gene is more Ph2 located on the short arm of chromosome 3D (3DS) (Mello-Sampayo, 1971; Mello-Sampayo and Lorente, 1968; Upadhyya and Swaminathan, 1967) and another suppressor of smaller magnitude located on the short arm of chromosome 3A (3AS) (Driscoll, 1972; Mello-Sampayo and Canas, 1973).

The *Ph2* locus was attributed to chromosome 3D by (Mello-Sampayo, 1968, 1971) who reported multivalent formation at MI in the absence of chromosome 3D in pentaploid hybrids between *T. aestivum* and *T. durum* and *T. aestivum* and *Aegilops*. Since then, two *Ph2* mutants have been discovered: an X-ray induced mutant with a substantial deletion (Sears, 1982) and the EMS-induced mutant *ph2b* [197]. The *Ph2* phenotype was investigated using both mutants, and the locus was narrowed down to 80 Mb located on the terminal portion of the short arm of 3D (S3D), according to the synteny in the analyzed wheat and rice regions (Sutton et al., 2003). (Svačina et al., 2020) svacina studies reported that this loss encompasses roughly 125 Mb of the short arm of chromosome 3D. The identification of a number of

potential meiotic genes on 3DS has come from researches aiming at *Ph2* identification. Some of them are the genes WM1 (Ji & Langridge, 1994; Whitford, 2002), WM3 (Letarte, 1996), WM5 (Dong et al., 2005) and TaMSH7 (Dong et al., 2002; A. H. Lloyd et al., 2007). Despite these efforts, the region is too large to conclusively allow the *Ph2* causal sequence. The EMS-induced *ph2b* mutant (Wall et al., 1971), which has a point mutation at *Ph2* locus provides a hope for finding the candidate sequence (Serra et al., 2021).

The *Ph2* locus differs from *Ph1*, having less influence on homologues pairing in wheat (Benavente et al., 1998; Martinez et al., 2001). Both (Martinez et al., 2001) Martinez and (Sánchez-Morán et al., 2001) Sánchez moran noticed no discernible effect on homoeologous chiasmata when *Ph1* is present but *Ph2* is absent, with the exception of an increase univalents. (Sears, 1977, 1982) sears 1977 1982 had previously demonstrated that in wheat and closely similar species-hybrids, a moderate incidence of homoeologous chiasmata occurred in the absence of *Ph2* but in the presence of *Ph1*. In the case of wheat-rye hybrids lacking the *Ph2* locus, (Prieto et al., 2005) also found a moderate amount of homoeologous chiasmata; nevertheless, chromosomal associations exclusively occur between wheat chromosomes, whereas chromosome associations in wheat-rye hybrids are infrequent. When homologues are present, *Ph2* has a reduced functional role; it may, however, inhibit connections between homoeologues in the absence of homologues. Furthermore, *Ph2* is not involved in the identification of homologues but instead impacts the development of synapsis (Martinez et al., 2001; Prieto et al., 2005). As highlighted by (Boden et al. 2009) 211 studies, interaction between *Ph1* and *Ph2* should not be overlooked.

Comparative genetics was performed by (Sutton et al., 2003) Sutton to investigate the potential genes implicated in the *Ph2* phenotype; however, no candidate responsible for a mutant phenotype equivalent to the *ph2a* was found. Single nucleotide polymorphism (SNP) based-genotyping and exome analysis with the goal of accurately delineating the *ph2a* deletion breakpoint were performed and the *Ph2* locus was found to be within a 14.3 Mb genomic gap, and 24 genes were discovered within the deleted region. The gene TraesCS3D02G119400 coding for a DNA mismatch repair protein (TaMSH7-3D) was found in the 14,3 Mb interval: it has 17 exons and 16 introns with a total length of 9747 bp (Serra et al., 2021).

On the basis of RNA-seq data analysis, TaMSH7-3D is expressed in anthers at PI. Together with TaMSH7-3A and 3B homoeologues, TaMSH7-3D is expressed throughout PI, lending support to a function for TaMSH7-3D in homoeologous recombination regulation (Alabdullah et al., 2019). TaMSH7 (*MutS* homologue 7) is a DNA mismatch repair (MMR) family member found only in plants. These highly conserved proteins are critical for genome integrity because they ensure the first stage of the MMR pathway (Reyes et al., 2015). In a hexaploid wheat x *Aegilops variabilis* hybrid, the lack of functioning TaMSH7-3D causes a 5.5-fold increase in CO frequency and is thought to play function in recombination partner selection (homologous vs. homoeologous) by increasing the instability of homoeologous recombination. MMR proteins have been shown to have a role in detecting mismatches in heteroduplex DNA (after DNA strand exchange) and encouraging the dissociation of invading strand DNA, a process known as heteroduplex rejection (Chakraborty & Alani, 2016). MSH7 may also play a role in limiting ectopic recombination, a cause of highly deleterious chromosomal rearrangements in diploid species, and could potentially provide an immediate advantage to newly allopolyploids by ensuring meiotic stability and, as a result, fertility, in newly formed allopolyploids. The discovery of TaZIP4-B2 and TaMSH7-3D, the two major genes governing homoeologous recombination in bread wheat, opened up the possibility of understanding their action and interactions. TaZIP4-B2 promotes homologous bivalent formation by preventing recombination between homoeologous chromosomes from

generating COs, according to new research from the ‘G. Moore group’ (Martín et al., 2014, 2017). TaMSH7-3D and TaZIP4-B2 may operate sequentially with distinct modes of action, implying that homoeologous recombination in polyploid bread wheat is a multilayered mechanism. Sears (1976) revealed that *Ph1* is twice as strong as *Ph2*, and that these changes have an additive impact in increasing homoeologous recombination, as seen in wheat x *Aegilops* hybrids (Ceoloni & Donini, 1993). Combining TaZIP4-B2 and TaMSH7-3D mutations may thus provide a way to increase the effectiveness and simplicity of introducing wild related chromosomal regions into wheat, allowing for the production of genetically distinct and attractive wheat cultivars (Serra et al., 2021).

### 2.13. Brassica and the prevalence of bivalent pairing

The Brassiceae is one of the most morphologically distinct tribes within the Brassicaceae family (Cruciferae). It is a monophyletic group of species has undergone a whole-genome triplication [215]. Extensive chromosome rearrangements, including fusions and/or fissions, resulted in chromosome number variation for the three diploid *Brassica* species, *B. nigra* (BB;  $2n = 16$ ), *B. oleracea* (CC;  $2n = 18$ ), and *B. rapa* (AA;  $2n = 20$ ) (Lysak et al., 2005). Subsequent spontaneous hybridization between the ancestors of these three diploid species, followed by chromosome doubling (Nagaharu, 1935), introduced an additional layer of duplication within the genomes of the three allotetraploids, *B. juncea* (AABB;  $2n = 36$ ), *B. napus* (AACC;  $2n = 38$ ) and *B. carinata* (BBCC;  $2n = 34$ ). Alignment of the A- and C-genome of *B. napus* allowed identification of regions with primary homoeology (i.e., regions from the A and C genomes that share a recent common ancestry) (Inaba & Nishio, 2002).

Natural euploid *B. napus* (AACC,  $2n = 38$ ) exhibits predominantly 19 bivalents at MI, with a preference for homologous chromosome pairing and disomic inheritance. In the resynthesized *B. napus*, preferential CO formation between homologues was reported as an immediate response to polyploidization and a clear predominance of bivalent formation, with 80–85% of pollen mother cells (PMCs) exhibiting 19 bivalents (Attia & Röbbelen, 1986; Inomata, 1980).

However, not all resynthesized *B. napus* bivalents are formed between homologues. Some allosyndetic bivalents between A and C homoeologues were observed (Inaba & Nishio, 2002), and these bivalents are formed in two ways: through regions of intra- or intergenomic homology, which arose by whole-genome duplications in the common ancestor of *B. rapa* and *B. oleracea* (Lysak et al., 2005; I. A. P. Parkin et al., 2003); or through homoeologues carrying segmental duplications that occurred after the polyploidy events (I. A. P. Parkin et al., 2005; T. J. Yang et al., 2006). Univalents and multivalents were also observed in resynthesized plants, confirming that meiotic behavior was not fully diploidized. Therefore, in comparison, to natural *B. napus*, the irregular meiosis of resynthesized *B. napus* generates a higher proportion of homoeologous exchanges generating HNRTs (I. A. Parkin et al., 1995; Udall et al., 2005).

Notably, (Jenczewski et al., 2003) Jenczewski et al. 2003 showed that the distribution of the number of univalents among haploids was consistent with the segregation of a biallelic gene, *Pairing regulator in B. napus (PrBn)*, against a background of polygenic variation. This study reported a high level (75%) and of 2 to 3 bivalents in the haploid varieties Darmor-bzh and Yudal, respectively, resulting from both auto- and allosyndesis within and between the A and C genomes of oilseed rape. In *B. oleracea* and *B. rapa* the pairing of two homoeologues originating from the same genome (autosyndesis) has been reported (K. C. Armstrong &



Keller, 1982) as a result of intragenomic duplications (Prakash, 1980; Schmidt et al., 2001). Previously, high-pairing haploids of oilseed rape exhibited meiotic behavior similar to those hybrids between *B. rapa* x *B. oleracea* (Attia & Röbbelen, 1986). In other words, these haploids provide evidence that the differences between the high- and low-pairing haploids are genetically controlled [146].

### 2.13.1. PrBn molecular characterization and function

Following Jenczewski et al. (2003) report, new insights into the genetic architecture of *PrBn* showing that the hereditary components of homoeologues pairing are polygenic were provided (Z. Liu et al., 2006). Using molecular markers, namely RAPD and AFLP, one linkage group of ~70 cM was identified in which the *PrBn* locus was mapped (10–20 cM interval) on a linkage group designated DY15 attributed to chromosome C9. Also, 3 to 6 minor quantitative trait loci (QTL), on C1 and C6, have minor additive effects on the number of univalents but do not seem to interact with *PrBn*. A further 2–3 loci that interact epistatically with *PrBn* were also detected.

In *B. napus*, recurrent polyploidy has driven extensive variation in the determinants of CO suppression between homoeolog. The natural variation in meiotic behavior among *B. napus* allohaploids is consistent with the segregation of two *PrBn* alleles, which is the expected composition resulting from a *B. napus* double origin.

The current understanding of CO variation in *B. napus* is based on cytological observations at MI and on genetic surveys of intergenomic exchanges in the *B. napus* allohaploids progenies. (Nicolas et al., 2009) Nicolas 2009 discovered that the *PrBn* locus (and the genes it interacts with) control the frequency, but not the distribution of COs between homoeologues in *B. napus* haploids, and between homologues during meiosis of triploid ArAnC (Ar = *B. rapa*; An = *B. napus*) hybrid plants. The threefold difference in the number of COs formed between homoeologues is the causal of the meiotic behaviors observed in Darmor-bzh (high-pairing) and Yudal (low-pairing) haploids. Given that, the action of *PrBn* and the genes with which it interacts genetically determines these two meiotic phenotypes. It was concluded that these loci influence recombination between homoeologues; however, *PrBn* does not affect the level of homologous recombination in tetraploid ArAnCC hybrids, suggesting that its effect on recombination depends on the background karyotype.

Although the exact origin of the karyotypic influence on CO variation is uncertain, at least two ideas have been presented proposed. Firstly, it was proposed a *PrBn* dosage effect on the *B. napus* C genome. One copy of the gene(s) carried by the Yudal C genome would lead to fewer COs than one copy of the gene(s) carried by the Darmor-bzh C genome, but two copies of gene(s) carried by the C genomes would provide the same numbers of COs (Cifuentes, Eber, et al., 2010; Cui et al., 2012; Jenczewski et al., 2003; Nicolas et al., 2009). Dosage effects have been shown to be common among the genes regulating chromosome pairing and recombination in polyploids (Mason & Wendel, 2020; Pecinka et al., 2012), including *Brassica* (Mason et al., 2010, 2011). Secondly, the presence of chromosomes that remain unpaired during meiosis (in haploids and triploids, but less frequently in tetraploids) may trigger genotype-dependent changes in the progression/completion of meiotic steps (Carlton et al., 2006; Martinez-Perez & Moore, 2008).

Synthetic *Brassica* allohexaploids (Gaebelein & Mason, 2018) and allotetraploids (Prakash et al., 1999) have long been known to be meiotically unstable, and synthetic *B. napus* is often extremely unstable, putatively due to the close relationship between the A and

C genomes (K. Song et al., 1995; Szadkowski et al., 2010; Xiong et al., 2011). In contrast, natural allotetraploid species *B. juncea*, *B. carinata*, and *B. napus* are fully stable and fertile. More recently, Tian et al. (2010) produced *B. rapa* × *B. carinata* allohexaploids exhibiting increased fertility and percentages of offspring with  $2n = 54$  up to the 4<sup>th</sup> generation using different genotype combinations. Also, (Zhou et al., 2016) Zhou 2016 found high fertility and stable breeding behavior in allohexaploids from *B. rapa* × *B. carinata* and *B. juncea* × *B. oleracea*, and lower fertility in allohexaploids from newly combined diploid genomes.

Fertility and meiotic stability in novel *Brassica* allohexaploids have been investigated for determining which factor could influence these traits and studies on homozygous (A2) and heterozygous (H2) allohexaploids showed a variation in fertility traits and meiotic configuration. For example, A2 displays low pollen fertility and a high level of chromosome loss, whereas in H2 high pollen fertility and an average of 49 chromosomes were found (Mwathi et al., 2017). The direction of unbalanced homoeologous exchanges (which subgenome was lost or duplicated, a potential mechanism for biased fractionation), loss or presence of univalent chromosomes, and inheritance of particular genomic regions from the allotetraploid parents have been all identified as major factors influencing the fertility and meiotic stability of novel allohexaploid hybrids. Replacing an A-genome fragment by a C-genome fragment was found to compromise fertility in allohexaploid hybrids and synthetic *B. napus*, bias in the directionality of translocations is a driving force for genome size reduction and biased fractionation, whereby gene copies from one subgenome are preferentially lost [241]. Interestingly, it has been proposed that a subgenome with a higher number of transposable elements is more likely to be lost in allopolyploids as a result of biased genome fractionation (Cheng et al., 2016; S. Liu et al., 2014; I. A. P. Parkin et al., 2014; Woodhouse et al., 2014). A preferential loss of the larger, transposable-element-rich C genome originated in *B. oleracea* has been shown to occur over evolutionary time (S. Liu et al., 2014; Schiessl et al., 2017; Q. Song & Chen, 2015).

### 2.13.2. *BnaPh1*

Higgins et al. (2021) are the first authors who described the *BnaPh1* locus. Established and resynthesized *B. napus* lines were compared to search for possible QTL that may influence mispairing and subsequent homoeologues' recombination in a segregating doubled-haploid (SGDH) population. The quantification of recombination events on the homoeologues allowed putative meiosis-specific genes to be identified.

A *B. napus* SGDH was used by Clarke et al. (2016) to generate a genomic map with 21,000 SNPs, and the *BnaPh1* (*B. napus* Pairing homoeologous 1) locus was mapped on chromosome BnaA9, this QTL explained 32–58 %, depending on the dataset, of the overall variance and two minor QTLs were positioned on the BnaA3 and BnaC7 chromosomes. With a length of 12.8 Mb, the BnaA9 QTL comprises the centromeric region; as expected, it exhibited low homologous CO rates and significant linkage disequilibrium.

Both *A. thaliana* and *B. napus* are cruciferous species; then, on the basis of those QTL locations, *A. thaliana* meiosis-related genes were investigated to search for orthologues in the *B. napus* genome. Reciprocal exchange, deletion/duplication, and synaptic partner switch QTLs on BnaA3, BnaA9, and BnaC7 were found to have 12 candidate genes (E. E. Higgins et al., 2021).

The RPA1C (Replication Protein A 1C) and MUS81 (MMS and UV Sensitive 81) are 2 of the 5 genes found to be associated with the BnaA9 QTL. RPA1C acts in double-strand break repair at early meiosis in *A. thaliana* (Aklilu et al., 2014). A further DNA repair protein implicated in the interference-free CO route is the endonuclease MUS81 (Berchowitz et al., 2007; J. D. Higgins et al., 2008). Researchers had previously exploited the BnaC9 copies of MUS81 and RPA1C in regard to the *PrBn* locus, but they found no significant differences in their expression between the respective high and low homoeologous pairing lines, leading them to conclude that neither genes were responsible for the *PrBn* phenotype (Blary, 2017). However, because the *BnaPh1* locus was mapped in allotetraploids rather than allohaploids, and because levels of meiotic transcription in wheat have been shown to be stable in the presence and absence of the *Ph1* locus (Martín et al., 2018), either MUS81 or RPA1C, or possibly an unidentified gene, could be responsible for the QTL discovered.

Other two smaller QTLs harboring 4 and 3 meiotic genes, respectively, one on BnaA3 and the other in the homologous region on BnaC7. MSH3, is one of the genes found on the minor QTLs, a homologue of the *MutS* gene, which controls mismatch repair in *E. coli* (Kunkel & Erie, 2005). In *A. thaliana*, six *MutS* homologues are present, MSH4 and MSH5 have recognized functions in meiotic recombination (J. D. Higgins et al., 2004, 2005), whereas MSH2, MSH3, MSH6, and MSH7 are crucial for DNA repair in *A. thaliana* (Culligan & Hays, 2000). MSH2 on chromosome C3 was one of the potential meiotic instability loci discovered by Gaebelein et al. (2019) 241 in *B. napus*, whereas, MSH7 has also been identified as a potential *Ph2* gene in wheat (Dong et al., 2002; A. H. Lloyd et al., 2007; Serra et al., 2021).

Gonzalo et al. (2019) 185 found that homologous recombination in *B. napus* allohaploids was reduced when MSH4 was reduced to one functional copy, while homologous recombination in allotetraploids was unaffected. Due to the low incidence of naturally occurring homoeologous recombination in *B. napus*, the effect of MSH4 decrease on the rate of homoeologous recombination in allotetraploids could not be established. This indicates either that *BnaPh1* is haplo-insufficient or that it does not specifically oppose the formation of early recombination intermediates and COs between homoeologues. Therefore, *BnaPh1* would rather help promote the maturation of recombination intermediates between the two homologues in the euploid lines, but it does not prevent COs between homoeologues in haploid lines (Sourdille & Jenczewski, 2021). This research suggests that lowering the number of functional gene copies for meiotic genes might be an essential evolutionary adaptation for polyploid meiotic stability.

The *PrBn* QTL was mapped to chromosome BnaC9 in segregating allohaploid lines (Z. Liu et al., 2006), interestingly the BnaC9 locus appears to be in a homoeologous region to the BnaA9 locus. The corresponding region for the *BnaPh1* locus in diploid *B. rapa* was explored to determine if genes present in the presumed progenitor had been deleted from *B. napus*, however there was no evidence of missing meiosis-related genes for this region (E. E. Higgins et al., 2021). As a result, the presence of meiotic controlling genes in homeologous regions could be attributed to the process of polyploidization, which results in the generation of paralogous genes. However further research on both QTLs is needed to support this hypothesis.

## 2.14. Meiotic proteins and crossover formation

Many proteins that have a role in CO formation have been identified (Boden et al., 2009; Chelysheva et al., 2007; Dubois et al., 2019; Martín et al., 2014). Since the study of (Riley & Chapman, 1958) Riley and Chapman (1958), how meiosis has adapted to deal with allopolyploidy has been deciphered only in wheat. A duplication of the *ZIP4* gene within the *Ph1* locus prevents maturation of COs between non-homologous chromosomes (Chelysheva et al., 2007; Martín et al., 2014; M. D. Rey et al., 2017; Riley & Chapman, 1958; Shen et al., 2012). The CO Class I or ZMM pathway includes a set of critical proteins in plants, such as MER3, MSH4, MSH5, SHOC1, HEI10, PTD, and ZIP4. The possible impact of genetic regulation on CO formation was illustrated by grandont (Grandont et al., 2014), whose findings showed that, during PI, the spatial-temporal localization of HEI10 is the same in *B. napus* euploids as in *A. thaliana* and rice (Chelysheva et al., 2012; Wang et al., 2012; Ziolkowski et al., 2017). Thus, the relocation of HEI10 in *B. napus* reflects the progressive formation of recombination intermediates in the ZMM CO pathway. This progression varies among genotypes. For instance, in Yudal the transition from early to late HEI10 occurs in earlier stages of PI compared to Darmor-bzh.

Both *Brassica* allohaploids (Darmor-bzh and Yudal) form distinct numbers of class I Cos, according to the immunolocalization of MLH1 I, suggesting that the progression of early meiotic recombination is essentially the same regardless of whether recombination intermediates are formed between homologues or homoeologues. Only a small fraction of HEI10 and MLH1 foci were found to be colocalized at diakinesis in *B. napus* allohaploids, whereas this was systematically found in euploids. As proposed for haploid *Arabidopsis* (Cifuentes et al., 2013) and hexaploid wheat (Martín et al., 2014), the ‘stand-alone’ MLH1 foci could mark the locations where COs eventually failed or occurred between sister chromatids. A fraction of late recombination intermediates may still be in the process of resolution at diakinesis in *B. napus* allohaploids, resulting in some HEI10 foci persisting longer than usual on chromosomes without producing the conditions required for MLH1 loading. Separate HEI10 and MLH1 loci may also reflect aberrant behavior of meiotic proteins, with MLH1 loading and off-loading irrespective of HEI10 (Grandont et al., 2014).

In *Brassica*, there was reduction in copy number for genes encoding MSH4, MSH5, MER3, and ZIP4 following independent WGDs, although SHOC1 and HEI10 showed higher duplicate retention rates. Higher HEI10 duplicate retention is consistent with the most widely accepted theory that explains the fate of gene duplicates post-WGD. MSH4 is essential to ensure normal CO numbers between homologous chromosomes, and is therefore required to ensure fertility. Normal levels of homologous CO mitigate against MSH4 gene duplicate loss; thus, CO formation between homologous chromosomes fluctuates in a dosage-sensitive manner. CO formation is at its maximum when all MSH4 copies are functional, and gradually decreases with the number of copies, approximating zero when all MSH4 copies are non-functional (Gonzalo et al., 2019).

Therefore, the modulation of the entire the ZMM pathway, or at least part of it, could contribute to meiotic stabilization in allopolyploids. It is unclear whether MSH4 and ZIP4 act on the same step of the ZMM pathway, or even whether their specific roles are conserved between species.

## 2.15. The consequences of meiosis for genetic mapping in auto- and allopolyploids

The use of genetic analysis in polyploids can be traced back to the work of Muller (1914), 263 who investigated data on the tetraploid *Primula sinensis* previously published by Gregory (1914), 264 and proposed the first polysomic segregation model. In the first half of the twentieth century, several authors addressed the complex inheritance patterns and genetic linkage properties in polyploid organisms (Dawson, 1941; de Winton & Haldane, 1931; B. A. FISHER & MATHER, 1940; Fisher, 1941; Fisher R. A., 1947; R. A. FISHER, 1954; R. A. FISHER & MATHER, 1942, 1943; Haldane, 1930; Lawrence, 1929; Mather, 1935, 1936). Although these studies offered key insights into polyploid inheritance theory, they were in practice limited to scarce morphological markers. A few traits were studied, such as color and shape of the stigma (Gregory, 1914; Muller, 1914), petal color (Lawrence, 1929), and style length (R. A. FISHER & MATHER, 1942). In addition to the low availability of these traits, the complexity of their segregation in experimental populations hindered application in real scenarios, which meant that linkage studies on polyploid species lagged behind studies on diploids. This situation eventually changed with the advancement of recombinant DNA technology in the early 1990s. Wu et al. (1992) 277 and Sorrells (1992) 278 proposed the use of single-dose (SD, or simplex) molecular markers based on restriction fragments to assess allelic variation in polyploids. SD markers display genetic polymorphisms in a single parental homologous chromosome (for example, Aaaa vs. aaaa in tetraploids). When present in one parent, the single variation results in a 1:1 segregation ratio. This approach allows standard diploid techniques to be used for linkage analysis and map construction. Since SD-based mapping does not depend on regular polyploid meiosis (Sorrells, 1992), it is to this day an extremely valuable technique, even after the development of modern genotyping technologies.

In allopolyploids, bivalent pairing between specific pairs of chromosomes will occur most of the time. Thus, there is no essential difference between the analytical linkage procedures for diploids and allopolyploids when constructing genetic maps. On the other hand, as stated earlier, chromosome pairing in autopolyploids is often unpredictable, and complex meiotic configurations can occur (Doerge & Craig, 2000). Three different types of autopolyploid chromosomal segregation have been proposed:

1. *random chromosome segregation* (Muller, 1914), where the gametes are formed by  $p/2$  homologous chromosomes selected from  $p$  chromosomes. For example, in an autotetraploid genotype where  $p = 4$ , the genotype ( $A_1, A_2, A_3, A_4$ ) can yield six different balanced gametes ( $A_1A_2, A_1A_3, A_1A_4, A_2A_3, A_2A_4, \text{ and } A_3A_4$ ) with same expected proportions of  $1/6$ .
2. *random chromatid segregation* (Haldane, 1930), where the gamete is formed by  $p/2$  homologous chromosomes selected at random from  $2p$  possible chromatids due to double reductional segregation. Thus, in addition to the heterozygous classes presented in the previous autotetraploid example, four extra homozygous types are expected ( $A_1A_1, A_2A_2, A_3A_3, A_4A_4$ ), with proportions of  $1/7$  for heterozygous classes and  $1/28$  for homozygous classes
3. *maximum equational segregation* (Mather, 1935, 1936): where a double-reduction coefficient ( $\alpha$ ) is used to regulate the proportion of extreme cases described in items 1 and 2 above.

**Table 1. Number of possible gametes for one locus with no double-reduction, and number of possible genotypes generated by their combination given even ploidy levels.**

Ploidy Level	Number of Gametes $\binom{p}{\frac{p}{2}}$	Number of Genotypes $\binom{p}{\frac{p}{2}}^2$
2	2	4
4	6	36
6	20	400
8	70	4900
10	252	63,504
12	924	853,776

The number of possible genotypes in a cross between two autopolyploid individuals with random chromosome segregation is given by the square of the number of gametes. Table 1 gives examples of gamete and genotype numbers in a biparental cross for different even ploidy levels. Note that a linear increment in the ploidy level results in a steep increment in the possible genotype numbers.

In recent years, most polyploid mapping studies have been based on SNPs identified through pre-assembled arrays or genotyping-by-sequencing (GBS) techniques (Bourke et al., 2015; Cappai et al., 2020; Hackett et al., 2013; Mollinari et al., 2020; van Geest et al., 2017). As a result of these techniques and the biallelic quantitative nature of these platforms, the high number of polyploid genotypic classes in Table 1 is expressed in terms of *dosages*. Thus, regardless of the 36 possible genotypic classes in tetraploid biparental populations, they are scored in up to five genotypic classes, i.e., AAAA, AAAa, AAaa, Aaaa, or aaaa. This means that when dosage-based markers are used, the multiple genotypes in a polyploid biparental cross collapse into a lower number of classes if biallelic markers are used (Figure 3).

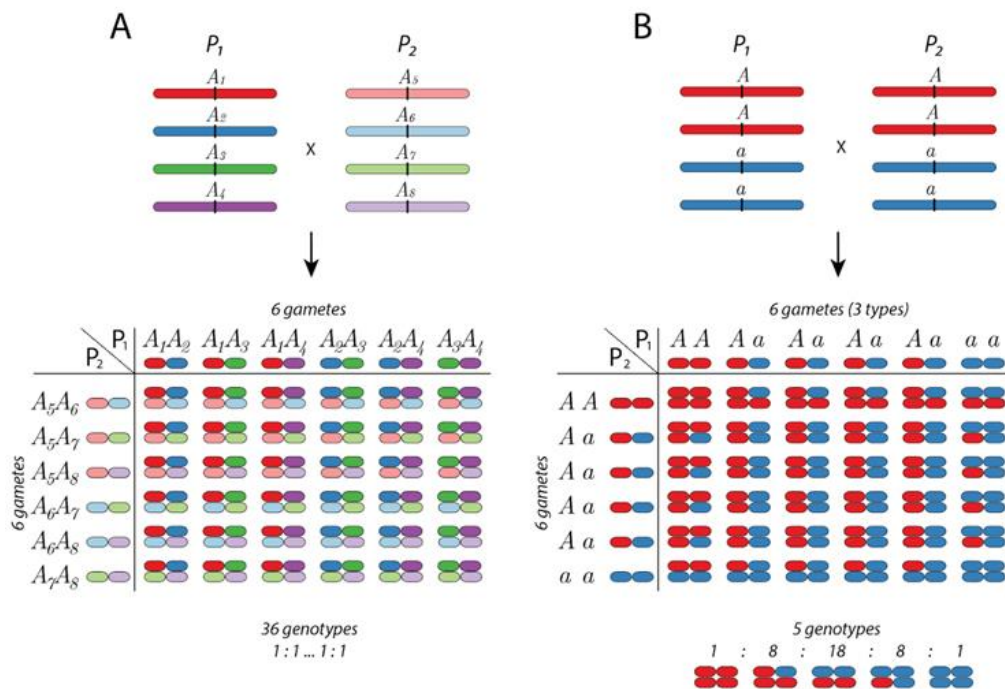


**Figure 2. Thirty-six possible genotypes in an autotetraploid cross.** A) Completely informative multiallelic scenario, in which all the genotypes formed by the combination of 6 gametes can be differentiated and segregated with equal probability. B) Biallelic scenario, in which both parents have two doses (duplex marker), in which case the genotypes collapse into five different classes segregating in a 1:8:18:8:1 ratio.

Several methods and computer programs have been implemented to convert quantitative molecular inputs into binary dosage markers (Clark et al., 2019; Gerard et al., 2018; Serang et al., 2012; Voorrips et al., 2011). The corresponding output produces dosage scores for SNPs along the genomes of all individuals in the population, used as the starting point for further genetic mapping analysis.

Genetic mapping in polyploid species began with the use of SD molecular markers (K. K. Wu et al., 1992). As a result, separate maps were generated, one for each homologous chromosome for each parent, i.e., the expected number of linkage groups is the basic chromosome number multiplied by the parent's ploidy level. A plethora of genetic maps was constructed using this approach in potato (Bourke et al., 2015; Li et al., 1998), sugarcane (Aitken et al., 2005, 2014; Al-Janabi et al., 1993; Garcia et al., 2006; Ming et al., 2002), sweet potato (Shirasawa et al., 2017; Yamamoto et al., 2019), strawberry (Hossain et al., 2019; Tennessen et al., 2014), rose (Rajapakse et al., 2001), and many other species. Some of these studies incorporated multiple-dose (MD) markers into a framework of SD-based maps. However, limitations in the genotyping technology and the complex nature of polyploid inheritance mean that the potential of MD markers cannot be fully exploited in a complete haplotypic inheritance analysis.

The use of multiple-dose markers in polyploid genetic mapping became more widespread with the advent of high-throughput DNA technologies, which allowed thousands of genomic positions to be assessed using SNPs. For a review of genetic analysis in polyploids using SD and MD markers [see (Bourke et al., 2018)]. In the following section, we describe two examples of polyploid maps constructed using the GBS approach. In the first, a sugarcane genetic map was built using exclusively SD markers. The second relates to the autohexaploid sweet potato, and involves the use of a variety of dosage-based markers to

build a multilocus genetic map. The sweet potato multilocus map facilitated a detailed study of the transmission patterns and meiotic characteristics of this complex hexaploid species.

## 2.16. Case studies

### *Sugarcane*

Sugarcane (*Saccharum* spp.) belongs to the Poaceae family and is a highly complex polyploid with a recent interspecific hybridization (D'Hont et al., 1998). Cultivated sugarcane was produced by crossing high sugar content species *S. officinarum* ( $2n = 80$ ,  $x = 10$ ) and *S. spontaneum* ( $2n = 40-128$ ,  $x = 8$ ), a wild species with high fiber content (Grivet et al., 2003). This cross resulted in the so-called *Saccharum* complex with ploidy levels varying from 5 to 16, often with aneuploidy (D'Hont et al., 1998; Garcia et al., 2013; Grivet & Arruda, 2002). Most of the sugarcane linkage maps to date were produced using SD markers, adding a few duplex and triplex markers (Aitken et al., 2005, 2014; Al-Janabi et al., 1993; Garcia et al., 2006; Guimarães et al., 1999; Ming et al., 2002). SD markers are usually the most practical choice for complex polyploid linkage studies because their inheritance is not affected by the ploidy type or level. Although they contain little or no information for assigning homolog chromosomes to homology groups, double SD markers (present in both parents, segregating 3:1 or 1:2:1) can be used to merge the genetic maps of both parents in a biparental population. Garcia et al. (2006) used double SD markers to integrate parental maps for a sugarcane population derived from a cross between two commercial varieties. The authors implemented a joint maximum likelihood method to build maps using simplex and double simplex markers. The double-simplex markers were used to establish linkages between simplex markers, integrating information from both parents into a joint map.

More recently, the introduction of platforms for genotyping by high-throughput DNA sequencing led to the construction of saturated genetic maps for sugarcane. Balsalobre et al. (2017) used GBS-based and gel-based SSR markers to build a single-dose map, subsequently mapping yield-related quantitative trait loci (QTL). After discovering the SNPs and performing genotype calling, the authors obtained 7,678 single-dose high-quality SNPs to build the genetic map. Nine hundred and ninety-three markers were positioned in the final linkage map and distributed over 223 linkage groups clustered in 18 homologous and homoeologous groups (HGs). (You et al., 2019) you 2019 used a 100K Affymetrix Axiom Sugarcane SNP array to genotype a full-sib family derived from the Green German and IND81-146 varieties, and a selfing population derived from CP80-1827. The maps obtained revealed higher numbers of markers than previous studies, ranging from 3482 mapped single-dose markers for the Green German parent to 536 for CP80-1827 [see Table 2 in (You et al., 2019)].

Although sugarcane genetic maps are becoming denser and covering higher fractions of this complex genome, the lack of high-quality multiple-dose markers precludes any appropriate assignment of homologs to homology groups. Other less complex species, such as potato, rose, blueberry, chrysanthemum and sweet potato have benefited from multiple markers, resulting in more effective QTL mapping and meiotic studies, as described in the following case study.



### *Sweet potato*

The hexaploid sweet potato (*Ipomea batatas* (L.) Lam.  $2n = 6x = 90$ ) is an important crop worldwide, serving as a staple food in several developing countries due to its high nutritional value (Loebenstein, 2009). It is a naturally occurring polyploid with two polyploidization events traced back to 0.8 and 0.5 million years ago (J. Yang et al., 2017). As observed by Gustafsson and Gadd (1965) 310 and Magoon et al. (1970), 311 meiosis in the cultivated sweet potato is regular, with a prevalence of bivalent formations and a constant hexaploid level. Thus, in contrast to sugarcane, the study of inheritance patterns is manageable using appropriate genomic tools and analytical pipelines. In common with sugarcane, the first genetic maps constructed for sweet potatoes were based on simplex markers, incorporating multiple-dose markers into the existing framework map built using simplex markers (Cervantes-Flores et al., 2008; Kriegner et al., 2003; Monden & Tahara, 2017; Shirasawa et al., 2017; Ukoskit & Thompson, 1997; Yamamoto et al., 2019).

Mollinari et al. (2020) used GBS-based SNP markers to study the inheritance system in a biparental hexaploid sweet potato cross between the Beauregard and Tanzania cultivars. The genomes of two related diploid sweet potatoes were used to anchor *I. trifida* and *I. triloba* SNPs. The authors obtained 30,684 high-quality markers, 60.7% simplex and double-simplex and 39.3% multiplex, combined with a recently developed algorithm to construct multilocus genetic maps in complex polyploids (Mollinari & Garcia, 2019). Due to the abundance of high-quality multiplex markers and novel mapping methods, they assembled an integrated map for both parents and phased homology groups for all parental homologous chromosomes. The resulting map indicated 96.5% and 83.1% collinearity between *I. batatas* and its diploid relatives *I. trifida* and *I. triloba*, respectively. The offspring's haplotypic composition was inferred in terms of the probability of inheritance of the parental homologous chromosomes, and several meiotic characteristics were investigated. The authors also found that 73.3% of the parents' meiotic configurations were resolved into bivalents, 15.7% into multivalent signatures, and 11.0% were inconclusive.

Moreover, the studied population exhibited vastly hexasomic inheritance mechanisms in all linkage groups, providing stable allele transmission. A similar analysis was also conducted on the tetraploid potato. The meiotic configuration estimated using the phased map strongly corroborated the results obtained using cytological techniques (da Silva Pereira et al., 2021), advantageous for evaluating meiosis by straight-forward extension of map construction.

## References

- Abraham, K.; Nemorin, A.; Lebot, V.; Arnau, G. Meiosis and Sexual Fertility of Autotetraploid Clones of Greater Yam *Dioscorea alata* L. *Genet. Resour. Crop Evol.* **2013**, *60*, 819–823, doi:10.1007/s10722-013-9973-4.
- Aitken, K.S.; Jackson, P.A.; McIntyre, C.L. A Combination of AFLP and SSR Markers Provides Extensive Map Coverage and Identification of Homo(Eo)Logous Linkage Groups in a Sugarcane Cultivar. *Theor. Appl. Genet.* **2005**, *110*, 789–801, doi:10.1007/s00122-004-1813-7.
- Aitken, K.S.; McNeil, M.D.; Hermann, S.; Bundock, P.C.; Kilian, A.; Heller-Uszynska, K.; Henry, R.J.; Li, J. A Comprehensive Genetic Map of Sugarcane That Provides Enhanced Map Coverage and Integrates High-Throughput Diversity Array Technology (DArT) Markers. *BMC Genom.* **2014**, *15*, 152, doi:10.1186/1471-2164-15-152.
- Aklilu, B.B.; Soderquist, R.S.; Culligan, K.M. Genetic Analysis of the Replication Protein A Large Subunit Family in *Arabidopsis* Reveals Unique and Overlapping Roles in DNA Repair, Meiosis and DNA Replication. *Nucleic Acids Res.* **2014**, *42*, 3104–3118, doi:10.1093/nar/gkt1292.
- Alabdullah, A.K.; Borrill, P.; Martin, A.C.; Ramirez-Gonzalez, R.H.; Hassani-Pak, K.; Uauy, C.; Shaw, P.; Moore, G. A Co-Expression Network in Hexaploid Wheat Reveals Mostly Balanced Expression and Lack of Significant Gene Loss of Homeologous Meiotic Genes Upon Polyploidization. *Front. Plant Sci.* **2019**, *10*, 1–24, doi:10.3389/fpls.2019.01325.
- Alabdullah, A.K.; Moore, G.; Martín, A.C. A Duplicated Copy of the Meiotic Gene ZIP4 Preserves up to 50% Pollen Viability and Grain Number in Polyploid Wheat. *Biology* **2021**, *10*, 290, doi:10.3390/biology10040290.
- Alexandrow, M.G.; Hamlin, J.L. Chromatin Decondensation in S-Phase Involves Recruitment of Cdk2 by Cdc45 and Histone H1 Phosphorylation. *J. Cell Biol.* **2005**, *168*, 875–886, doi:10.1083/jcb.200409055.
- Al-Janabi, S.M.; Honeycutt, R.J.; McClelland, M.; Sobral, B.W.S. A Genetic Linkage Map of *Saccharum spontaneum* L. “SES 208.” *Genetics* **1993**, *134*, 1249–1260, doi:10.1093/genetics/134.4.1249.
- Al-Kaff, N.; Knight, E.; Bertin, I.; Foote, T.; Hart, N.; Griffiths, S.; Moore, G. Detailed Dissection of the Chromosomal Region Containing the Ph1 Locus in Wheat *Triticum aestivum*: With Deletion Mutants and Expression Profiling. *Ann. Bot.* **2008**, *101*, 863–872, doi:10.1093/aob/mcm252.
- Anderson, L.K.; Stack, S.M. Recombination Nodules in Plants. *Cytogenet. Genome Res.* **2005**, *109*, 198–204, doi:10.1159/000082400.
- Armstead, I.P.; Bollard, A.; King, I.P.; Forster, J.W.; Hayward, M.D.; Evans, G.M.; Thomas, H.M. Chromosome Pairing in *Lolium perenne* × *L. Temulentum* Diploid Hybrids: Genetic and Cytogenetic Evaluation. *Heredity* **1999**, *83*, 298–303, doi:10.1038/sj.hdy.6885730.
- Armstrong, K.C.; Keller, W.A. Chromosome Pairing in Haploids of *Brassica oleracea*. *Theor. Appl. Genet.* **1982**, *24*, 49–52, doi:10.1007/BF00275776.
- Armstrong, S.J.; Caryl, A.P.; Jones, G.H.; Franklin, F.C.H. Asy1, a Protein Required for Meiotic Chromosome Synapsis, Localizes to Axis-Associated Chromatin in *Arabidopsis* and *Brassica*. *J. Cell Sci.* **2002**, *115*, 3645–3655, doi:10.1242/jcs.00048.

- Armstrong, S.J.; Franklin, F.C.H.; Jones, G.H. Nucleolus-Associated Telomere Clustering and Pairing Precede Meiotic Chromosome Synapsis in *Arabidopsis thaliana*. *J. Cell Sci.* **2001**, *114*, 4207–4217, doi:10.1242/jcs.114.23.4207.
- Ashley, T.; Walpita, D.; De Rooij, D.G. Localization of Two Mammalian Cyclin Dependent Kinases during Mammalian Meiosis. *J. Cell Sci.* **2001**, *114*, 685–693.
- Attia, T.; Röbbelen, G. Meiotic Pairing in Haploids and Amphidiploids of Spontaneous versus Synthetic Origin in Rape, *Brassica napus* L. *Can. J. Genet. Cytol.* **1986**, *28*, 330–334, doi:10.1139/g86-049.
- Avivi, L.; Feldman, M. Arrangement of Chromosomes in the Interphase Nucleus of Plants. *Hum. Genet.* **1980**, *55*, 281–295, doi:10.1007/BF00290206.
- Balsalobre, T.W.A.; da Silva Pereira, G.; Margarido, G.R.A.; Gazaffi, R.; Barreto, F.Z.; Anoni, C.O.; Cardoso-Silva, C.B.; Costa, E.A.; Mancini, M.C.; Hoffmann, H.P.; et al. GBS-Based Single Dosage Markers for Linkage and QTL Mapping Allow Gene Mining for Yield-Related Traits in Sugarcane. *BMC Genom.* **2017**, *18*, 72, doi:10.1186/s12864-016-3383-x.
- Bass, H.W.; Marshall, W.F.; Sedat, J.W.; Agard, D.A.; Cande, W.Z. Telomeres Cluster De Novo before the Initiation of Synapsis: A Three-Dimensional Spatial Analysis of Telomere Positions before and during Meiotic Prophase. *J. Cell Biol.* **1997**, *137*, 5–18, doi:10.1083/jcb.137.1.5.
- Bass, H.W.; Riera-Lizarazu, O.; Ananiev, E.V.; Bordoli, S.J.; Rines, H.W.; Phillips, R.L.; Sedat, J.W.; Agard, D.A.; Cande, W.Z. Evidence for the Coincident Initiation of Homolog Pairing and Synapsis during the Telomere-Clustering (Bouquet) Stage of Meiotic Prophase. *J. Cell Sci.* **2000**, *113*, 1033–1042, doi:10.1242/jcs.113.6.1033.
- Benavente, E.; Orellana, J.; Fernández-Calvín, B. Comparative Analysis of the Meiotic Effects of Wheat Ph1b and Ph2b Mutations in Wheat×rye Hybrids. *Theor. Appl. Genet.* **1998**, *96*, 1200–1204, doi:10.1007/s001220050857.
- Bennett, M.D. Centromere Arrangements in *Triticum aestivum* and Their Relationship to Synapsis. *Heredity* **1979**, *43*, 157.
- Berchowitz, L.E.; Francis, K.E.; Bey, A.L.; Copenhaver, G.P. The Role of AtMUS81 in Interference-Insensitive Crossovers in *A. Thaliana*. *PLoS Genet.* **2007**, *3*, 1355–1364, doi:10.1371/journal.pgen.0030132.
- Bhatt, A.M.; Lister, C.; Page, T.; Franz, P.; Findlay, K.; Jones, G.H.; Dickinson, H.G.; Dean, C. The DIF1 Gene of *Arabidopsis* Is Required for Meiotic Chromosome Segregation and Belongs to the REC8/RAD21 Cohesin Gene Family. *Plant J.* **1999**, *19*, 463–472, doi:10.1046/j.1365-313X.1999.00548.x.
- Bhullar, R.; Nagarajan, R.; Bennypaul, H.; Sidhu, G.K.; Sidhu, G.; Rustgi, S.; von Wettstein, D.; Gill, K.S. Silencing of a Metaphase I-Specific Gene Results in a Phenotype Similar to That of the Pairing Homeologous 1 (Ph1) Gene Mutations. *Proc. Natl. Acad. Sci.* **2014**, *111*, 14187–14192, doi:10.1073/pnas.1416241111.
- Bingham, E.T.; Burnham, C.R.; Gates, C.E. Double and Single Backcross Linkage Estimates in Autotetraploid Maize. *Genetics* **1968**, *59*, 399.
- Blanc, G.; Wolfe, K.H. Functional Divergence of Duplicated Genes Formed by Polyploidy during *Arabidopsis* Evolution. *Plant Cell* **2004**, *16*, 1679–1691, doi:10.1105/tpc.021410.

- Blary, A. *Towards a Functional Characterization of Meiotic Recombination in Rapeseed: Analysis of the Meiotic Transcriptome and Hyper-Recombinant Mutants*; Universite Paris-Saclay: Saint-Aubin, France, 2017.
- Boden, S.A.; Langridge, P.; Spangenberg, G.; Able, J.A. TaASY1 Promotes Homologous Chromosome Interactions and Is Affected by Deletion of Ph1. *Plant J.* **2009**, *57*, 487–497, doi:10.1111/j.1365-313X.2008.03701.x.
- Bombliès, K.; Higgins, J.D.; Yant, L. Meiosis Evolves: Adaptation to External and Internal Environments. *New Phytol.* **2015**, *208*, 306–323, doi:10.1111/nph.13499.
- Bombliès, K.; Jones, G.; Franklin, C.; Zickler, D.; Kleckner, N. The Challenge of Evolving Stable Polyploidy: Could an Increase in “Crossover Interference Distance” Play a Central Role? *Chromosoma* **2016**, *125*, 287–300, doi:10.1007/s00412-015-0571-4.
- Bourke, P.M.; Voorrips, R.E.; Visser, R.G.F.; Maliepaard, C. The Double-Reduction Landscape in Tetraploid Potato as Revealed by a High-Density Linkage Map. *Genetics* **2015**, *201*, 853–863, doi:10.1534/genetics.115.181008.
- Bourke, P.M.; Voorrips, R.E.; Visser, R.G.F.; Maliepaard, C. Tools for Genetic Studies in Experimental Populations of Polyploids. *Front. Plant Sci.* **2018**, *9*, 1–17, doi:10.3389/fpls.2018.00513.
- Brubaker, C.L.; Paterson, A.H.; Wendel, J.F. Comparative Genetic Mapping of Allotetraploid Cotton and Its Diploid Progenitors. *Genome* **1999**, *42*, 184–203, doi:10.1139/gen-42-2-184.
- Buggs, R.J.A.; Chamala, S.; Wu, W.; Tate, J.A.; Schnable, P.S.; Soltis, D.E.; Soltis, P.S.; Barbazuk, W.B. Rapid, Repeated, and Clustered Loss of Duplicate Genes in Allopolyploid Plant Populations of Independent Origin. *Curr. Biol.* **2012**, *22*, 248–252, doi:10.1016/j.cub.2011.12.027.
- Cai, X.; Dong, F.; Edelman, R.E.; Makaroff, C.A. The *Arabidopsis* SYN1 Cohesin Protein Is Required for Sister Chromatid Arm Cohesion and Homologous Chromosome Pairing. *J. Cell Sci.* **2003**, *116*, 2999–3007, doi:10.1242/jcs.00601.
- Cappai, F.; Amadeu, R.R.; Benevenuto, J.; Cullen, R.; Garcia, A.; Grossman, A.; Ferrão, L.F. V.; Munoz, P. High-Resolution Linkage Map and QTL Analyses of Fruit Firmness in Autotetraploid Blueberry. *Front. Plant Sci.* **2020**, *11*, 1–11, doi:10.3389/fpls.2020.562171.
- Carlton, P.M.; Farruggio, A.P.; Dernburg, A.F. A Link between Meiotic Prophase Progression and Crossover Control. *PloS Genet.* **2006**, *2*, 119–128, doi:10.1371/journal.pgen.0020012.
- Carvalho, A.; Delgado, M.; Barão, A.; Frescatada, M.; Ribeiro, E.; Pikaard, C.S.; Viegas, W.; Neves, N. Chromosome and DNA Methylation Dynamics during Meiosis in the Autotetraploid *Arabidopsis arenosa*. *Sex. Plant Reprod.* **2010**, *23*, 29–37, doi:10.1007/s00497-009-0115-2.
- Caryl, A.P.; Armstrong, S.J.; Jones, G.H.; Franklin, F.C.H. A Homologue of the Yeast HOP1 Gene Is Inactivated in the *Arabidopsis* Meiotic Mutant *Asy1*. *Chromosoma* **2000**, *109*, 62–71, doi:10.1007/s004120050413.
- Ceoloni, C.; Donini, P. Combining Mutations for the Two Homoeologous Pairing Suppressor Genes Ph1 and Ph2 in Common Wheat and in Hybrids with Alien Triticeae. *Genome* **1993**, *36*, 377–386, doi:10.1139/g93-052.

- Cervantes-Flores, J.C.; Yenchu, G.C.; Kriegner, A.; Pecota, K.V.; Faulk, M.A.; Mwanga, R.O.M.; Sosinski, B.R. Development of a Genetic Linkage Map and Identification of Homologous Linkage Groups in Sweetpotato Using Multiple-Dose AFLP Markers. *Mol. Breed.* **2008**, *21*, 511–532, doi:10.1007/s11032-007-9150-6.
- Chakraborty, U.; Alani, E. Understanding How Mismatch Repair Proteins Participate in the Repair/Anti-Recombination Decision. *FEMS Yeast Res.* **2016**, *16*, fow071, doi:10.1093/femsyr/fow071.
- Chambon, A.; West, A.; Vezon, D.; Horlow, C.; De Muyt, A.; Chelysheva, L.; Ronceret, A.; Darbyshire, A.; Osman, K.; Heckmann, S.; et al. Identification of ASYNAPTIC4, a Component of the Meiotic Chromosome Axis. *Plant Physiol.* **2018**, *178*, 233–246, doi:10.1104/pp.17.01725.
- Chelysheva, L.; Diallo, S.; Vezon, D.; Gendrot, G.; Vrielynck, N.; Belcram, K.; Rocques, N.; Márquez-Lema, A.; Bhatt, A.M.; Horlow, C.; et al. AtREC8 and AtSCC3 Are Essential to the Monopolar Orientation of the Kinetochores during Meiosis. *J. Cell Sci.* **2005**, *118*, 4621–4632, doi:10.1242/jcs.02583.
- Chelysheva, L.; Gendrot, G.; Vezon, D.; Doutriaux, M.-P.; Mercier, R.; Grelon, M. Zip4/Spo22 Is Required for Class I CO Formation but Not for Synapsis Completion in *Arabidopsis thaliana*. *PLoS Genetics* **2007**, *3*, e83, doi:10.1371/journal.pgen.0030083.
- Chelysheva, L.; Vezon, D.; Chambon, A.; Gendrot, G.; Pereira, L.; Lemhemdi, A.; Vrielynck, N.; Le Guin, S.; Novatchkova, M.; Grelon, M. The *Arabidopsis* HEI10 Is a New ZMM Protein Related to Zip3. *PloS Genet.* **2012**, *8*, e1002799, doi:10.1371/journal.pgen.1002799.
- Cheng, F.; Sun, R.; Hou, X.; Zheng, H.; Zhang, F.; Zhang, Y.; Liu, B.; Liang, J.; Zhuang, M.; Liu, Y.; et al. Subgenome Parallel Selection Is Associated with Morphotype Diversification and Convergent Crop Domestication in *Brassica rapa* and *Brassica oleracea*. *Nat. Genet.* **2016**, *48*, 1218–1224, doi:10.1038/ng.3634.
- Chester, M.; Gallagher, J.P.; Symonds, V.V.; Cruz da Silva, A.V.; Mavrodiev, E.V.; Leitch, A.R.; Soltis, P.S.; Soltis, D.E. Extensive Chromosomal Variation in a Recently Formed Natural Allopolyploid Species, *Tragopogon miscellus* (Asteraceae). *Proc. Natl. Acad. Sci.* **2012**, *109*, 1176–1181, doi:10.1073/pnas.1112041109.
- Chikashige, Y.; Ding, D.Q.; Imai, Y.; Yamamoto, M.; Haraguchi, T.; Hiraoka, Y. Meiotic Nuclear Reorganization: Switching the Position of Centromeres and Telomeres in the Fission Yeast *Schizosaccharomyces pombe*. *EMBO J.* **1997**, *16*, 193–202, doi:10.1093/emboj/16.1.193.
- Choi, K.; Zhao, X.; Tock, A.J.; Lambing, C.; Underwood, C.J.; Hardcastle, T.J.; Serra, H.; Kim, J.; Cho, H.S.; Kim, J.; et al. Nucleosomes and DNA Methylation Shape Meiotic DSB Frequency in *Arabidopsis thaliana* Transposons and Gene Regulatory Regions. *Genome Res.* **2018**, *28*, 532–546, doi:10.1101/gr.225599.117.
- Cifuentes, M.; Eber, F.; Lucas, M.O.; Lode, M.; Chevre, A.M.; Jenczewskia, E. Repeated Polyploidy Drove Different Levels of Crossover Suppression between Homoeologous Chromosomes in *Brassica napus* Allohaploids. *Plant Cell* **2010**, *22*, 2265–2276, doi:10.1105/tpc.109.072991.
- Cifuentes, M.; Grandont, L.; Moore, G.; Marie, A.; Jenczewski, E.; Chèvre, A.M.; Jenczewski, E. Genetic Regulation of Meiosis in Polyploid Species: New Insights into an Old Question. *New Phytol.* **2010**, *186*, 29–36, doi:10.1111/j.1469-8137.2009.03084.x.
- Cifuentes, M.; Rivard, M.; Pereira, L.; Chelysheva, L.; Mercier, R. Haploid Meiosis in *Arabidopsis*: Double-Strand Breaks Are Formed and Repaired but Without Synapsis and Crossovers. *PLoS ONE* **2013**, *8*, e72431, doi:10.1371/journal.pone.0072431.

- Clancy, S. Genetic Recombination. *Nat. Educ.* **2008**, *1*, 40.
- Clark, L.V.; Lipka, A.E.; Sacks, E.J. PolyRAD: Genotype Calling with Uncertainty from Sequencing Data in Polyploids and Diploids. *G3 Genes Genomes Genet.* **2019**, *9*, 663–673, doi:10.1534/g3.118.200913.
- Clarke, W.E.; Higgins, E.E.; Plieske, J.; Wieseke, R.; Sidebottom, C.; Khedikar, Y.; Batley, J.; Edwards, D.; Meng, J.; Li, R.; et al. A High-Density SNP Genotyping Array for *Brassica napus* and Its Ancestral Diploid Species Based on Optimised Selection of Single-Locus Markers in the Allotetraploid Genome. *Theor. Appl. Genet.* **2016**, *129*, 1887–1899, doi:10.1007/s00122-016-2746-7.
- Cohen, P.E.; Pollack, S.E.; Pollard, J.W. Genetic Analysis of Chromosome Pairing, Recombination, and Cell Cycle Control during First Meiotic Prophase in Mammals. *Endocr. Rev.* **2006**, *27*, 398–426, doi:10.1210/er.2005-0017.
- Colas, I.; Shaw, P.; Prieto, P.; Wanous, M.; Spielmeier, W.; Mago, R.; Moore, G. Effective Chromosome Pairing Requires Chromatin Remodeling at the Onset of Meiosis. *Proc. Natl. Acad. Sci.* **2008**, *105*, 6075–6080, doi:10.1073/pnas.0801521105.
- Comai, L. The Advantages and Disadvantages of Being Polyploid. *Nat. Rev. Genet.* **2005**, *6*, 836–846, doi:10.1038/nrg1711.
- Comai, L.; Tyagi, A.P.; Lysak, M.A. FISH Analysis of Meiosis in *Arabidopsis* Allopolyploids. *Chromosome Res.* **2003**, *11*, 217–226, doi:10.1023/A:1022883709060.
- Cowan, C.R.; Carlton, P.M.; Cande, W.Z. The Polar Arrangement of Telomeres in Interphase and Meiosis. Rabl Organization and the Bouquet. *Plant Physiol.* **2001**, *125*, 532–538, doi:10.1104/pp.125.2.532.
- Cremer, T.; Cremer, M. Chromosome Territories. *Cold Spring Harb. Perspect. Biol.* **2010**, *2*, 1–23, doi:10.1101/cshperspect.a003889.
- Crowley, J.G.; Rees, H. Fertility and Selection in Tetraploid *Lolium*. *Chromosoma* **1968**, *24*, 300–308, doi:10.1007/BF00336197.
- Cui, C.; Ge, X.; Gautam, M.; Kang, L.; Li, Z. Cytoplasmic and Genomic Effects on Meiotic Pairing in *Brassica* Hybrids and Allotetraploids from Pair Crosses of Three Cultivated Diploids. *Genetics* **2012**, *191*, 725–738, doi:10.1534/genetics.112.140780.
- Culligan, K.M.; Hays, J.B. *Arabidopsis* MutS Homologs—AtMSH2, AtMSH3, AtMSH6, and a Novel AtMSH7—Form Three Distinct Protein Heterodimers with Different Specificities for Mismatched DNA. *Plant Cell* **2000**, *12*, 991–1002, doi:10.1105/tpc.12.6.991.
- Cuñado, N.; Callejas, S.; García, M.J.; Fernández, A.; Santos, J.L. The Pattern of Zygotene and Pachytene Pairing in Allotetraploid *Aegilops* Species Sharing the U Genome. *Theor. Appl. Genet.* **1996**, *93*, 1152–1155, doi:10.1007/BF00230139.
- D’Hont, A.; Ison, D.; Alix, K.; Roux, C.; Glaszmann, J.C. Determination of Basic Chromosome Numbers in the Genus *Saccharum* by Physical Mapping of Ribosomal RNA Genes. *Genome* **1998**, *41*, 221–225, doi:10.1139/gen-41-2-221.
- da Silva Pereira, G.; Mollinari, M.; Schumann, M.J.; Clough, M.E.; Zeng, Z.-B.; Yenko, G.C. The Recombination Landscape and Multiple QTL Mapping in a *Solanum Tuberosum* Cv. ‘Atlantic’-Derived F1 Population. *Heredity* **2021**, *126*, 817–830, doi:10.1038/s41437-021-00416-x.
- Dawson, C.D.R. Tetrasomic Inheritance in *Lotus corniculatus* L. *J. Genet.* **1941**, *42*, 49–72, doi:10.1007/BF02982510.

- De Muyt, A.; Mercier, R.; Mézard, C.; Grelon, M. Meiotic Recombination and Crossovers in Plants. *Genome Dyn.* **2009**, *5*, 14–25, doi:10.1159/000166616.
- de Muyt, A.; Pyatnitskaya, A.; Andréani, J.; Ranjha, L.; Ramus, C.; Laureau, R.; Fernandez-Vega, A.; Holoch, D.; Girard, E.; Govin, J.; et al. A Meiotic XPF–ERCC1-like Complex Recognizes Joint Molecule Recombination Intermediates to Promote Crossover Formation. *Genes Dev.* **2018**, *32*, 283–296, doi:10.1101/gad.308510.117.
- de Winton, D.; Haldane, J.B.S. Linkage in the Tetraploid *Primula Sinensis*. *J. Genet.* **1931**, *24*, 121–144.
- Desai, A.; Chee, P.W.; Rong, J.; May, O.L.; Paterson, A.H. Chromosome Structural Changes in Diploid and Tetraploid A Genomes of *Gossypium*. *Genome* **2006**, *49*, 336–345, doi:10.1139/g05-116.
- Dhaliwal, H.S.; Gill, B.S.; Waines, J.G. Analysis of Induced Homoeologous Pairing in a Ph Mutant Wheat X Rye Hybrid. *J. Hered.* **1977**, *68*, 207–209, doi:10.1093/oxfordjournals.jhered.a108815.
- Ding, D.-Q.; Matsuda, A.; Okamasa, K.; Nagahama, Y.; Haraguchi, T.; Hiraoka, Y. Meiotic Cohesin-Based Chromosome Structure Is Essential for Homologous Chromosome Pairing in *Schizosaccharomyces Pombe*. *Chromosoma* **2016**, *125*, 205–214, doi:10.1007/s00412-015-0551-8.
- Dixon, J.R.; Gorkin, D.U.; Ren, B. Chromatin Domains: The Unit of Chromosome Organization. *Mol. Cell* **2016**, *62*, 668–680, doi:10.1016/j.molcel.2016.05.018.
- Doerge, R.W.; Craig, B.A. Model Selection for Quantitative Trait Locus Analysis in Polyploids. *Proc. Natl. Acad. Sci. USA* **2000**, *97*, 7951–7956, doi:10.1073/pnas.97.14.7951.
- Dong, C.; Thomas, S.; Becker, D.; Lörz, H.; Whitford, R.; Sutton, T.; Able, J.A.; Langridge, P. WM5: Isolation and Characterisation of a Gene Expressed during Early Meiosis and Shoot Meristem Development in Wheat. *Funct. Plant Biol.* **2005**, *32*, 249, doi:10.1071/FP04198.
- Dong, C.; Whitford, R.; Langridge, P. A DNA Mismatch Repair Gene Links to the Ph2 Locus in Wheat. *Genome* **2002**, *45*, 116–124, doi:10.1139/g01-126.
- Drouaud, J.; Camilleri, C.; Bourguignon, P.Y.; Canaguier, A.; Bérard, A.; Vezon, D.; Giancola, S.; Brunel, D.; Colot, V.; Prum, B.; et al. Variation in Crossing-over Rates across Chromosome 4 of *Arabidopsis thaliana* Reveals the Presence of Meiotic Recombination “Hot Spots.” *Genome Res.* **2006**, *16*, 106–114, doi:10.1101/gr.4319006.
- Dubois, E.; De Muyt, A.; Soyer, J.L.; Budin, K.; Legras, M.; Piolot, T.; Debuchy, R.; Kleckner, N.; Zickler, D.; Espagne, E. Building Bridges to Move Recombination Complexes. *Proc. Natl. Acad. Sci. USA* **2019**, *116*, 12400–12409, doi:10.1073/pnas.1901237116.
- Edlinger, B.; Schlögelhofer, P. Have a Break: Determinants of Meiotic DNA Double Strand Break (DSB) Formation and Processing in Plants. *J. Exp. Bot.* **2011**, *62*, 1545–1563, doi:10.1093/jxb/erq421.
- Evans, G.M.; Davies, E.W. The Genetics of Meiotic Chromosome Pairing in *Lolium Temulentum* × *Lolium Perenne* Tetraploids. *Appl. Genet.* **1985**, *71*, 185–192.
- Ferdous, M.; Higgins, J.D.; Osman, K.; Lambing, C.; Roitinger, E.; Mechtler, K.; Armstrong, S.J.; Perry, R.; Pradillo, M.; Cuñado, N.; et al. Inter-Homolog Crossing-Over and Synapsis in *Arabidopsis* Meiosis Are Dependent on the Chromosome Axis Protein AtASY3. *PLoS Genet.* **2012**, *8*, e1002507, doi:10.1371/journal.pgen.1002507.
- Fisher, B.A.; Mather, K. Non-Lethality of the Mid Factor in *Lythrum Salicaria*. *Nature* **1940**, *146*, 521–521, doi:10.1038/146521a0.

- Fisher, R.A. *Statistical Methods for Research Workers*; DinOliver and Boyd Ltd.: London, UK, 1954.
- Fisher, R.A. The Theoretical Consequences of Polyploid Inheritance For The Mid Style Form of *Lythrum Salicaria*. *Ann. Eugen.* **1941**, *11*, 31–38, doi:10.1111/j.1469-1809.1941.tb02268.x.
- Fisher, R.A. The Theory of Linkage in Polysomic Inheritance. *Philos. Trans. R. Soc. Lond. Ser. B Biol. Sci.* **1947**, *233*, 55–87, doi:10.1098/rstb.1947.0006.
- Fisher, R.A.; Mather, K. Polyploid Inheritance in *Lythrum Salicaria*. *Nature* **1942**, *150*, 430–430, doi:10.1038/150430a0.
- Fisher, R.A.; Mather, K. The Inheritance of Style Length in *Lythrum Salicaria*. *Ann. Eugen.* **1943**, *12*, 1–23, doi:10.1111/j.1469-1809.1943.tb02307.x.
- Fransz, P.; De Jong, J.H.; Lysak, M.; Castiglione, M.R.; Schubert, I. Interphase Chromosomes in *Arabidopsis* Are Organized as Well Defined Chromocenters from Which Euchromatin Loops Emanate. *Proc. Natl. Acad. Sci. USA* **2002**, *99*, 14584–14589, doi:10.1073/pnas.212325299.
- Gaebelein, R.; Mason, A.S. Allohexaploids in the Genus *Brassica*. *Crit. Rev. Plant Sci.* **2018**, *37*, 422–437, doi:10.1080/07352689.2018.1517143.
- Gaebelein, R.; Schiessl, S.V.; Samans, B.; Batley, J.; Mason, A.S. Inherited Allelic Variants and Novel Karyotype Changes Influence Fertility and Genome Stability in *Brassica* Allohexaploids. *New Phytol.* **2019**, *223*, 965–978, doi:10.1111/nph.15804.
- Gaeta, R.T.; Chris Pires, J. Homoeologous Recombination in Allopolyploids: The Polyploid Ratchet. *New Phytol.* **2010**, *186*, 18–28, doi:10.1111/j.1469-8137.2009.03089.x.
- Gaeta, R.T.; Pires, J.C.; Iniguez-Luy, F.; Leon, E.; Osborn, T.C. Genomic Changes in Resynthesized *Brassica napus* and Their Effect on Gene Expression and Phenotype. *Plant Cell* **2007**, *19*, 3403–3417, doi:10.1105/TPC.107.054346.
- Garcia, A.A.F.; Kido, E.A.; Meza, A.N.; Souza, H.M.B.; Pinto, L.R.; Pastina, M.M.; Leite, C.S.; Da Silva, J.A.G.; Ulian, E.C.; Figueira, A.; et al. Development of an Integrated Genetic Map of a Sugarcane (*Saccharum* Spp.) Commercial Cross, Based on a Maximum-Likelihood Approach for Estimation of Linkage and Linkage Phases. *Theor. Appl. Genet.* **2006**, *112*, 298–314, doi:10.1007/s00122-005-0129-6.
- Garcia, A.A.F.; Mollinari, M.; Marconi, T.G.; Serang, O.R.; Silva, R.R.; Vieira, M.L.C.; Vicentini, R.; Costa, E.A.; Mancini, M.C.; Garcia, M.O.S.; et al. SNP Genotyping Allows an In-Depth Characterisation of the Genome of Sugarcane and Other Complex Autopolyploids. *Sci. Rep.* **2013**, *3*, 1–10, doi:10.1038/srep03399.
- Gauthier, F.M.; McGinnis, R.C. The Meiotic Behavior of a Nulli-Haploid Plant in *Avena Sativa* L. *Can. J. Genet. Cytol.* **1968**, *10*, 186–189, doi:10.1139/g68-025.
- Gerard, D.; Ferrão, L.F.V.; Garcia, A.A.F.; Stephens, M. Genotyping Polyploids from Messy Sequencing Data. *Genetics* **2018**, *210*, 789–807, doi:10.1534/genetics.118.301468.
- Gillies, C.B. An Electron Microscopic Study of Synaptonemal Complex Formation at Zygotene in Rye. *Chromosoma* **1985**, *92*, 165–175, doi:10.1007/BF00348690.
- Gillies, C.B. *Chromosome Pairing and Fertility in Polyploids*; CRC Press: Boca Raton, FL, USA, 1989.
- Gillies, C.B. Synaptonemal Complex and Chromosome Structure. *Annu. Rev. Genet.* **1975**, *9*, 91–109.
- Golubovskaya, I.N.; Hamant, O.; Timofejeva, L.; Wang, C.-J.R.; Braun, D.; Meeley, R.; Cande, W.Z. Alleles of Afd1 Dissect REC8 Functions during Meiotic Prophase I. *J. Cell Sci.* **2006**, *119*, 3306–3315, doi:10.1242/jcs.03054.



- Gonzalo, A.; Lucas, M.O.; Charpentier, C.; Sandmann, G.; Lloyd, A.; Jenczewski, E. Reducing MSH4 Copy Number Prevents Meiotic Crossovers between Non-Homologous Chromosomes in *Brassica napus*. *Nat. Commun.* **2019**, *10*, 1–9, doi:10.1038/s41467-019-10010-9.
- Grandont, L.; Cuñado, N.; Coriton, O.; Huteau, V.; Eber, F.; Chèvre, A.M.; Grelon, M.; Chelysheva, L.; Jenczewski, E. Homoeologous Chromosome Sorting and Progression of Meiotic Recombination in *Brassica napus*: Ploidy Does Matter! *Plant Cell* **2014**, *26*, 1448–1463, doi:10.1105/tpc.114.122788.
- Grandont, L.; Jenczewski, E.; Lloyd, A. Meiosis and Its Deviations in Polyploid Plants. *Cytogenet. Genome Res.* **2013**, *140*, 171–184, doi:10.1159/000351730.
- Grant, V. *Genetics of Flowering Plants*.; Columbia University Press: New York, NY, USA, 1978.
- Greer, E.; Martı, A.C.; Moore, G.; Shaw, P. The Ph1 Locus Suppresses Cdk2-Type Activity during Premeiosis and Meiosis in Wheat. *Plant Cell* **2012**, *24*, 152–162, doi:10.1105/tpc.111.094771.
- Gregory, R.P. On the Genetics of Tetraploid Plants in *Primula Sinensis*. *Proc. R. Soc. Lond. Ser. B Contain. Pap. A Biol. Character* **1914**, *87*, 484–492, doi:10.1098/rspb.1914.0035.
- Griffiths, S.; Sharp, R.; Foote, T.N.; Bertin, I.; Wanous, M.; Reader, S.; Colas, I.; Moore, G. Molecular Characterization of Ph1 as a Major Chromosome Pairing Locus in Polyploid Wheat. *Nature* **2006**, *439*, 749–752, doi:10.1038/nature04434.
- Grivet, L.; Arruda, P. Sugarcane Genomics: Depicting the Complex Genome of an Important Tropical Crop. *Curr. Opin. Plant Biol.* **2002**, *5*, 122–127, doi:10.1016/S1369-5266(02)00234-0.
- Grivet, L.; Glaszmann, J.C.; Vincentz, M.; Da Silva, F.; Arruda, P. ESTs as a Source for Sequence Polymorphism Discovery in Sugarcane: Example of the Adh Genes. *Theor. Appl. Genet.* **2003**, *106*, 190–197, doi:10.1007/s00122-002-1075-1.
- Grusz, A.L.; Sigel, E.M.; Witherup, C. Homoeologous Chromosome Pairing across the Eukaryote Phylogeny. *Mol. Phylogenet. Evol.* **2017**, *117*, 83–94, doi:10.1016/j.ympev.2017.05.025.
- Guimarães, C.T.; Honeycutt, R.J.; Sills, G.R.; Sobral, B.W.S. Genetic Maps of *Saccharum officinarum* L. and *Saccharum Robustum* Brandes & Jew. Ex Grassl. *Genet. Mol. Biol.* **1999**, *22*, 125–132, doi:10.1590/S1415-47571999000100024.
- Gustafsson, Å.; Gadd, I. Mutations and Crop Improvement. Iii. *Ipomoea batatas* (L.) Poir. (Convolvulaceae). *Hereditas* **1965**, *53*, 77–89, doi:10.1111/j.1601-5223.1965.tb01981.x.
- Hackett, C.A.; McLean, K.; Bryan, G.J. Linkage Analysis and QTL Mapping Using SNP Dosage Data in a Tetraploid Potato Mapping Population. *PLoS ONE* **2013**, *8*, e63939, doi:10.1371/journal.pone.0063939.
- Haldane, J.B.S. Theoretical Genetics of Autopolyploids. *J. Genet.* **1930**, *22*, 359–372.
- Hamant, O.; Ma, H.; Cande, W.Z. Genetics of Meiotic Prophase I in Plants. *Annu. Rev. Plant Biol.* **2006**, *57*, 267–302, doi:10.1146/annurev.arplant.57.032905.105255.
- Hazarika, M.H.; Rees, H. Genotypic Control of Chromosome Behaviour in Rye X. Chromosome Pairing and Fertility in Autotetraploids. *Heredity* **1967**, *22*, 317–332, doi:10.1038/hdy.1967.44.
- He, Y.; Wang, M.; Dukowic-Schulze, S.; Zhou, A.; Tiang, C.-L.; Shilo, S.; Sidhu, G.K.; Eichten, S.; Bradbury, P.; Springer, N.M.; et al. Genomic Features Shaping the Landscape of Meiotic Double-Strand-Break Hotspots in Maize. *Proc. Natl. Acad. Sci.* **2017**, *114*, 12231–12236, doi:10.1073/pnas.1713225114.

- Henry, I.M.; Dilkes, B.P.; Tyagi, A.; Gao, J.; Christensen, B.; Comaia, L. The BOY NAMED SUE Quantitative Trait Locus Confers Increased Meiotic Stability to an Adapted Natural Allopolyploid of *Arabidopsis*. *Plant Cell* **2014**, *26*, 181–194, doi:10.1105/tpc.113.120626.
- Higgins, E.E.; Howell, E.C.; Armstrong, S.J.; Parkin, I.A.P. A Major Quantitative Trait Locus on Chromosome A9, *BnaPh1*, Controls Homoeologous Recombination in *Brassica Napus*. *New Phytologist* **2021**, *229*, 3281–3293, doi:10.1111/nph.16986.
- Higgins, J.D.; Armstrong, S.J.; Franklin, F.C.H.; Jones, G.H. The *Arabidopsis* MutS Homolog AtMSH4 Functions at an Early Step in Recombination: Evidence for Two Classes of Recombination in *Arabidopsis*. *Genes Dev.* **2004**, *18*, 2557–2570, doi:10.1101/gad.317504.
- Higgins, J.D.; Buckling, E.F.; Franklin, F.C.H.; Jones, G.H. Expression and Functional Analysis of AtMUS81 in *Arabidopsis* Meiosis Reveals a Role in the Second Pathway of Crossing-Over. *Plant J.* **2008**, *54*, 152–162, doi:10.1111/j.1365-313X.2008.03403.x.
- Higgins, J.D.; Sanchez-Moran, E.; Armstrong, S.J.; Jones, G.H.; Franklin, F.C.H. The *Arabidopsis* Synaptonemal Complex Protein ZYP1 Is Required for Chromosome Synapsis and Normal Fidelity of Crossing Over. *Genes Dev.* **2005**, *19*, 2488–2500, doi:10.1101/gad.354705.
- Hobolth, P. Chromosome Pairing in Allohexaploid Wheat Var. Chinese Spring. Transformation of Multivalents into Bivalents, a Mechanism for Exclusive Bivalent Formation. *Carlsberg Res. Commun.* **1981**, *46*, 129–173, doi:10.1007/BF02910465.
- Hollister, J.D.; Arnold, B.J.; Svedin, E.; Xue, K.S.; Dilkes, B.P.; Bomblies, K. Genetic Adaptation Associated with Genome-Doubling in Autotetraploid *Arabidopsis arenosa*. *PLoS Genet.* **2012**, *8*, e1003093, doi:10.1371/journal.pgen.1003093.
- Holm, P.B. Chromosome Pairing and Chiasma Formation in Allohexaploid Wheat, *Triticum aestivum* Analyzed by Spreading of Meiotic Nuclei. *Carlsberg Res. Commun.* **1986**, *51*, 239–294, doi:10.1007/BF02906837.
- Holm, P.B.; Wang, X. The Effect of Chromosome 5B on Synapsis and Chiasma Formation in Wheat, *Triticum aestivum* Cv. Chinese Spring. *Carlsberg Res. Commun.* **1988**, *53*, 191–208, doi:10.1007/BF02907179.
- Hossain, M.R.; Natarajan, S.; Kim, H.T.; Jesse, D.M.I.; Lee, C.G.; Park, J.I.; Nou, I.S. High Density Linkage Map Construction and QTL Mapping for Runner Production in Allo-Octoploid Strawberry *Fragaria* × *Ananassa* Based on DdRAD-Seq Derived SNPs. *Sci. Rep.* **2019**, *9*, 1–11, doi:10.1038/s41598-019-39808-9.
- Hunter, N.; Kleckner, N. The Single-End Invasion: An Asymmetric Intermediate at the Double-Strand Break to Double-Holliday Junction Transition of Meiotic Recombination. *Cell* **2001**, *106*, 59–70, doi:10.1016/S0092-8674(01)00430-5.
- Idziak, D.; Robaszkiewicz, E.; Hasterok, R. Spatial Distribution of Centromeres and Telomeres at Interphase Varies among Brachypodium Species. *J. Exp. Bot.* **2015**, *66*, 6623–6634, doi:10.1093/jxb/erv369.
- Inaba, R.; Nishio, T. Phylogenetic Analysis of Brassiceae Based on the Nucleotide Sequences of the S-Locus Related Gene, SLR1. *Theor. Appl. Genet.* **2002**, *105*, 1159–1165, doi:10.1007/s00122-002-0968-3.
- Inomata, N. Hybrid Progenies of the Cross, *Brassica campestris* × *B. oleracea*. I. Cytogenetical Studies on F1 Hybrids. *Jpn. J. Genet.* **1980**, *55*, 189–202, doi:10.1266/jjg.55.189.
- Jannoo, N.; Grivet, L.; David, J.; D’Hont, A.; Glaszmann, J.C. Differential Chromosome Pairing Affinities at Meiosis in Polyploid Sugarcane Revealed by Molecular Markers. *Heredity* **2004**, *93*, 460–467, doi:10.1038/sj.hdy.6800524.

- Jauhar, P.P. Genetic Control of Diploid-like Meiosis in Hexaploid Tall Fescue. *Nature* **1975**, *254*, 595–597, doi:10.1038/254595a0.
- Jauhar, P.P. Inter- and Intragenomic Chromosome Pairing in Haploids of Durum Wheat. *J. Hered.* **1999**, *90*, 437–445, doi:10.1093/jhered/90.4.437.
- Jenczewski, E.; Alix, K. From Diploids to Allopolyploids: The Emergence of Efficient Pairing Control Genes in Plants. *Crit. Rev. Plant Sci.* **2004**, *23*, 21–45, doi:10.1080/07352680490273239.
- Jenczewski, E.; Chèvre, A.M.; Alix, K. Chromosomal and Gene Expression Changes in *Brassica* Allopolyploids. In *Polyploid and Hybrid Genomics*; Wiley: New York, NY, USA, 2013; pp. 171–186, doi:10.1002/9781118552872.CH10.
- Jenczewski, E.; Eber, F.; Grimaud, A.; Huet, S.; Lucas, M.O.; Monod, H.; Chèvre, A.M. PrBn, a Major Gene Controlling Homeologous Pairing in Oilseed Rape (*Brassica napus*) Haploids. *Genetics* **2003**, *164*, 645–653, doi:10.1093/genetics/164.2.645.
- Jenkins, G. Chromosome pairing and fertility in plant hybrids. In *Fertility and Chromosome Pairing: Recent Studies in Plants and Animals*; Taylor & Francis: Oxfordshire, UK, 1989; pp. 109–135, ISBN 9781003068433.
- Jenkins, G. Synaptonemal Complex Formation in Hybrids of *Lolium temulentum* × *Lolium perenne* (L.)—II. Triploid. *Chromosoma* **1985**, *92*, 387–390, doi:10.1007/BF00327471.
- Jenkins, G.; Rees, H. Strategies of Bivalent Formation in Allopolyploid Plants. *Proc. R. Soc. B: Biol. Sci.* **1991**, *243*, 209–214, doi:10.1098/rspb.1991.0033.
- Ji, L.-H.; Langridge, P. An Early Meiosis CDNA Clone from Wheat. *Mol. Gen. Genet. MGG* **1994**, *243*, 17–23, doi:10.1007/BF00283871.
- John, B.; Henderson, S.A. Asynapsis and Polyploidy in *Schistocerca Paranensis*. *Chromosoma* **1962**, *13*, 111–147, doi:10.1007/BF00326567.
- Jones, G.H.; Khazanehdari, K.A.; Ford-Lloyd, B.V. Meiosis in the Leek (*Allium porrum* L.) Revisited. II. Metaphase I Observations. *Heredity* **1996**, *76*, 186–191, doi:10.1038/hdy.1996.26.
- Keeney, S.; Giroux, C.N.; Kleckner, N. Meiosis-Specific DNA Double-Strand Breaks Are Catalyzed by Spo11, a Member of a Widely Conserved Protein Family. *Cell* **1997**, *88*, 375–384, doi:10.1016/S0092-8674(00)81876-0.
- Kim, S.; Plagnol, V.; Hu, T.T.; Toomajian, C.; Clark, R.M.; Ossowski, S.; Ecker, J.R.; Weigel, D.; Nordborg, M. Recombination and Linkage Disequilibrium in *Arabidopsis thaliana*. *Nat. Genet.* **2007**, *39*, 1151–1155, doi:10.1038/ng2115.
- King, J.; Grewal, S.; Yang, C.Y.; Hubbart, S.; Scholefield, D.; Ashling, S.; Edwards, K.J.; Allen, A.M.; Burridge, A.; Bloor, C.; et al. A Step Change in the Transfer of Interspecific Variation into Wheat from *Amblyopyrum muticum*. *Plant Biotechnol. J.* **2017**, *15*, 217–226, doi:10.1111/pbi.12606.
- Kleckner, N. Chiasma Formation: Chromatin/Axis Interplay and the Role(s) of the Synaptonemal Complex. *Chromosoma* **2006**, *115*, 175–194, doi:10.1007/s00412-006-0055-7.
- Knight, E.; Greer, E.; Draeger, T.; Thole, V.; Reader, S.; Shaw, P.; Moore, G. Inducing Chromosome Pairing through Premature Condensation: Analysis of Wheat Interspecific Hybrids. *Funct. Integr. Genom.* **2010**, *10*, 603–608, doi:10.1007/s10142-010-0185-0.

- Kollmann, F. *Allium Ampeloprasum*—a Polyploid Complex II. Meiosis and Relationships between the Ploidy Types. *Caryologia* **1972**, *25*, 295–312, doi:10.1080/00087114.1972.10796484.
- Krasinska, L.; Besnard, E.; Cot, E.; Dohet, C.; Méchali, M.; Lemaitre, J.-M.; Fisher, D. Cdk1 and Cdk2 Activity Levels Determine the Efficiency of Replication Origin Firing in *Xenopus*. *EMBO J.* **2008**, *27*, 758–769, doi:10.1038/emboj.2008.16.
- Kriegner, A.; Cervantes, J.C.; Burg, K.; Mwanga, R.O.M.; Zhang, D. A Genetic Linkage Map of Sweetpotato [*Ipomoea batatas* (L.) Lam.] Based on AFLP Markers. *Mol. Breed.* **2003**, *11*, 169–185, doi:10.1023/A:1022870917230.
- Kunkel, T.A.; Erie, D.A. DNA Mismatch Repair. *Annu. Rev. Biochem.* **2005**, *74*, 681–710, doi:10.1146/annurev.biochem.74.082803.133243.
- Lam, W.S.; Yang, X.; Makaroff, C.A. Characterization of *Arabidopsis thaliana* SMC1 and SMC3: Evidence That AtSMC3 May Function beyond Chromosome Cohesion. *J. Cell Sci.* **2005**, *118*, 3037–3048, doi:10.1242/jcs.02443.
- Lambing, C.; Kuo, P.C.; Tock, A.J.; Topp, S.D.; Henderson, I.R. ASY1 Acts as a Dosage-Dependent Antagonist of Telomere-Led Recombination and Mediates Crossover Interference in *Arabidopsis*. *Proc. Natl. Acad. Sci.* **2020**, *117*, 13647–13658, doi:10.1073/pnas.1921055117.
- Lambing, C.; Tock, A.J.; Topp, S.D.; Choi, K.; Kuo, P.C.; Zhao, X.; Osman, K.; Higgins, J.D.; Franklin, F.C.H.; Henderson, I.R. Interacting Genomic Landscapes of REC8-Cohesin, Chromatin, and Meiotic Recombination in *Arabidopsis*. *Plant Cell* **2020**, *32*, 1218–1239, doi:10.1105/tpc.19.00866.
- Lavania, U.C. High Bivalent Frequencies in Artificial Autopolyploids of *Hyoscyamus muticus* L. *Can. J. Genet. Cytol.* **1986**, *28*, 7–11, doi:10.1139/g86-002.
- Lavania, U.C. Polyploid Breeding: Meiosis in the Diploid Progenitor and Its Predictive Value for Fertility in the Autotetraploid. *Proc. Indian Nat. Sci. Acad. B.* **1991**, *57*, 17–24.
- Lawrence, W.J.C. The Genetics and Cytology of Dahlia Species. *J. Genet.* **1929**, *21*, 125–159, doi:10.1007/BF02984203.
- Leflon, M.; Grandont, L.; Eber, F.; Huteau, V.; Coriton, O.; Chelysheva, L.; Jenczewski, E.; Chèvre, A.-M. Crossovers Get a Boost in *Brassica* Allotriploid and Allotetraploid Hybrids. *Plant Cell* **2010**, *22*, 2253–2264, doi:10.1105/TPC.110.075986.
- Leitch, A.R.; Leitch, I.J. Genomic Plasticity and the Diversity of Polyploid Plants. *Science* **2008**, *320*, 481–484, doi:10.1111/j.1365-313X.2008.03432.x.
- Letarte, J. *Identification and Characterisation of Early Meiotic Genes in Wheat*; University of Adelaide: Adelaide, Australia, 1996.
- Lhuissier, F.G.P.; Offenberg, H.H.; Wittich, P.E.; Vischer, N.O.E.; Heyting, C. The Mismatch Repair Protein MLH1 Marks a Subset of Strongly Interfering Crossovers in Tomato. *Plant Cell* **2007**, *19*, 862–876, doi:10.1105/tpc.106.049106.
- Li, X.; Van Eck, H.J.; Rouppe Van Der Voort, J.N.A.M.; Huigen, D.J.; Stam, P.; Jacobsen, E. Autotetraploids and Genetic Mapping Using Common AFLP Markers: The R2 Allele Conferring Resistance to *Phytophthora infestans* Mapped on Potato Chromosome 4. *Theor. Appl. Genet.* **1998**, *96*, 1121–1128, doi:10.1007/s001220050847.

- Liu, S.; Liu, Y.; Yang, X.; Tong, C.; Edwards, D.; Parkin, I.A.P.; Zhao, M.; Ma, J.; Yu, J.; Huang, S.; et al. The *Brassica oleracea* Genome Reveals the Asymmetrical Evolution of Polyploid Genomes. *Nat. Commun.* **2014**, *5*, 3930, doi:10.1038/ncomms4930.
- Liu, Z.; Adamczyk, K.; Manzanares-Dauleux, M.; Eber, F.; Lucas, M.O.; Delourme, R.; Chèvre, A.M.; Jenczewski, E. Mapping PrBn and Other Quantitative Trait Loci Responsible for the Control of Homeologous Chromosome Pairing in Oilseed Rape (*Brassica napus* L.) Haploids. *Genetics* **2006**, *174*, 1583–1596, doi:10.1534/genetics.106.064071.
- Lloyd, A.; Bomblies, K. Meiosis in Autopolyploid and Allopolyploid *Arabidopsis*. *Curr. Opin. Plant Biol.* **2016**, *30*, 116–122, doi:10.1016/j.pbi.2016.02.004.
- Lloyd, A.H.; Milligan, A.S.; Langridge, P.; Able, J.A. TaMSH7: A Cereal Mismatch Repair Gene That Affects Fertility in Transgenic Barley (*Hordeum vulgare* L.). *BMC Plant Biol.* **2007**, *7*, 67, doi:10.1186/1471-2229-7-67.
- Lloyd, A.H.; Ranoux, M.; Vautrin, S.; Glover, N.; Fourment, J.; Charif, D.; Choulet, F.; Lassalle, G.; Marande, W.; Tran, J.; et al. Meiotic Gene Evolution: Can You Teach a New Dog New Tricks? *Mol. Biol. Evol.* **2014**, *31*, 1724–1727, doi:10.1093/molbev/msu119.
- Loebenstein, G. Origin, Distribution and Economic Importance. In *The Sweetpotato*; Loebenstein, G., Thottappilly, G., Eds.; Springer Netherlands: Dordrecht, The Netherlands, 2009; Volume 49, pp. 9–12, ISBN 978-1-4020-9474-3.
- Lohmiller, L.D.; De Muyt, A.; Howard, B.; Offenberg, H.H.; Heyting, C.; Grelon, M.; Anderson, L.K. Cytological Analysis of MRE11 Protein during Early Meiotic Prophase I in *Arabidopsis* and Tomato. *Chromosoma* **2008**, *117*, 277–288, doi:10.1007/s00412-007-0147-z.
- Loidl, J. Synaptonemal Complex Spreading in Allium. II. Tetraploid A. Vineale. *Can. J. Genet. Cytol.* **1986**, *28*, 754–761, doi:10.1139/g86-106.
- Loidl, J.; Ehrendorfer, F.; Schweizer, D. EM Analysis of Meiotic Chromosome Pairing in a Pentaploid Achillea Hybrid. *Heredity* **1990**, *65*, 11–20, doi:10.1038/hdy.1990.64.
- Loidl, J.; Jones, G.H. Synaptonemal Complex Spreading in Allium. *Chromosoma* **1986**, *93*, 420–428, doi:10.1007/bf00285824.
- Lysak, M.A.; Koch, M.A.; Pecinka, A.; Schubert, I. Chromosome Triplication Found across the Tribe Brassiceae. *Genome Res.* **2005**, *15*, 516–525, doi:10.1101/gr.3531105.
- Magoon, M.L.; Krishnan, R.; Vijaya Bai, K. Cytological Evidence on the Origin of Sweet Potato. *Theor. Appl. Genet.* **1970**, *40*, 360–366, doi:10.1007/BF00285415.
- Marburger, S.; Monnahan, P.; Seear, P.J.; Martin, S.H.; Koch, J.; Paajanen, P.; Bohutínská, M.; Higgins, J.D.; Schmickl, R.; Yant, L. Interspecific Introgression Mediates Adaptation to Whole Genome Duplication. *Nat. Commun.* **2019**, *10*, 5218, doi:10.1038/s41467-019-13159-5.
- Marston, A.L.; Amon, A. Meiosis: Cell-Cycle Controls Shuffle and Deal. *Nat. Rev. Mol. Cell Biol.* **2004**, *5*, 983–997, doi:10.1038/nrm1526.
- Martín, A.C.; Borrill, P.; Higgins, J.; Alabdullah, A.; Ramírez-gonzález, R.H.; Swarbreck, D.; Uauy, C.; Shaw, P.; Moore, G. Genome-Wide Transcription During Early Wheat Meiosis Is Independent of Synapsis, Ploidy Level, and the Ph1 Locus. *Front. Plant Sci.* **2018**, *9*, 1–19, doi:10.3389/fpls.2018.01791.

- Martín, A.C.; Rey, M.D.; Shaw, P.; Moore, G.; Moore, G. Dual Effect of the Wheat Ph1 Locus on Chromosome Synapsis and Crossover. *Chromosoma* **2017**, *126*, 669–680, doi:10.1007/s00412-017-0630-0.
- Martín, A.C.; Shaw, P.; Phillips, D.; Reader, S.; Moore, G.; Marti, A.C. Licensing MLH1 Sites for Crossover during Meiosis. *Nat. Commun.* **2014**, *5*, 1–5, doi:10.1038/ncomms5580.
- Martinez, M.; Cuñado, N.; Carcelén, N.; Romero, C. The Ph1 and Ph2 Loci Play Different Roles in the Synaptic Behaviour of Hexaploid Wheat *Triticum aestivum*. *Theor. Appl. Genet.* **2001**, *103*, 398–405, doi:10.1007/s00122-001-0543-3.
- Martinez-Perez, E.; Moore, G. To Check or Not to Check? The Application of Meiotic Studies to Plant Breeding. *Curr. Opin. Plant Biol.* **2008**, *11*, 222–227, doi:10.1016/j.pbi.2008.01.001.
- Martinez-Perez, E.; Shaw, P.; Reader, S.; Aragon-Alcaide, L.; Miller, T.; Moore, G. Homologous Chromosome Pairing in Wheat. *J. Cell Sci.* **1999**, *112*, 1761–1769, doi:10.1242/jcs.112.11.1761.
- Martinez-Perez, E.; Shaw, P.J.; Moore, G. Polyploidy Induces Centromere Association. *J. Cell Biol.* **2000**, *148*, 233–238, doi:10.1083/jcb.148.2.233.
- Mason, A.S.; Huteau, V.; Eber, F.; Coriton, O.; Yan, G.; Nelson, M.N.; Cowling, W.A.; Chèvre, A.M. Genome Structure Affects the Rate of Autosynopsis and Allosynopsis in AABC, BBAC and CCAB *Brassica* Interspecific Hybrids. *Chromosome Res.* **2010**, *18*, 655–666, doi:10.1007/s10577-010-9140-0.
- Mason, A.S.; Nelson, M.N.; Yan, G.; Cowling, W.A. Production of Viable Male Unreduced Gametes in *Brassica* Interspecific Hybrids Is Genotype Specific and Stimulated by Cold Temperatures. *BMC Plant Biol.* **2011**, *11*, doi:10.1186/1471-2229-11-103.
- Mason, A.S.; Wendel, J.F. Homoeologous Exchanges, Segmental Allopolyploidy, and Polyploid Genome Evolution. *Front. Genet.* **2020**, *11*, 1–10, doi:10.3389/fgene.2020.01014.
- Mather, K. Reductional and Equational Separation of the Chromosomes in Bivalents and Multivalents. *J. Genet.* **1935**, *30*, 53–78, doi:10.1007/BF02982205.
- Mather, K. Segregation and Linkage in Autotetraploids. *J. Genet.* **1936**, *32*, 287–314, doi:10.1007/BF02982683.
- Matsuoka, Y. Evolution of Polyploid *Triticum* Wheats under Cultivation: The Role of Domestication, Natural Hybridization and Allopolyploid Speciation in Their Diversification. *Plant Cell Physiol.* **2011**, *52*, 750–764, doi:10.1093/pcp/pcr018.
- McCollum, G.D. Comparative Studies of Chromosome Pairing in Natural and Induced Tetraploid *Dactylis*. *Chromosoma* **1957**, *9*, 571–605, doi:10.1007/BF02568094.
- Mello-Sampayo, T. Genetic Regulation of Meiotic Chromosome Pairing by Chromosome 3D of *Triticum aestivum*. *Nat. New Biol.* **1971**, *230*, 22–23, doi:10.1038/newbio230022a0.
- Mello-Sampayo, T. Homoeologous Chromosome Pairing in Pentaploid Hybrids of Wheat. In Proceedings of the Third International Wheat Genetics Symposium, Canberra, Australia, 5–9 August 1968; Finlay, K.W., Shepherd, K.W., Eds.; pp. 179–184.
- Mercier, R.; Grelon, M. Meiosis in Plants: Ten Years of Gene Discovery. *Cytogenet. Genome Res.* **2008**, *120*, 281–290, doi:10.1159/000121077.
- Mézard, C. Meiotic Recombination Hotspots in Plants. *Biochem. Soc. Trans.* **2006**, *34*, 531–534, doi:10.1042/BST0340531.
- Mézard, C.; Vignard, J.; Drouaud, J.; Mercier, R. The Road to Crossovers: Plants Have Their Say. *Trends Genet.* **2007**, *23*, 91–99, doi:10.1016/j.tig.2006.12.007.

- Mikhailova, E.I.; Sosnikhina, S.P.; Kirillova, G.A.; Tikholiz, O.A.; Smirnov, V.G.; Jones, R.N.; Jenkins, G. Nuclear Dispositions of Subtelomeric and Pericentromeric Chromosomal Domains during Meiosis in Asynaptic Mutants of Rye (*Secale cereale* L.). *J. Cell Sci.* **2001**, *114*, 1875–1882.
- Ming, R.; Liu, S.C.; Bowers, J.E.; Moore, P.H.; Irvine, J.E.; Paterson, A.H. Construction of a *Saccharum* Consensus Genetic Map from Two Interspecific Crosses. *Crop Sci.* **2002**, *42*, 570–583, doi:10.2135/cropsci2002.5700.
- Mollinari, M.; Garcia, A.A.F. Linkage Analysis and Haplotype Phasing in Experimental Autopolyploid Populations with High Ploidy Level Using Hidden Markov Models. *G3 Genes Genomes Genet.* **2019**, *9*, 3297–3314, doi:10.1534/g3.119.400378.
- Mollinari, M.; Olukolu, B.A.; Da Pereira, G.S.; Khan, A.; Gemenet, D.; Craig Yench, G.; Zeng, Z.B. Unraveling the Hexaploid Sweetpotato Inheritance Using Ultra-Dense Multilocus Mapping. *G3 Genes Genomes Genet.* **2020**, *10*, 281–292, doi:10.1534/g3.119.400620.
- Monden, Y.; Tahara, M. Genetic Linkage Analysis Using DNA Markers in Sweetpotato. *Breed. Sci.* **2017**, *67*, 41–51, doi:10.1270/jsbbs.16142.
- Moore, G. Meiosis in Allopolyploids—the Importance of ‘Teflon’ Chromosomes. *Trends Genet.* **2002**, *18*, 456–463, doi:10.1016/S0168-9525(02)02730-0.
- Moran, E.S.; Armstrong, S.J.; Santos, J.L.; Franklin, F.C.H.; Jones, G.H. Chiasma Formation in *Arabidopsis thaliana* Accession Wassileskija and in Two Meiotic Mutants. *Chromosome Res.* **2001**, *9*, 121–128, doi:10.1023/a:1009278902994.
- Morgan, C.; Zhang, H.; Henry, C.E.; Franklin, F.C.H.; Bomblies, K. Derived Alleles of Two Axis Proteins Affect Meiotic Traits in Autotetraploid *Arabidopsis arenosa*. *Proc. Natl. Acad. Sci.* **2020**, *117*, 8980–8988, doi:10.1073/pnas.1919459117.
- Muller, H.J. A New Mode of Segregation in Gregory’s Tetraploid Primulas. *Am. Nat.* **1914**, *48*, 508–512, doi:10.1086/279426.
- Mwathi, M.W.; Gupta, M.; Atri, C.; Banga, S.S.; Batley, J.; Mason, A.S. Segregation for Fertility and Meiotic Stability in Novel Brassica Allohexaploids. *Theor. Appl. Genet.* **2017**, *130*, 767–776, doi:10.1007/s00122-016-2850-8.
- Nagaharu, U. Genome Analysis in *Brassica* with Special Reference to the Experimental Formation of B. Napus and Peculiar Mode of Fertilization. *Jpn. J. Bot.* **1935**, *7*, 389–452.
- Neale, M.J.; Keeney, S. Clarifying the Mechanics of DNA Strand Exchange in Meiotic Recombination. *Nature* **2006**, *442*, 153–158, doi:10.1038/nature04885.
- Newton, W.C.F.; Darlington, C.D. Meiosis in Polyploids: Part I. Triploid and Pentaploid Tulips. *J. Genet.* **1929**, *21*, 1–15, doi:10.1007/BF02983355.
- Nicolas, S.D.; Leflon, M.; Monod, H.; Eber, F.; Coriton, O.; Huteau, V.; Chevre, A.-M.; Jenczewski, E. Genetic Regulation of Meiotic Cross-Overs between Related Genomes in *Brassica napus* Haploids and Hybrids. *Plant Cell* **2009**, *21*, 373–385, doi:10.1105/tpc.108.062273.
- Niwa, O.; Shimanuki, M.; Miki, F. Telomere-Led Bouquet Formation Facilitates Homologous Chromosome Pairing and Restricts Ectopic Interaction in Fission Yeast Meiosis. *EMBO J.* **2000**, *19*, 3831–3840, doi:10.1093/emboj/19.14.3831.

- Nonomura, K.I.; Nakano, M.; Eiguchi, M.; Suzuki, T.; Kurata, N. PAIR2 Is Essential for Homologous Chromosome Synapsis in Rice Meiosis I. *J. Cell Sci.* **2006**, *119*, 217–225, doi:10.1242/jcs.02736.
- Oleszczuk, S.; Lukaszewski, A.J. The Origin of Unusual Chromosome Constitutions among Newly Formed Allopolyploids. *Am. J. Bot.* **2014**, *101*, 318–326, doi:10.3732/ajb.1300286.
- Otto, S.P.; Whitton, J. Polyploid Incidence and Evolution. *Annu. Rev. Genet.* **2000**, *34*, 401–437, doi:10.1146/annurev.genet.34.1.401.
- Page, S.L.; Hawley, R.S. The Genetics and Molecular Biology of the Synaptonemal Complex. *Annu. Rev. Cell Dev. Biol.* **2004**, *20*, 525–558, doi:10.1146/annurev.cellbio.19.111301.155141.
- Parisod, C.; Alix, K.; Just, J.; Petit, M.; Sarilar, V.; Mhiri, C.; Ainouche, M.; Chalhoub, B.; Grandbastien, M.A. Impact of Transposable Elements on the Organization and Function of Allopolyploid Genomes. *New Phytol.* **2010**, *186*, 37–45, doi:10.1111/j.1469-8137.2009.03096.x.
- Parkin, I.A.; Sharpe, A.G.; Keith, D.J.; Lydiate, D.J. Identification of the A and C Genomes of amphidiploid *Brassica napus* (Oilseed rape). *Genome* **1995**, *38*, 1122–1131, doi:10.1139/g95-149.
- Parkin, I.A.P.; Gulden, S.M.; Sharpe, A.G.; Lukens, L.; Trick, M.; Osborn, T.C.; Lydiate, D.J. Segmental Structure of the *Brassica napus* Genome Based on Comparative Analysis with *Arabidopsis thaliana*. *Genetics* **2005**, *171*, 765–781, doi:10.1534/genetics.105.042093.
- Parkin, I.A.P.; Koh, C.; Tang, H.; Robinson, S.J.; Kagale, S.; Clarke, W.E.; Town, C.D.; Nixon, J.; Krishnakumar, V.; Bidwell, S.L.; et al. Transcriptome and Methylome Profiling Reveals Relics of Genome Dominance in the Mesopolyploid *Brassica oleracea*. *Genome Biol.* **2014**, *15*, 1–18, doi:10.1186/gb-2014-15-6-r77.
- Parkin, I.A.P.; Sharpe, A.G.; Lydiate, D.J. Patterns of Genome Duplication within the *Brassica napus* Genome. *Genome* **2003**, *46*, 291–303, doi:10.1139/g03-006.
- Pecinka, A.; Fang, W.; Rehmsmeier, M.; Levy, A.A.; Mittelsten Scheid, O. Polyploidization Increases Meiotic Recombination Frequency in *Arabidopsis*. *BMC Biol.* **2011**, *9*, 24, doi:10.1186/1741-7007-9-24.
- Pecinka, A.; Fang, W.; Rehmsmeier, M.; Levy, A.A.; Mittelsten Scheid, O. Polyploidization Increases Meiotic Recombination Frequency in *Arabidopsis*. *BMC Biology* **2012**, *10*, doi:10.1186/1741-7007-10-33.
- Pelé, A.; Falque, M.; Trotoux, G.; Eber, F.; Nègre, S.; Gilet, M.; Huteau, V.; Lodé, M.; Jousseau, T.; Dechaumet, S.; et al. Amplifying Recombination Genome-Wide and Reshaping Crossover Landscapes in Brassicas. *PLoS Genet.* **2017**, *13*, e1006794, doi:10.1371/journal.pgen.1006794.
- Pelé, A.; Rousseau-Gueutin, M.; Chèvre, A.-M.M. Speciation Success of Polyploid Plants Closely Relates to the Regulation of Meiotic Recombination. *Front. Plant Sci.* **2018**, *9*, 1–9, doi:10.3389/fpls.2018.00907.
- Pradillo, M.; Knoll, A.; Oliver, C.; Varas, J.; Corredor, E.; Puchta, H.; Santos, J.L. Involvement of the Cohesin Cofactor PDS5 (SPO76) During Meiosis and DNA Repair in *Arabidopsis thaliana*. *Front. Plant Sci.* **2015**, *6*, 1–14, doi:10.3389/fpls.2015.01034.
- Prakash, S. Taxonomy, Cytogenetics and Origin of Crop Brassica, a Review. *Opera Bot.* **1980**, *55*, 1–57.
- Prakash, S.; Takahata, Y.; Kirti, P.B.; Chopra, V.L. Cytogenetics. In *Biology of Brassica coenospecies*; Gomez-Campo, C., Ed.; Elsevier Science: Amsterdam, The Netherlands, 1999; pp. 59–106, ISBN 9780080528021.
- Prieto, P.; Moore, G.; Reader, S. Control of Conformation Changes Associated with Homologue Recognition during Meiosis. *Theor. Appl. Genet.* **2005**, *111*, 505–510, doi:10.1007/s00122-005-2040-6.



- Prieto, P.; Naranjo, T. Analytical Methodology of Meiosis in Autopolyploid and Allopolyploid Plants. In *Plant Meiosis*; Pradillo, M., Heckmann, S., Eds.; Methods in Molecular Biology; Springer New York: New York, NY, USA, 2020; Volume 2061, pp. 141–168, ISBN 9781493998173.
- Prieto, P.; Shaw, P.; Moore, G. Homologue Recognition during Meiosis Is Associated with a Change in Chromatin Conformation. *Nat. Cell Biol.* **2004**, *6*, 906–908, doi:10.1038/ncb1168.
- Rajapakse, S.; Byrne, D.H.; Zhang, L.; Anderson, N.; Arumuganathan, K.; Ballard, R.E. Two Genetic Linkage Maps of Tetraploid Roses. *Theor. Appl. Genet.* **2001**, *103*, 575–583, doi:10.1007/PL00002912.
- Ramanna, M.S.; Jacobsen, E. Relevance of Sexual Polyploidization for Crop Improvement—A Review. *Euphytica* **2003**, *133*, 3–8, doi:10.1023/A:1025600824483.
- Ramsey, J.; Schemske, D.W. Neopolyploidy in Flowering Plants. *Annu. Rev. Ecol. Syst.* **2002**, *33*, 589–639, doi:10.1146/annurev.ecolsys.33.010802.150437.
- Rey, M.; Martín, A.C.; Smedley, M.; Hayta, S.; Harwood, W.; Shaw, P.; Moore, G. Magnesium Increases Homoeologous Crossover Frequency During Meiosis in ZIP4 (Ph1 Gene) Mutant Wheat-Wild Relative Hybrids. *Front. Plant Sci.* **2018**, *9*, 1–12, doi:10.3389/fpls.2018.00509.
- Rey, M.D.; Martín, A.C.; Higgins, J.; Swarbreck, D.; Uauy, C.; Shaw, P.; Moore, G. Exploiting the ZIP4 Homologue within the Wheat Ph1 Locus Has Identified Two Lines Exhibiting Homoeologous Crossover in Wheat-Wild Relative Hybrids. *Mol. Breed.* **2017**, *37*, 95, doi:10.1007/s11032-017-0700-2.
- Reyes, G.X.; Schmidt, T.T.; Kolodner, R.D.; Hombauer, H. New Insights into the Mechanism of DNA Mismatch Repair. *Chromosoma* **2015**, *124*, 443–462, doi:10.1007/s00412-015-0514-0.
- Riley, R.; Chapman, V. Genetic Control of the Cytologically Diploid Behaviour of Hexaploid Wheat. *Nature* **1958**, *182*, 713–715, doi:10.1038/182713a0.
- Roberts, M.A.; Reader, S.M.; Dalgliesh, C.; Miller, T.E.; Foote, T.N.; Fish, L.J.; Snape, J.W.; Moore, G. Induction and Characterization of Ph1 Wheat Mutants. *Genetics* **1999**, *153*, 1909–1918, doi:10.1093/genetics/153.4.1909.
- Roeder, G.S. Meiotic Chromosomes: It Takes Two to Tango. *Genes Dev.* **1997**, *11*, 2600–2621, doi:10.1101/gad.11.20.2600.
- Sánchez-Morán, E.; Benavente, E.; Orellana, J. Analysis of Karyotypic Stability of Homoeologous-Pairing (Ph) Mutants in Allopolyploid Wheats. *Chromosoma* **2001**, *110*, 371–377, doi:10.1007/s004120100156.
- Sanchez-Moran, E.; Osman, K.; Higgins, J.D.; Pradillo, M.; Cuñado, N.; Jones, G.H.; Franklin, F.C.H. ASY1 Coordinates Early Events in the Plant Meiotic Recombination Pathway. *Cytogenet. Genome Res.* **2008**, *120*, 302–312, doi:10.1159/000121079.
- Sanchez-Moran, E.; Santos, J.L.; Jones, G.H.; Franklin, F.C.H. ASY1 Mediates AtDMC1-Dependent Interhomolog Recombination during Meiosis in *Arabidopsis*. *Genes Dev.* **2007**, *21*, 2220–2233, doi:10.1101/gad.439007.
- Santos, J.L.; Alfaro, D.; Sanchez-Moran, E.; Armstrong, S.J.; Franklin, F.C.H.; Jones, G.H. Partial Diploidization of Meiosis in Autotetraploid *Arabidopsis thaliana*. *Genetics* **2003**, *165*, 1533–1540, doi:10.1093/genetics/165.3.1533.
- Schiessl, S.; Huettel, B.; Kuehn, D.; Reinhardt, R.; Snowdon, R. Post-Polyploidisation Morphotype Diversification Associates with Gene Copy Number Variation. *Sci. Rep.* **2017**, *7*, 1–18, doi:10.1038/srep41845.

- Schiessl, S.; Katche, E.; Ihien, E.; Chawla, H.S.; Mason, A.S. ScienceDirect The Role of Genomic Structural Variation in the Genetic Improvement of Polyploid Crops. *Crop J.* **2019**, *7*, 127–140, doi:10.1016/j.cj.2018.07.006.
- Schmidt, R.; Acarkan, A.; Boivin, K. Comparative Structural Genomics in the Brassicaceae Family. *Plant Physiol. Biochem.* **2001**, *39*, 253–262, doi:10.1016/S0981-9428(01)01239-6.
- Schubert, I.; Shaw, P. Organization and Dynamics of Plant Interphase Chromosomes. *Trends Plant Sci.* **2011**, *16*, 273–281, doi:10.1016/j.tplants.2011.02.002.
- Schuermann, D.; Molinier, J.; Fritsch, O.; Hohn, B. The Dual Nature of Homologous Recombination in Plants. *Trends Genet.* **2005**, *21*, 172–181, doi:10.1016/j.tig.2005.01.002.
- Sears, E.R. A Wheat Mutation Conditioning an Intermediate Level of Homoeologous Chromosome Pairing. *Can. J. Genet. Cytol.* **1982**, *24*, 715–719, doi:10.1139/g82-076.
- Sears, E.R. An Induced Mutant with Homoeologous Pairing in Common Wheat. *Can. J. Genet. Cytol.* **1977**, *19*, 585–593, doi:10.1139/g77-063.
- Sears, E.R. Genetic Control of Chromosome Pairing in Wheat. *Annu. Rev. Genet.* **1976**, *10*, 31–51, doi:10.1146/annurev.ge.10.120176.000335.
- Sears, E.R.; Okamoto, M. Intergenomic Chromosome Pairing in Hexaploid Wheat. *Proc. Int. Congr. Genet.* **1958**, *2*, 258–259.
- Seear, P.J.; France, M.G.; Gregory, C.L.; Heavens, D.; Schmickl, R.; Yant, L.; Higgins, J.D. A Novel Allele of ASY3 Is Associated with Greater Meiotic Stability in Autotetraploid *Arabidopsis lyrata*. *PLoS Genet.* **2020**, *16*, 1–21, doi:10.1371/journal.pgen.1008900.
- Serang, O.; Mollinari, M.; Garcia, A.A.F. Efficient Exact Maximum a Posteriori Computation for Bayesian SNP Genotyping in Polyploids. *PLoS ONE* **2012**, *7*, 1–13, doi:10.1371/journal.pone.0030906.
- Serra, H.; Svačina, R.; Baumann, U.; Whitford, R.; Sutton, T.; Bartoš, J.; Sourdille, P. Ph2 Encodes the Mismatch Repair Protein MSH7-3D That Inhibits Wheat Homoeologous Recombination. *Nat. Commun.* **2021**, *12*, 803, doi:10.1038/s41467-021-21127-1.
- Shen, Y.; Tang, D.; Wang, K.; Wang, M.; Huang, J.; Luo, W.; Luo, Q.; Hong, L.; Li, M.; Cheng, Z. ZIP4 in Homologous Chromosome Synapsis and Crossover Formation in Rice Meiosis. *J. Cell Sci.* **2012**, *125*, 2581–2591, doi:10.1242/jcs.090993.
- Shirasawa, K.; Tanaka, M.; Takahata, Y.; Ma, D.; Cao, Q.; Liu, Q.; Zhai, H.; Kwak, S.S.; Cheol Jeong, J.; Yoon, U.H.; et al. A High-Density SNP Genetic Map Consisting of a Complete Set of Homologous Groups in Autohexaploid Sweetpotato (*Ipomoea Batatas*). *Sci. Rep.* **2017**, *7*, 1–8, doi:10.1038/srep44207.
- Sidhu, G.K.; Warzecha, T.; Pawlowski, W.P. Evolution of Meiotic Recombination Genes in Maize and Teosinte. *BMC Genom.* **2017**, *18*, 1–17, doi:10.1186/s12864-017-3486-z.
- Silkova, O.G.; Adonina, I.G.; Krivosheina, E.A.; Shchapova, A.I.; Shumny, V.K. Chromosome Pairing in Meiosis of Partially Fertile Wheat/Rye Hybrids. *Plant Reprod.* **2013**, *26*, 33–41, doi:10.1007/s00497-012-0207-2.
- Song, K.; Lu, P.; Tang, K.; Osborn, T.C. Rapid Genome Change in Synthetic Polyploids of *Brassica* and Its Implications for Polyploid Evolution. *Proc. Natl. Acad. Sci.* **1995**, *92*, 7719–7723, doi:10.1073/PNAS.92.17.7719.

- Song, Q.; Chen, J.Z. Epigenetic and Developmental Regulation in Plant Polyploids. *Curr. Opin. Plant Biol.* **2015**, *24*, 101–109, doi:10.1016/j.pbi.2015.02.007.
- Sorrells, M.E. Development and Application of RFLPs in Polyploids. *Crop Sci.* **1992**, *32*, 1086–1091, doi:10.2135/cropsci1992.0011183x003200050003x.
- Sourdille, P.; Jenczewski, E. Homoeologous Exchanges in Allopolyploids: How *Brassica napus* Established Self-control! *New Phytol.* **2021**, *229*, 3041–3043, doi:10.1111/nph.17222.
- Stebbins, G.L. *Chromosomal Evolution in Higher Plants*; Edward Arnold Ltd.: London, UK, 1971; ISBN 9780713122879.
- Stebbins, G.L. Types of Polyploids: Their Classification and Significance. *Adv. Genet.* **1947**, *1*, 403–429, doi:10.1016/S0065-2660(08)60490-3.
- Suay, L.; Zhang, D.; Eber, F.; Jouy, H.; Lodé, M.; Huteau, V.; Coriton, O.; Szadkowski, E.; Leflon, M.; Martin, O.C.; et al. Crossover Rate between Homologous Chromosomes and Interference Are Regulated by the Addition of Specific Unpaired Chromosomes in *Brassica*. *New Phytol.* **2014**, *201*, 645–656, doi:10.1111/nph.12534.
- Sutton, T.; Whitford, R.; Baumann, U.; Dong, C.; Able, J.A.; Langridge, P. The Ph2 Pairing Homoeologous Locus of Wheat (*Triticum aestivum*): Identification of Candidate Meiotic Genes Using a Comparative Genetics Approach. *Plant J.* **2003**, *36*, 443–456, doi:10.1046/j.1365-313X.2003.01891.x.
- Svačina, R.; Sourdille, P.; Kopecký, D.; Bartoš, J. Chromosome Pairing in Polyploid Grasses. *Front. Plant Sci.* **2020**, *11*, 1–17, doi:10.3389/fpls.2020.01056.
- Sybenga, J. Chromosome Pairing Affinity and Quadrivalent Formation in Polyploids: Do Segmental Allopolyploids Exist? *Genome* **1996**, *39*, 1176–1184, doi:10.1139/g96-148.
- Sybenga, J. *Meiotic Configurations*; Springer: Berlin, Germany, 1975; ISBN 3540073477.
- Szadkowski, E.; Eber, F.; Huteau, V.; Lodé, M.; Huneau, C.; Belcram, H.; Coriton, O.; Manzaneres-Dauleux, M.J.; Delourme, R.; King, G.J.; et al. The First Meiosis of Resynthesized *Brassica napus*, a Genome Blender. *New Phytologist* **2010**, *186*, 102–112, doi:10.1111/j.1469-8137.2010.03182.x.
- Tate, J.A.; Joshi, P.; Soltis, K.A.; Soltis, P.S.; Soltis, D.E. On the Road to Diploidization? Homoeolog Loss in Independently Formed Populations of the Allopolyploid *Tragopogon miscellus* (Asteraceae). *BMC Plant Biol.* **2009**, *9*, 11, doi:10.1186/1471-2229-9-80.
- Tennessen, J.A.; Govindarajulu, R.; Ashman, T.L.; Liston, A. Evolutionary Origins and Dynamics of Octoploid Strawberry Subgenomes Revealed by Dense Targeted Capture Linkage Maps. *Genome Biol. Evol.* **2014**, *6*, 3295–3313, doi:10.1093/gbe/evu261.
- Thomas, H. Sid: A Mendelian Locus Controlling Thylakoid Membrane Disassembly in Senescing Leaves of *Festuca pratensis*. *Theor. Appl. Genet.* **1987**, *73*, 551–555, doi:10.1007/BF00289193.
- Tian, E.; Jiang, Y.; Chen, L.; Zou, J.; Liu, F.; Meng, J. Synthesis of a *Brassica* Trigenomic Allohexaploid (*B. carinata* × *B. rapa*) de Novo and Its Stability in Subsequent Generations. *Theor. Appl. Genet.* **2010**, *121*, 1431–1440, doi:10.1007/s00122-010-1399-1.
- Tiang, C.L.; He, Y.; Pawlowski, W.P. Chromosome Organization and Dynamics during Interphase, Mitosis, and Meiosis in Plants. *Plant Physiol.* **2012**, *158*, 26–34, doi:10.1104/pp.111.187161.
- Trelles-Sticken, E.; Loidl, J.; Scherthan, H. Bouquet Formation in Budding Yeast: Initiation of Recombination Is Not Required for Meiotic Telomere Clustering. *J. Cell Sci.* **1999**, *112*, 651–658, doi:10.1242/jcs.112.5.651.

- Udall, J.A.; Quijada, P.A.; Osborn, T.C. Detection of Chromosomal Rearrangements Derived from Homeologous Recombination in Four Mapping Populations of *Brassica napus* L. *Genetics* **2005**, *169*, 967–979, doi:10.1534/genetics.104.033209.
- Ukoskit, K.; Thompson, P.G. Autopolyploidy versus Allopolyploidy and Low-Density Randomly Amplified Polymorphic DNA Linkage Maps of Sweetpotato. *J. Am. Soc. Hortic. Sci.* **1997**, *122*, 822–828, doi:10.21273/JASHS.122.6.822.
- Underwood, C.J.; Choi, K.; Lambing, C.; Zhao, X.; Serra, H.; Borges, F.; Simorowski, J.; Ernst, E.; Jacob, Y.; Henderson, I.R.; et al. Epigenetic Activation of Meiotic Recombination near *Arabidopsis thaliana* Centromeres via Loss of H3K9me2 and Non-CG DNA Methylation. *Genome Res.* **2018**, *28*, 519–531, doi:10.1101/gr.227116.117.
- van Geest, G.; Bourke, P.M.; Voorrips, R.E.; Marasek-Ciolakowska, A.; Liao, Y.; Post, A.; van Meeteren, U.; Visser, R.G.F.; Maliepaard, C.; Arens, P. An Ultra-Dense Integrated Linkage Map for Hexaploid Chrysanthemum Enables Multi-Allelic QTL Analysis. *Theor. Appl. Genet.* **2017**, *130*, 2527–2541, doi:10.1007/s00122-017-2974-5.
- Viera, A.; Rufas, J.S.; Martínez, I.; Barbero, J.L.; Ortega, S.; Suja, J.A. CDK2 Is Required for Proper Homologous Pairing, Recombination and Sex-Body Formation during Male Mouse Meiosis. *J. Cell Sci.* **2009**, *122*, 2149–2159, doi:10.1242/jcs.046706.
- Vincent, J.E.; Jones, G.H. Meiosis in Autopolyploid *Crepis Capillaris* I. Triploids and Trisomics; Implications for Models of Chromosome Pairing. *Chromosoma* **1993**, *102*, 195–206, doi:10.1139/g94-069.
- Voorrips, R.E.; Gort, G.; Vosman, B. Genotype Calling in Tetraploid Species from Bi-Allelic Marker Data Using Mixture Models. *BMC Bioinform.* **2011**, *12*, 172, doi:10.1186/1471-2105-12-172.
- Waines, J.G. A Model for the Origin of Diploidizing Mechanisms in Polyploid Species. *Am. Nat.* **1976**, *110*, 415–430, doi:10.1086/283077.
- Wall, A.M.; Riley, R.; Chapman, V. Wheat Mutants Permitting Homoeologous Meiotic Chromosome Pairing. *Genet. Res.* **1971**, *18*, 311–328, doi:10.1017/S0016672300012714.
- Wang, K.; Wang, M.; Tang, D.; Shen, Y.; Miao, C.; Hu, Q.; Lu, T.; Cheng, Z. The Role of Rice HEI10 in the Formation of Meiotic Crossovers. *PLoS Genet.* **2012**, *8*, e1002809, doi:10.1371/journal.pgen.1002809.
- Weiss, H.; Maluszynska, J. Chromosomal Rearrangement in Autotetraploid Plants of *Arabidopsis thaliana*. *Hereditas* **2001**, *133*, 255–261, doi:10.1111/j.1601-5223.2000.00255.x.
- West, A.M.; Rosenberg, S.C.; Ur, S.N.; Lehmer, M.K.; Ye, Q.; Hagemann, G.; Caballero, I.; Usón, I.; MacQueen, A.J.; Herzog, F.; et al. A Conserved Filamentous Assembly Underlies the Structure of the Meiotic Chromosome Axis. *eLife* **2019**, *8*, 1–27, doi:10.7554/eLife.40372.
- Whitford, R. *From Intimate Chromosome Associations to Wild Sex in Wheat (Triticum aestivum)*; University of Adelaide: Adelaide, Australia, 2002.
- Wolf, P.G.; Soltis, P.S.; Soltis, D.E. Tetrasomic Inheritance and Chromosome Pairing Behaviour in the Naturally Occurring Autotetraploid *Heuchera Grossulariifolia* (Saxifragaceae). *Genome* **1989**, *32*, 655–659, doi:10.1139/g89-494.
- Woodhouse, M.R.; Cheng, F.; Pires, J.C.; Lisch, D.; Freeling, M.; Wang, X. Origin, Inheritance, and Gene Regulatory Consequences of Genome Dominance in Polyploids. *Proc. Natl. Acad. Sci.* **2014**, *111*, 6527–6527, doi:10.1073/pnas.1405833111.

- Wu, J.H.; Datson, P.M.; Manako, K.I.; Murray, B.G. Meiotic Chromosome Pairing Behaviour of Natural Tetraploids and Induced Autotetraploids of *Actinidia Chinensis*. *Tag. Theor. Appl. Genet. Theor. Angew. Genet.* **2014**, *127*, 549–557, doi:10.1007/s00122-013-2238-y.
- Wu, K.K.; Burnquist, W.; Sorrells, M.E.; Tew, T.L.; Moore, P.H.; Tanksley, S.D. The Detection and Estimation of Linkage in Polyploids Using Single-Dose Restriction Fragments. *Theor. Appl. Genet.* **1992**, *83*, 294–300, doi:10.1007/BF00224274.
- Xiong, Z.; Gaeta, R.T.; Pires, J.C. Homoeologous Shuffling and Chromosome Compensation Maintain Genome Balance in Resynthesized Allopolyploid *Brassica napus*. *Proc. Natl. Acad. Sci. USA* **2011**, *108*, 7908–7913, doi:10.1073/pnas.1014138108.
- Yamamoto, E.; Shirasawa, K.; Kimura, T.; Monden, Y.; Tanaka, M.; Isobe, S. Genetic Mapping in Autohexaploid Sweet Potato with Low-Coverage NGS-Based Genotyping Data. *bioRxiv* **2019**, *10*, 2661–2670, doi:10.1101/789198.
- Yang, J.; Moeinzadeh, M.H.; Kuhl, H.; Helmuth, J.; Xiao, P.; Haas, S.; Liu, G.; Zheng, J.; Sun, Z.; Fan, W.; et al. Haplotype-Resolved Sweet Potato Genome Traces Back Its Hexaploidization History. *Nat. Plants* **2017**, *3*, 696–703, doi:10.1038/s41477-017-0002-z.
- Yang, T.J.; Kim, J.S.; Kwon, S.J.; Lim, K.B.; Choi, B.S.; Kim, J.A.; Jin, M.; Park, J.Y.; Lim, M.H.; Kim, H. II; et al. Sequence-Level Analysis of the Diploidization Process in the Triplicated FLOWERING LOCUS C Region of *Brassica rapa*. *Plant Cell* **2006**, *18*, 1339–1347, doi:10.1105/tpc.105.040535.
- Yant, L.; Hollister, J.D.; Wright, K.M.; Arnold, B.J.; Higgins, J.D.; Franklin, F.C.H.; Bomblies, K. Meiotic Adaptation to Genome Duplication in *Arabidopsis Arenosa*. *Current biology : CB* **2013**, *23*, 2151–2156, doi:10.1016/j.cub.2013.08.059.
- Yelina, N.E.; Lambing, C.; Hardcastle, T.J.; Zhao, X.; Santos, B.; Henderson, I.R. DNA Methylation Epigenetically Silences Crossover Hot Spots and Controls Chromosomal Domains of Meiotic Recombination in *Arabidopsis*. *Genes Dev.* **2015**, *29*, 2183–2202, doi:10.1101/gad.270876.115.
- You, Q.; Yang, X.; Peng, Z.; Islam, M.S.; Sood, S.; Luo, Z.; Comstock, J.; Xu, L.; Wang, J. Development of an Axiom Sugarcane100K SNP Array for Genetic Map Construction and QTL Identification. *Theor. Appl. Genet.* **2019**, *132*, 2829–2845, doi:10.1007/s00122-019-03391-4.
- Zamariola, L.; Tiang, C.L.; De Storme, N.; Pawlowski, W.; Geelen, D. Chromosome Segregation in Plant Meiosis. *Front. Plant Sci.* **2014**, *5*, 1–19, doi:10.3389/fpls.2014.00279.
- Zhang, H.; Bian, Y.; Gou, X.; Zhu, B.; Xu, C.; Qi, B.; Li, N.; Rustgi, S.; Zhou, H.; Han, F.; et al. Persistent Whole-Chromosome Aneuploidy Is Generally Associated with Nascent Allohexaploid Wheat. *Proc. Natl. Acad. Sci. USA* **2013**, *110*, 3447–3452, doi:10.1073/pnas.1300153110.
- Zhang, L.Q.; Yen, Y.; Zheng, Y.L.; Liu, D.C. Meiotic Restriction in Emmer Wheat Is Controlled by One or More Nuclear Genes That Continue to Function in Derived Lines. *Sex. Plant Reprod.* **2007**, *20*, 159–166, doi:10.1007/s00497-007-0052-x.
- Zheng, T.; Nibau, C.; Phillips, D.W.; Jenkins, G.; Armstrong, S.J.; Doonan, J.H. CDKG1 Protein Kinase Is Essential for Synapsis and Male Meiosis at High Ambient Temperature in *Arabidopsis thaliana*. *Proc. Natl. Acad. Sci. USA* **2014**, *111*, 2182–2187, doi:10.1073/pnas.1318460111.
- Zhou, J.; Tan, C.; Cui, C.; Ge, X.; Li, Z. Distinct Subgenome Stabilities in Synthesized *Brassica* Allohexaploids. *Theor. Appl. Genet.* **2016**, *129*, 1257–1271, doi:10.1007/s00122-016-2701-7.

- Zickler, D.; Kleckner, N. Meiotic Chromosomes: Integrating Structure and Function. *Annu. Rev. Genet.* **1999**, *33*, 603–754, doi:10.1146/annurev.genet.33.1.603.
- Zickler, D.; Kleckner, N. Recombination, Pairing, and Synapsis of Homologs during Meiosis. *Cold Spring Harb. Perspect. Biol.* **2015**, *7*, a016626, doi:10.1101/cshperspect.a016626.
- Zielinski, M.-L.; Mittelsten Scheid, O. Meiosis in Polyploid Plants. In *Polyploidy and Genome Evolution*; Soltis, P., Soltis, D.E., Eds.; Springer: Berlin/Heidelberg, Germany, 2012; Volume 3 , pp. 33–55, ISBN 9783642314421.
- Ziolkowski, P.A.; Underwood, C.J.; Lambing, C.; Martinez-Garcia, M.; Lawrence, E.J.; Ziolkowska, L.; Griffin, C.; Choi, K.; Franklin, F.C.H.; Martienssen, R.A.; et al. Natural Variation and Dosage of the HEI10 Meiotic E3 Ligase Control *Arabidopsis* Crossover Recombination. *Genes Dev.* **2017**, *31*, 306–317, doi:10.1101/gad.295501.116.

### 3. IN SITU EVIDENCE OF GENOMIC RELATIONSHIPS AMONG THE FOUNDING ANCESTRAL GENOMES OF *SACCHARUM* SPP.<sup>2</sup>

#### Abstract

*Saccharum spontaneum*, *S. robustum* and *S. officinarum* are the founding polyploid genomes of the modern varieties of sugarcane (*Saccharum* spp.). The crop is one of the world's major sugar and biomass-producing crops, potential sources of renewable energy. Understanding the genomic relationships among the founding genomes is crucial if we are to develop disease/drought resistant varieties to counter the threat posed by climate change. *Saccharum* cytogenetics is a growing field and significant progress has been achieved particularly in *S. spontaneum* ( $x = 8$ ,  $2n = 8x = 64$ ) and *S. officinarum* ( $x = 10$ ,  $2n = 8x = 80$ ). However, only a few studies on *S. robustum* ( $x = 10$ ,  $2n = 6-20x = 60-200$ ) have been conducted, which is thought to be the wild ancestor of *S. officinarum*, a legitimate species, commonly known as noble cane. Herein, using fluorescent *in situ* hybridization with centromeric probes we found clear evidence that *S. robustum* meiosis is regular ( $2n = 100$ ), exhibiting 50 bivalents, with no univalents or multivalent associations. In addition, using genomic *in situ* hybridization, we found a close relationship between *S. robustum* and *S. officinarum*, and divergence from *S. spontaneum*.

Keywords: In situ hybridization · Meiosis · *Saccharum robustum* · sugarcane

#### 3.1. Introduction

*Saccharum* species originated in Papua New Guinea. The earliest record of domestication dates back to around 8,000 BCE. Cultivation gradually spread along human migration routes to Southeast Asia and India. This long history of cultivation has facilitated the generation of a diversified germplasm, including the modern varieties of sugarcane (*Saccharum* spp.) conserved by vegetative means at experimental stations worldwide. The *Saccharum* complex comprises two wild species (*S. spontaneum* and *S. robustum*) and four cultivated species (*S. officinarum*, known as noble cane, *S. barberi*, *S. sinense* and *S. edule*). The last three have been accorded the status of species, but there is a consensus to consider them as cultigens (see Irvine 1999; Grivet et al. 2004; Grivet et al. 2006). *Saccharum robustum* is thought to be the wild ancestor of *S. officinarum*. They share the same geographical origin and are closely related (Lu et al. 1994; Schenck 2004; Zhang et al. 2018; Pompidor et al. 2021). Importantly, *S. spontaneum* ( $x = 8, 9, 10$ ), *S. robustum* ( $x = 10$ ) and *S. officinarum* ( $x = 10$ ) are the founding polyploid genomes of the modern varieties of sugarcane (Piperidis and D'Hont 2020). Understanding the genomic relationships in *Saccharum* is crucial if we are to develop disease/drought resistant varieties to counter the threat posed by climate change (see Thirugnanasambandam et al. 2022).

Classical and molecular cytogenetics have played a major role in elucidating *Saccharum* species classification, genome structure and evolution (see Wang et al. 2022). For instance, genomic *in situ* hybridization (GISH) is fast becoming the method of choice for identifying sugarcane parental chromosomes, verifying the occurrence of chromosomal rearrangements, and comparing physical and genetic maps<sup>13,14,58-60</sup>. In this study, we used FISH to investigate

---

<sup>2</sup> The text corresponds to that of the article published by Soares et al. (2023) in *Brazilian Journal of Botany*.

male meiosis in *S. robustum*, including chromosome association at diakinesis, and GISH to infer the genomic relationships of *S. robustum* with *S. officinarum* and *S. spontaneum*.

### 3.2. Material and Methods

The following genotypes were used: (i) “NG5712” ( $2n = 100$ ,  $x = 10$ , a decaploid accession), (ii) “Caiana Fita” ( $2n = 80$ ,  $x = 10$ , an octaploid accession) and (iii) “SES205A” ( $2n = 64$ ,  $x = 8$ , an octaploid accession), representatives of *S. robustum*, *S. officinarum* and *S. spontaneum* respectively. Immature panicles and leaves of *S. robustum* were collected from field plants kept at the Sugarcane Hybridization Station (Agronomic Institute) in Uruçuca ( $14^{\circ}35'34''$  S,  $3917'2''$  W), Bahia State, Brazil. Sugarcane stalks were collected from *S. officinarum*, and *S. spontaneum* field plants kept at Escola Superior de Agricultura "Luiz de Queiroz" in Piracicaba ( $22^{\circ}43'31''$  S,  $47^{\circ}38'57''$  W), São Paulo State, Brazil.

#### 3.2.1. Microsporogenesis and chromosome association analysis in *S. robustum*

Immature inflorescences were fixed in Carnoy solution for 24 h at room temperature. The fixative solution was then replaced with a 70% ethanol solution, and flasks stored at  $4^{\circ}\text{C}$ . Slides were prepared using a standard protocol (Sharma and Sharma 1980). Meiotic cells from metaphase I to telophase II (including tetrads) were analyzed, and images captured using an OPTIKAM B3 camera (Optika) and Adobe Photoshop CS5 software (Adobe Systems). The percentage of cells with chromosome irregularities was estimated for a total of 347 cells.

Anthers containing cells at diakinesis were selected and slides prepared according to Murata and Motoyoshi (1995) and Vieira et al. (2018), with modifications. The slides were examined under high-contrast microscopy (Nikon E200) and selected for hybridization. Chromosome pairing was investigated, and centromeres detected using *in situ* hybridization with fluorescent probes. First, genomic DNA from *S. robustum* was extracted using the CTAB method described in Vieira et al. (2018), quantified with a Qubit4 Fluorometer (Invitrogen), and integrity was verified after standard agarose gel (1.2% w/v) electrophoresis stained with SYBR Safe  $0.5 \times$  (Invitrogen).

A primer pair designed to amplify sugarcane CENT repeats (137 bp) was then used (CENT1F: CATCGGGTGCGTCCAAAATG and CENT1R: CGTACCATAGGCTCATAATCC) <sup>53,63</sup> and the amplification reaction carried out according Oliveira et al. (2022). Standard gel electrophoresis was run to check the size of the PCR products, which were then purified using a Wizard SV Gel and PCR Clean-Up System kit (Promega). Purified products were labeled using a DIG-nick translation labeling kit (Roche) with digoxigenin-11-dUTP, following the manufacturer's instructions. FISH procedures were carried out according to Schwarzacher and Heslop-Harrison (2000) as detailed in Oliveira et al. (2022). The CENT probe was detected with anti-digoxigenin conjugated to rhodamine (Roche). Slides were assembled in DAPI-Vectashield (Vector Labs). Images at diakinesis were captured using a DFC365 FX digital camera (Leica) coupled to a DM 4000B fluorescence microscope (Leica). After processing selected images, the hybridization sites of the top 10 cells were analyzed to determine chromosome associations.



### 3.2.2. Mitotic chromosome preparation and genomic *in situ* hybridization (GISH)

*S. officinarum* and *S. spontaneum* sugarcane stalks were placed on trays containing damp sphagnum moss and kept at  $28^{\circ}\text{C}\pm 3^{\circ}\text{C}$  to induce rooting. Roots (~2 cm long) were excised and pre-treated with a blocking solution of 8-hydroxyquinoline (0.03% w/v; Sigma) and cycloheximide (25 ppm; Cayaman Chemical) (4h:30min, room temperature). The roots were then fixed and stored as mentioned above and prepared according to the protocol in Oliveira et al. (2022). Slides were examined under an Olympus BX50 microscope.

*S. robustum* genomic DNA was extracted, quantified and checked for integrity as mentioned above. DNA was labeled using the DIG-nick translation labeling kit (Roche) with digoxigenin-11-dUTP, following the manufacturer's instructions. For GISH analysis, previous protocols optimized for sugarcane were used (D'Hont et al. 1996; Piperidis et al. 2010; Oliveira et al. 2022). *S. robustum* labeled probes were detected with sheep anti-digoxigenin TRITC (Roche Biochemicals). Slides were mounted using Vectashield with 4',6-diamidino-2-phenylindole (DAPI) (Vector Labs). Mitotic chromosome images were captured by a DFC365 FX digital camera (Leica) coupled to a DM 4000B fluorescence microscope (Leica). After processing selected images, the hybridization patterns of the top 10 cells were analyzed to determine genomic affinity.

## 3.3. Results and Discussion

### 3.3.1. Microsporogenesis and chromosome association in *Saccharum robustum*

*Saccharum* cytogenetics is a growing field. Significant progress has been made since the early 1990s (see review in Wang et al. 2022). However, only a few cytogenetic studies on *S. robustum* have been conducted, most of them focusing on chromosome counting (Price 1957; 1965), classical microsporogenesis analysis (Moriya 1944) and basic chromosome number determination (D'Hont et al. 1998).

*S. robustum* exhibits very regular microsporogenesis. Irregularities were detected in only a few cells and consisted exclusively of asynchronous behavior during the second division, i.e., prophase/metaphase and metaphase/anaphase (Supplemental Table 1). Centromeric probes used to unveil chromosome associations revealed intense fluorescent signals and 50 bivalents, with no univalents or multivalent associations (Fig. 11 a-c). Our findings corroborate the classic paper by Moriya (1944) in which no irregularities and only bivalents were visualized in the 28 NG 251 genotype ( $2n = 80$ ). This is the only existing report on *S. robustum* meiotic behavior. When compared to the meiotic data available for *Saccharum* species, *S. robustum* is closer to *S. officinarum*, both have the same basic chromosome number  $x = 10$  and exhibit a regular microsporogenesis, where abnormalities were found in only less than 6% of cells, which is acceptable for an autopolyploid origin. In addition, the bivalent configuration prevailed for both species at diakinesis. However, *S. spontaneum* differs in all meiotic aspects, with basic chromosome number varying from  $x=8,9,10$ , being 8 the most common (Meng et al. 2020), and exhibiting over 50% of meiotic cells with irregularities, including univalent chromosomes during diakinesis (see Vieira et al. 2018; Oliveira et al. 2022).

### 3.3.2. Genomic relationships among the founding ancestral genomes using GISH

*S. robustum* DNA probes were hybridized on mitotic chromosome preparations of *S. officinarum* ( $x = 10$ ,  $2n = 8x = 80$ ) and *S. spontaneum* ( $x = 8$ ,  $2n = 8x = 64$ ). *S. officinarum* is thought to have evolved from *S. robustum* ( $x = 10$ ,  $2n = 6-20x = 60-200$ ). Our findings reveal that all 80 chromosomes of *S. officinarum* were fully labeled using the *S. robustum* probe, evidence of closely related species. All chromosome segments without exception exhibited hybridization (Fig. 11 d-f). In *S. spontaneum*, however, all 64 chromosomes were sparsely labeled by the *S. robustum* probe, primarily in telomeric and centromeric regions (Fig. 11 g-i). Telomeres are well-conserved sequences consisting of short minisatellites in tandem (see Watson and Riha 2010), matching the signals exhibited in *S. spontaneum*. The SCEN-like satellite is relatively conserved in the centromeres of *S. spontaneum*, *S. robustum*, *S. officinarum*, and modern sugarcane cultivars (Zhang et al. 2017).

Recently, conclusive proof has been found that *S. officinarum*, *S. robustum* and *S. spontaneum* are the founding ancestral genomes of sugarcane (Pompidor et al. 2021). Vital studies based on transcriptome-derived SNPs suggest that *S. officinarum* and *S. robustum* diverged about 385,000 years ago (well before the advent of agriculture in Papua New Guinea), and the whole-genome duplication events occurred after the speciation event, as evidenced by shared interchromosomal rearrangements. On the other hand, the common ancestor of *S. officinarum* diverged from *S. spontaneum* about 769,000 years ago, close to the divergence event between *S. robustum* and *S. spontaneum* (see Zhang et al. 2018). Our findings provide further evidence that there was a close relationship between *S. robustum* and *S. officinarum* but divergence from *S. spontaneum*.

Thus, cytological analysis provides an additional method for studying chromosomal evolution, which might give new insights into the genomic structure of sugarcane and increase our understanding of sugarcane evolution, which has a direct impact on sugarcane breeding programs.

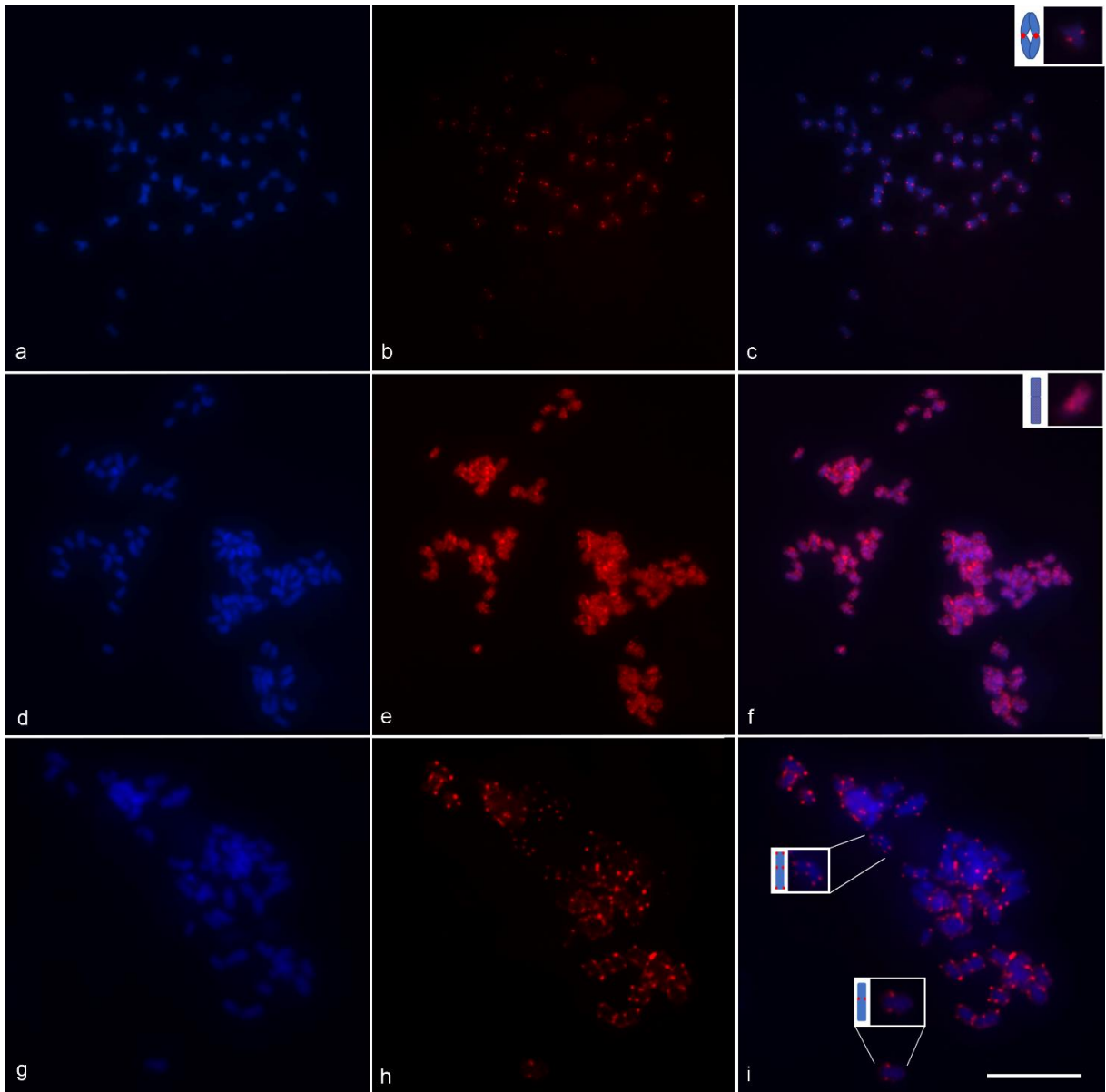


**Figure 3. Fluorescent *in situ* hybridization with centromeric probes on *Saccharum robustum* cells at diakinesis.** (a) Chromosomes stained with DAPI (blue); (b) Centromeric sites hybridized with the CENT probe detected with anti-DIG-rhodamine (red); (c) Merged images (a/b) showing 50 bivalents. The scheme represents a bivalent with the 2 centromeres in red. The inset shows a typical bivalent. Genomic *in situ* hybridization of *Saccharum officinarum* and *Saccharum spontaneum* mitotic chromosome preparations using labeled genomic DNA of *S. robustum*. (d) Mitotic metaphase of *S. officinarum* counterstained with DAPI; (e) red fluorescence (TRITC) indicates full hybridization with *S. robustum* DNA; (f) Merged images (d/e). The scheme represents. The inset shows the chromosome fully hybridized. (g) Mitotic metaphase of *S. spontaneum* counterstained with DAPI; (h) red fluorescence (TRITC) indicates localized hybridization with *S. robustum* DNA; (i) Merged images (g/h). The inset shows typical hybridized telomeric/centromeric regions. Bar, 10  $\mu$ m

## References

- D'Hont A (2005) Unraveling the genome structure of polyploids using FISH and GISH; examples of sugarcane and banana. *Cytogenet Genome Res* 109:27–33. <https://doi.org/10.1159/000082378>
- D'Hont A, Grivet L, Feldmann P, et al (1996) Characterisation of the double genome structure of modern sugarcane cultivars (*Saccharum* spp.) by molecular cytogenetics. *Mol Gen Genet* 250:405–413. <https://doi.org/10.1007/BF02174028>
- D'Hont A, Ison D, Alix K, et al (1998) Determination of basic chromosome numbers in the genus *Saccharum* by physical mapping of ribosomal RNA genes. *Genome* 41:221–225. <https://doi.org/10.1139/gen-41-2-221>
- D'Hont A, Paulet F, Glaszmann JC (2002) Oligoclonal interspecific origin of “North Indian” and “Chinese” sugarcanes. *Chromosome Res* 10:253–62. <https://doi.org/10.1023/a:1015204424287>
- Lu YH, D'Hont A, Walker DIT, et al (1994) Relationships among ancestral species of sugarcane revealed with RFLP using single copy maize nuclear probes. *Euphytica* 78:7–18. <https://doi.org/10.1007/BF00021393>
- Meng Z, Han J, Lin Y, et al (2020) Characterization of a *Saccharum spontaneum* with a basic chromosome number of  $x = 10$  provides new insights on genome evolution in genus *Saccharum*. *Theoretical and Applied Genetics* 133:187–199. <https://doi.org/10.1007/s00122-019-03450-w>
- Moriya A (1944) Contributions to the cytology of Genus *Saccharum*. *Cytologia (Tokyo)* 13:265–269. <https://doi.org/10.1508/cytologia.13.265>
- Murata M, Motoyoshi F (1995) Floral chromosomes of *Arabidopsis thaliana* for detecting low-copy DNA sequences by fluorescence in situ hybridization. *Chromosoma* 1995 104:1 104:39–43. <https://doi.org/10.1007/BF00352224>
- Nagaki K, Tsujimoto H, Sasakuma T (1998) A novel repetitive sequence of sugarcane, SCEN family, locating on centromeric regions. *Chromosome Research* 1998 6:4 6:295–302. <https://doi.org/10.1023/A:1009270824142>
- Oliveira GK, Soares NR, Costa ZP, et al (2022) Anormalidades meióticas na cana-de-açúcar (*Saccharum* spp.): Evidência de inversões peri e paracêntricas. *Res Sq.* <https://doi.org/https://doi.org/10.21203/rs.3.rs-2216232/v1>
- Piperidis G, Piperidis N, D'Hont A (2010) Molecular cytogenetic investigation of chromosome composition and transmission in sugarcane. *Molecular Genetics and Genomics* 284:65–73. <https://doi.org/10.1007/s00438-010-0546-3>
- Piperidis N, D'Hont A (2020) Sugarcane genome architecture decrypted with chromosome-specific oligo probes. *The Plant Journal* 103:2039–2051. <https://doi.org/10.1111/tpj.14881>
- Price S (1957) Cytological studies in *Saccharum* and allied genera. *Cytologia (Tokyo)* 22:40–52. <https://doi.org/10.1508/cytologia.22.40>
- Price S (1965) Cytology of *Saccharum robustum* and related sympatric species and natural hybrids
- Schenck S (2004) Genetic diversity and relationships in native Hawaiian *Saccharum officinarum* sugarcane. *Journal of Heredity* 95:327–331. <https://doi.org/10.1093/jhered/esh052>
- Schwarzacher T, Heslop-Harrison P (2000) Practical in situ hybridization. BIOS Scientific Publishers Ltd
- Sharma AK, Sharma A (1980) Chromosome techniques: theory and practice, 3rd edn. Elsevier

- Vieira MLC, Almeida CB, Oliveira CA, et al (2018) Revisiting meiosis in sugarcane: chromosomal irregularities and the prevalence of bivalent configurations. *Front Genet* 9:1–12. <https://doi.org/10.3389/fgene.2018.00213>
- Wang K, Zhang H, Khurshid H, et al (2022) Past and recent advances in sugarcane cytogenetics. *Crop J.* <https://doi.org/10.1016/J.CJ.2022.08.004>
- Watson JM, Riha K (2010) Comparative biology of telomeres: Where plants stand. *FEBS Lett* 584:3752–3759. <https://doi.org/10.1016/j.febslet.2010.06.017>
- Zhang J, Zhang Q, Li L, et al (2018) Recent polyploidization events in three *Saccharum* founding species. *Plant Biotechnol J* 17:264–274. <https://doi.org/10.1111/pbi.12962>
- Zhang W, Zuo S, Li Z, et al (2017) Isolation and characterization of centromeric repetitive DNA sequences in *Saccharum spontaneum*. *Sci Rep* 7:41659. <https://doi.org/10.1038/srep41659>

## 4. FIRST INVESTIGATION OF GENETIC CONTROL OF MEIOSIS IN SUGARCANE

### Abstract

Sugarcane (*Saccharum* spp.) has one of the most complex genomes. Modern varieties are highly polyploids and aneuploids, resulting from hybridization between *Saccharum officinarum* and *S. spontaneum*. Research on the meiotic control in polyploid species is limited, except for the wheat *Ph1* locus, carrying the gene *ZIP4* (*TaZIP4-B2*) which promotes pairing between homologous chromosomes, whilst suppressing crossover between homoeologues. In sugarcane, despite its interspecific origin, bivalent association is favored, and multivalents, if they occur, are resolved at the end of prophase I. Thus, our aim here was to investigate the supposedly genetic control of meiosis in the parental species and sugarcane. We have investigated the *ZIP4* gene and performed the immunolocalization of the synaptonemal complex proteins ZYP1 and ASY1. The sugarcane *ZIP4* gene is located on chromosome 2 and it is expressed more abundantly in flowers, a similar profile to that found for *TaZIP4-B2*. The *ZIP4* expression level is higher in *S. spontaneum* an neo-autopolyploid, and less expressed in *S. officinarum*, a stable octoploid species. The sugarcane *ZIP4* protein contains a TPR domain, essential for its scaffolding function. Its 3D-structure was also predicted. Likewise, it was very similar to that of *TaZIP4-B2*, may reflecting their function relatedness. The immunolocalization of the ASY1 and ZYP1 proteins revealed that *S. officinarum* completes synapsis. However, in *S. spontaneum* and SP80-3280 (a modern variety), no nuclei with complete synapsis were observed. Importantly, our results have implications for sugarcane genetic mapping and genomics, whose understanding of inheritance and genome organization remain somewhat obscure.

Keywords: *Saccharum*, Meiosis, ZIP4, Synapsis

### 4.1. Introduction

Sugarcane (*Saccharum* spp.) is an important economic crop, on average, it accounts for nearly 80% of global sugar production (<https://www.isosugar.org/sugarsector/sugar>) and is one of the main crop used as source of biomass to producing biofuels (sugar-based ethanol) and co-generating electricity (cane bagasse) (Long et al., 2015; Kline et al., 2017). Sugarcane originated in Papua, New Guinea. The region is one of the centers of early plant domestication, around 8,000 BCE, including sugarcane with subsequent dispersal in Southeast Asia, India, and China (see Denham, 2011). Its long history of cultivation has generated a diversified germplasm.

The *Saccharum* complex consists of two wild species, *S. spontaneum* ( $2n = 8x = 40-128$ ,  $x = 8, 9$  or  $10$ ) and *S. robustum* ( $2n = 60$ ,  $x = 10, 80$  to  $200$ ), and four cultivated species, *S. officinarum* ( $2n = 8x = 80$ ,  $x = 10$ ), *S. sinense*, *S. barberi* and *S. edule*, all polyploids. *S. robustum* is the most likely precursor of sugarcane and anthropic selection of plants with sweet juice and low fiber produced the first *S. officinarum* clones.

Subsequently, selection practices resulted in *S. officinarum* clones with a high sugar content, known as noble canes (Simmonds, 1975). In the late 19th century, new varieties emerged from interspecific hybridization between representatives of the noble canes and the wild *S. spontaneum*, the latter chosen due to ratooning capability and resistance to diseases (see Barreto et al., 2021; Cheavegatti-Gianotto et al., 2011; Grivet et al., 2004). These hybrids

were then successively backcrossed with *S. officinarum* to recover the sucrose content, a process that was called ‘nobilization’. In the first generations, the hybrid progenies received unreduced ( $2n$ ) gametes from *S. officinarum* and  $n$  gametes from *S. spontaneum* (Bielig et al., 2003; Bremer, 1961; Price, 1961), which accelerate the overrepresentation of the *S. officinarum* genome in the modern varieties which were released few generations (7, 8) after the interspecific cross. The resulting modern cultivars/varieties have a polyploid and aneuploid genome of interspecific constitution produced by human intervention, and with a complexity that exceeds most crops (Gouy et al., 2013). Current varieties have variable chromosome number ( $2n = 110$  to  $130$ ). According to molecular cytogenetic analysis, *S. officinarum* and *S. spontaneum* account respectively for 75-85% and 15-25% of their chromosomes, plus ~10% of recombinants, generated due to synapsis and crossover (CO) occurrences involving homoeologous chromosomes (Cuadrado, 2004; D’Hont et al., 1996; Piperidis et al., 2010; Piperidis & D’Hont, 2020).

From a meiotic point of view, classical cytogenetic analyses suggest that both parental species and interspecific hybrids predominantly form bivalents (Burner, 1991; Nair, 1975; Price, 1963a, 1963b; Suzuki, 1941). Recently, our group performed a comparative analysis of the meiotic behavior in one representative of the two species *S. officinarum* (clone Caiana Fita) and *S. spontaneum* (clone SES205A) and the Brazilian variety SP80-3280 (Oliveira et al., 2023). The two latter exhibited several abnormalities, while *S. officinarum*, a stable octoploid species, showed a regular meiotic chromosome segregation. Using centromeric probes and fluorescent in situ hybridization (FISH) allowed us to enumerate the bivalents, which prevailed, although in *S. spontaneum* and SP80-3280, up to 2 and 4 univalents were found in diakinesis, respectively. Furthermore, we also visualized the presence of dicentric chromosomes and a pericentric inversion that was evidenced in pachytene. In the same study, using genomic in situ hybridization (GISH), we have also determined the origin of lagging chromosomes. They were mainly detected from *S. spontaneum* and from interspecific recombination events, suggesting that there is a coordinated, not at random, meiotic chromosome segregation (Oliveira et al., 2023). Altogether, our previous studies have pointed to mechanisms regulating meiosis that need to be investigated in depth.

Meiosis is well studied in diploids, e.g., Arabidopsis, rice, maize, barley and tomato, however, in polyploid species, there are fewer studies, mainly focused on Brassica species and wheat (Wang et al., 2021). The example of cultivated wheat (*Triticum aestivum*,  $2n = 6x = 42$ , AABBDD) is noteworthy: it is a relatively recent allopolyploid (it dates to 8,000 BEC), whose ancestral genomes are syntenic and collinear (International Wheat Genome Sequencing Consortium, 2018). Despite the significant similarity between the homoeologous, wheat behaves as a diploid during meiosis, with every chromosome synapsing and recombining only with its true homolog. This phenotypic behavior has been predominantly attributed to the Ph1 locus (Pairing homoeologous 1) (Riley & Chapman, 1958; Sears, 1976). The Ph1 locus was lately assigned to a region on chromosome 5B containing a duplicated 3B chromosome segment carrying the major meiotic gene ZIP4 (TaZIP4-B2) (Al-Kaff et al., 2008; Griffiths et al., 2006; Martín et al., 2014, 2017; Rey et al., 2018). Previous studies showed that TaZIP4-B2 promotes pairing and synapsis between wheat homologous chromosomes, whilst suppressing CO between homoeologous chromosomes (Martín et al., 2017, 2021; Rey et al., 2017). The ZIP4 protein belongs to the ZMM group of proteins that bind to and stabilize CO-specific DNA intermediates that are formed during homologous recombination (Chelysheva et al., 2007; Lynn et al., 2007; Tsubouchi et al., 2006). In yeast, the ZIP4 protein acts as a scaffold (via tetratricopeptide repeats - TPRs) for the formation of multi-protein complexes, and it connects meiotic CO formation to the assembly of the synaptonemal complex (SC) (De Muyt et al., 2018; Pyatnitskaya et al., 2022).

During meiosis, homologous chromosomes are synapsed along their length by a proteinaceous structure, the synaptonemal complex (SC) (Zickler, 2006). It regulates cessation of DNA double-strand breaks, stabilizes homologous pairing and limits CO formation, ensuring normal interference-dependent CO patterning (Lenormand et al., 2016). The tripartite organization of SC is well-known, consisting of lateral elements (LEs) that hold the homologous sister chromatids together, a central element (CE) along the midline and an array of transverse filaments (TFs) that interconnect LEs generating a zipper-like structure (Gao & Colaiácovo, 2018). In higher plants, the protein ASY1 temporally associates with the meiotic chromosome axis, forming the LE, it stabilizes the axial core and CO formation (Armstrong et al., 2002; Cuacos et al., 2021). The ZYP1 protein, on the other hand, form parallel homodimers which overlap in the central space of the SC, where they associate with the LE, ensuring alignment and synapsis between homologous chromosomes (France et al., 2021; Capilla Perez et al., 2021).

In sugarcane, bivalent association is favored, and multivalents, a common meiotic irregularity in neo-polyploids, are resolved by the end of pachytene, forming bivalents due to the suppression of homeologous COs. Therefore, the hypothesis made is that a mechanism favoring regular chromosome segregation is put into action in the generations that followed the interspecific hybridization (*S. officinarum* × *S. spontaneum*) and the ‘nobilization’ process, very possibly when the genotypes begin to transmit  $n + n$  chromosomes (Vieira et al., 2018).

Our aim here was to investigate the supposedly genetic control of meiosis in sugarcane. We have identified the ZIP4 gene in both parental species (*S. officinarum* and *S. spontaneum*) and in two current varieties (R570 and SP80-3280), analyzing both gene and protein sequence conservation, protein domains, TPR distribution and predicting the 3D-protein structure. We have also investigated the ZIP4 level of expression in different sugarcane tissues. Using immunocytology, we were able to determine the SC polymerization during prophase I, using ASY1 and ZYP1 sugarcane specific antibodies, revealing synapsis defects in all genotypes, excepting *S. officinarum*. Our findings, in addition to being original, will have implications for sugarcane genetic mapping, genomics and molecular cytogenetics, since the crop is of commercial relevance, whose understanding of the agronomic trait architecture and inheritance and genome organization remain somewhat obscure.

## 4.2. Experimental procedures

### 4.2.1. Plant material

The following plant material was investigated: (i) the clone Caiana Fita ( $2n = 8x = 80$ ,  $x = 10$ ), representative of *Saccharum officinarum*; (ii) the clone SES205A ( $2n = 8x = 64$ ,  $x = 8$ ), representative of *S. spontaneum* and (iii) the Brazilian variety SP80-3280 ( $2n = 112$ ). Immature panicles (pre-emerged inflorescences still wrapped in the flag leaf sheath) from *S. officinarum* was collected at the Federal University of São Carlos, located in Araras (22° 21' S, 47° 23' W, São Paulo State, Brazil). *S. spontaneum* was collected in Piracicaba (22°43'14''S, 47°38'46''W, São Paulo State) and the cultivar SP80-3280 at the Flowering and Crossing Station of Serra do Ouro, Murici (09°13' S, 35°50' W, Alagoas State, Brazil).



#### 4.2.2. ZIP4 candidates

The CDS sequence corresponding to the ZIP4 gene located on the chromosome 5B in *Triticum aestivum* (TraesCS5B02G255100.1) was used as reference and aligned through BLAST against the sorghum genome (McCornicl et al, 2017, orthologous corresponding gene model SORBI\_3003G384100). This sorghum ZIP4 coding sequence was used as a query to BLAST against the available genomes of *S. officinarum* LA-purple (PRJNA744175), *S. spontaneum* AP85-441 (PRJNA483885) (Zhang et al., 2018), Brazilian cultivar SP80-3280 (PRJNA431722) (Souza et al., 2019) and French cultivar R570 (Garsmeur et al, 2018 and unpublished whole polyploid genome assembly). Only hits with  $\geq 80\%$  identity at the nucleotide level were retained. The genomic sequences were then aligned using MAFFT (Kato et al., 2019). Intron and exon structures were determined based on sorghum sequence using Gblocks (Castresana, 2000) and gene annotations were refined using Artemis (Carver et al, 2011). All CDS sequences were aligned using MAFFT (Kato et al., 2019).

#### 4.2.3. ZIP4 protein analyses

CDS sequences were translated into amino acids using Transeq (Madeira et al., 2022). Multiple protein sequence alignment was done using Clustal X (Higgins & Sharp, 1988; Larkin et al., 2007). Protein architecture was predicted by InterPro (Blum et al., 2021) and TPRs by TPRpred (Zimmermann et al., 2018). A graphical representation of the conserved residues in the aligned protein sequences was obtained using the Skyline webtool (<https://skylign.org/logo/>) (Wheeler et al., 2014). The secondary structure (2D) of the TPR domain was predicted by EMBOSS Protein plugin (Rice et al., 2000), and the three-dimensional (3D) protein structure was predicted by AlphaFold2 (Jumper et al., 2021) and the 3D protein structure alignment was performed using iCn3D (Wang et al., 2020). The TM-score was calculated according with Xu & Zhang (2010).

#### 4.2.4. RNA isolation and Real Time quantitative PCR (RT-qPCR)

Flowers from the base of immature panicles (comprising early meiotic stages), leaves and roots from *S. officinarum* (Caiana Fita), *S. spontaneum* (SES205A) and SP0-3280 were collected, frozen immediately in liquid nitrogen, and stored at  $-80\text{ }^{\circ}\text{C}$ . Total RNA from three biological replicates was extracted from 200 mg of tissue using Direct-zol RNA MiniPrep Plus (Zymo Research) with TRIzol reagent (Invitrogen, USA). RNA concentration was determined in Invitrogen Qubit 4 Fluorometer with a Qubit<sup>TM</sup> RNA BR Assay (Thermo Fisher Scientific, USA). The RNA quality was verified by both agarose gel electrophoresis and Qubit<sup>TM</sup> RNA IQ Assay Kit (Thermo Fisher Scientific, USA). Regarding cDNA synthesis, the GoScript Reverse Transcription System (Promega, USA) was used, starting from 0.5  $\mu\text{g}$  of RNA.

ZIP4 gene specific primers were designed using Geneious Prime 2023.1.2 (<https://www.geneious.com/>) according with the following parameters: 58–62  $^{\circ}\text{C}$  melting temperature ( $T_m$ ), 18–22 bp in length, and 100–200 bp, the expected length of the amplified fragments. Two housekeeping genes, GAPDH (glyceraldehyde-3-phosphate dehydrogenase) and TIPS-41 (Tonoplast Intrinsic Protein) were used as internal references (Silva Santos et al., 2021). The following primer sequences were used:

Gene	Forward	Reverse
<i>ZIP4</i>	5'CCTAACCGAAGCGCTTGATC3'	5'ATCACTTGGAGCTTTGGGGT3'
<i>GAPDH</i>	5'TTGGTTTCCACTGACTTCGTT3'	5'CTGTAGCCCCACTCGTTGT3'
<i>TIPS-4I</i>	5'CACCTGTTGAGGTTCTGCT3'	5'CACAGCATCACTCCCACAGT3'

We used two technical replicates for each biological replicate. Briefly, the reaction mixture consisted of 7.5  $\mu$ L Power up SYBR<sup>TM</sup> Green PCR Master Mix (Applied Biosystems, USA), 2  $\mu$ L of cDNA, 0.6  $\mu$ L of each primer at 5  $\mu$ M and nuclease-free water to a final reaction volume of 15  $\mu$ L. A reaction without cDNA was included. Amplification consisted of 95 °C for 10 min, followed by 40 cycles of 95 °C for 15 s and 60 °C for 1 min, plus a melting curve. Product specificity was evaluated by dissociation curves. Reaction efficiency and Ct values were determined with LinReg (Ramakers et al., 2003). The relative changes in expression level were calculated with REST (Pfaffl et al., 2002). The significance of the differences was verified by using a one-way analysis of variance (ANOVA) followed by the Tukey's test ( $p < 0.05$ ). All statistical analysis were performed using the R software (<http://www.r-project.org>).

#### 4.2.5. Antibodies

The anti-ASY1 and anti-ZYP1 antibodies were obtained by immunizing rat, and guinea pig, respectively, with a synthetic peptide conjugated with KLH (Eurogentec, <http://www.eurogentec.com>). The synthetic peptide consisted of 15-aa residues from the respective protein in *S. spontaneum* AP85-441 available genome (PRJNA483885) (Zhang et al., 2018). The following peptides were used for anti-ASY1 353-C+RASKDRYTVNQKTD-367 (646 aa, Sspon.02G0010810-4D-mRNA-1) and for anti-ZYP1 854-C+EGSLNPYADDPYAFG-cooh-868, (868 aa, Sspon.05G0025500-1P-mRNA-1). The working dilution of the purified serum used in the cytology assays was 1:100 for both antibodies.

#### 4.2.6. Immunocytology

Chromosome spreads and immunolocalization were performed on cells with preserved three-dimensional structures as described in Hurel et al. (2018) with modifications. Fresh inflorescences were collected and kept in water, the same day flower buds were carefully dissected, and anthers at prophase I with the appropriate size were selected: 0.55-1.0, 1.0-1.6 and 1.2-2.0 mm in *S. spontaneum* (SES205A), *S. officinarum* (Caiana Fita) and SP0-3280, respectively. Anthers were collected in buffer A (80 mM KCl, 20 mM NaCl, 15 mM Pipes–NaOH, 0.5 mM ethylene glycol tetra acetic acid (EGTA), 2 mM ethylene diamine tetra acetic acid (EDTA), 80 mM sorbitol, 1 mM dithiothreitol (DTT), 0.15 mM spermine, and 0.5 mM spermidine) and fixed by incubation in buffer A + 2% formaldehyde for 20 min. Anthers were then washed in buffer A for 10 min and digested at 37 °C for 25 min (4% cellulase, 4% pectolyase and 4% macerozyme in citrate buffer). After a wash in buffer A, digested anthers were kept on ice in buffer A. For embedding, five to eight anthers were placed in 12  $\mu$ L of buffer A on 18 mm  $\times$  18 mm coverslip, dissected and squashed to extrude the meiocytes. A 5- $\mu$ L drop of activated polyacrylamide solution (25  $\mu$ L 15% polyacrylamide in buffer A + 1.25  $\mu$ L of 20% sodium sulfite + 1.25  $\mu$ L of 20% ammonium persulfate) was added to the meiocytes, and a second coverslip was placed on the top with gentle pressure. The polyacrylamide gels

were left to polymerize for 1 h, and then the two coverslips were separated. The coverslips covered by a gel pad were incubated in 1× phosphate-buffered saline (PBsS), 1% Tween, and 1 mM EDTA for 1 h with agitation, followed by 2 h in blocking buffer (3% bovine serum albumin in 1× PBS + 0.1% Tween 20) at room temperature. Coverslips were then incubated with 200 µl of primary antibody, rat anti-ASY1 and guinea pig anti-ZYP1, in blocking buffer at 4 °C in a humid chamber for 48 h. Coverslips were washed four times for 30 min with 1× PBS 0.1% Tween 20. A total of 200 µl of Goat anti-Rat IgG Alexa Fluor 488 and Goat anti-Guinea pig Alexa Fluor 594 secondary antibodies in blocking buffer was applied (1: 250) and incubated at room temperature for 2 h in the dark. Gels were washed four times for 20 min with 1×PBS, 0.1% Tween 20. A total of 15 µl of DAPI Vectashield was used for mounting the coverslip with a slide that was sealed with nail polish.

Microscopic analysis was done under an epifluorescence microscope (Leica DM 5500), using the the follow settings: the DAPI fluorophore was observed under DAPI Filter (excitation:340-380nm; emission LP 425nm). To access ASY1 protein the Alexa Fluor 488 fluorophore was observed under L5 filter (Excitation: 460 to 500nm; Emission: 515 to 585 nm). At last, the ZYP1 protein were detect by the observation of Alexa Fluor 594 under N2.1 Filter (Excitation 515 to 560 nm; Emission 590nm). Individuaized cells were observed in a Z-stack position (~7um) and the digital projection reached. After the image capture, we submitted the digital projections including the layers of Z-stack to the deconvolution algorithm under Blind Method with 10 interactions on LAS AF software (Leica Microsystems), using a calculated point-spread function. A total of 50 cells was analyzed for each genotype. The percentage of each of the protein in pachytene cells was obtained counting pixels with the same color, using the computational program GIMP 2.10.34.

### 4.3. Results

#### 4.3.1. *ZIP4* gene characterization in *Saccharum*

The *ZIP4* gene was investigated in the available sugarcane genomes, including both representative of the parental species, *S. officinarum* cultivar LA-purple ( $2n = 8x = 80$ ,  $x = 10$ ), *S. spontaneum* clone AP85-441 ( $2n = 4x = 32$ ,  $x = 8$ , haploid constitution) and two current varieties SP80-3280 ( $2n = 112$ ) and R570 ( $2n = 12x = 114$ ,  $x = 10$ ). Three and four copies were found to occur in *S. officinarum* (LA-purple) and *S. spontaneum* (AP85-441), respectively. Eleven and four copies were discovered in R570 and SP80-3280, respectively (Figure 1). All copies were identified on chromosome 2, according to D'Hont et al., (2023) *Saccharum* chromosome nomenclature. Because the assembly was made up of contigs, the gene copies identified in SP80-3280 were not chromosome specific. In *S. spontaneum*, we were able to find one gene copy in each homologous chromosome, however, in the other available genomes there were missing copies. The R570 has 12 copies of chromosome 2, and 11 *ZIP4* copies were identified, one copy is missing. In *S. officinarum* and SP80-3280, a low copy number was found and some of the copies have missing segments, as both available genomes are incomplete.

In *Saccharum*, the *ZIP4* gene has a genomic sequence of 3,254 bp exhibiting a conserved structure of five exons and four introns in all copies (Figure 4a). The CDS is 2,901 bp long with 99.5 % pairwise identity among the copies (Figure 4b, Supplementary 1), excluding SP80-3280\_0083261 and SP80-3280\_0209934 which are incomplete copies.

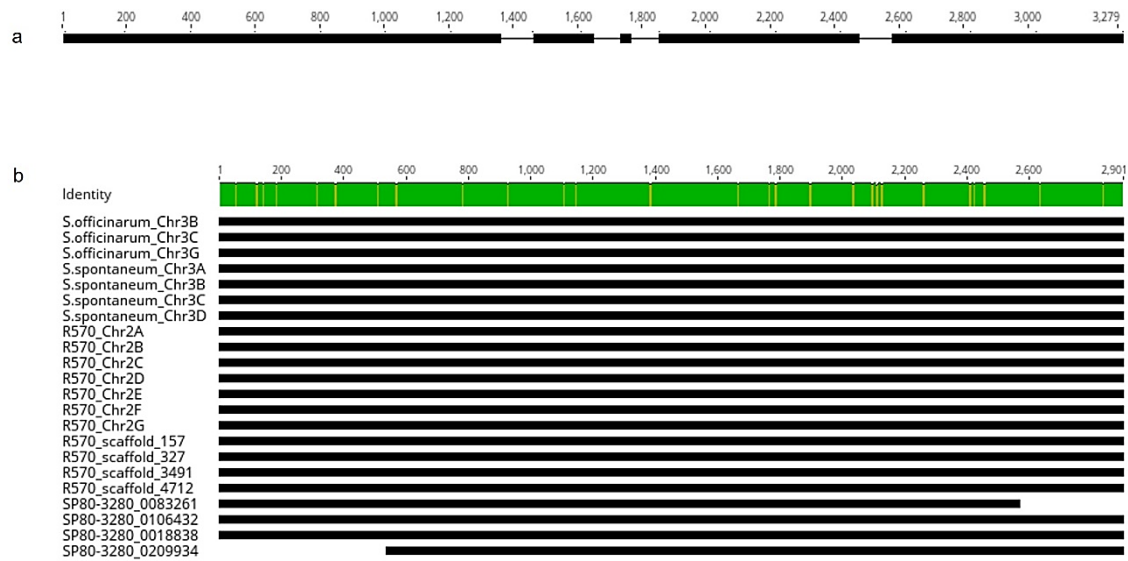


**Figure 4. Structure of the *ZIP4* gene in *Saccharum*.** a) *ZIP4* genomic sequence structure consisting of 5 exons (thick lines) and 4 introns (narrow lines). b) Aligned CDS sequences of the *ZIP4* gene copies in *S. officinarum*, *S. spontaneum*, R570 and SP80-3280 modern varieties. Polymorphisms are shown as vertical yellow lines at the identity bar (green).

The CDS sequences were *in silico* translated into amino acids, and the alignment generated a protein with 967 amino acids with 96.4% identity between them (Figure 5a, Supplementary 2). The following conserved regions were found in all copies: SPORULATION-SPECIFIC PROTEIN 22/Zip4 (PTHR40375), TPR-like (SSF48452), and Meiosis protein Spo22/Zip4 like (PF08631) (Figure 5b, Supplementary 3). Five copies of the TPRs comprising the TPR-like domain were found, excluding SP80-3280\_0209934 that has four copies due to a missing segment in its sequence (Figure 5c, Supplementary 4). TPRs are not evenly distributed throughout the domain, being located toward the extremities with a gap in the middle. Multiple alignments carried out to assess the level of sequence conservation between the TPR copies revealed similarity values ranging from 97 up to 100% in the species and varieties examined (Supplementary 5). The consensus sequence contains 34 residues, in which the only conserved position is A20 (Figure 5d). TPRs secondary structure similarity, in turn, was found to be divergent between all copies (1 – 5), however, the structure of each TPR copy is conserved among all examined sequences (Figure 5d, Supplementary 6). With that in mind, the TPR number and distribution within the *ZIP4* gene in some Poaceae was investigated revealing that these figures vary among species (Supplementary 7).

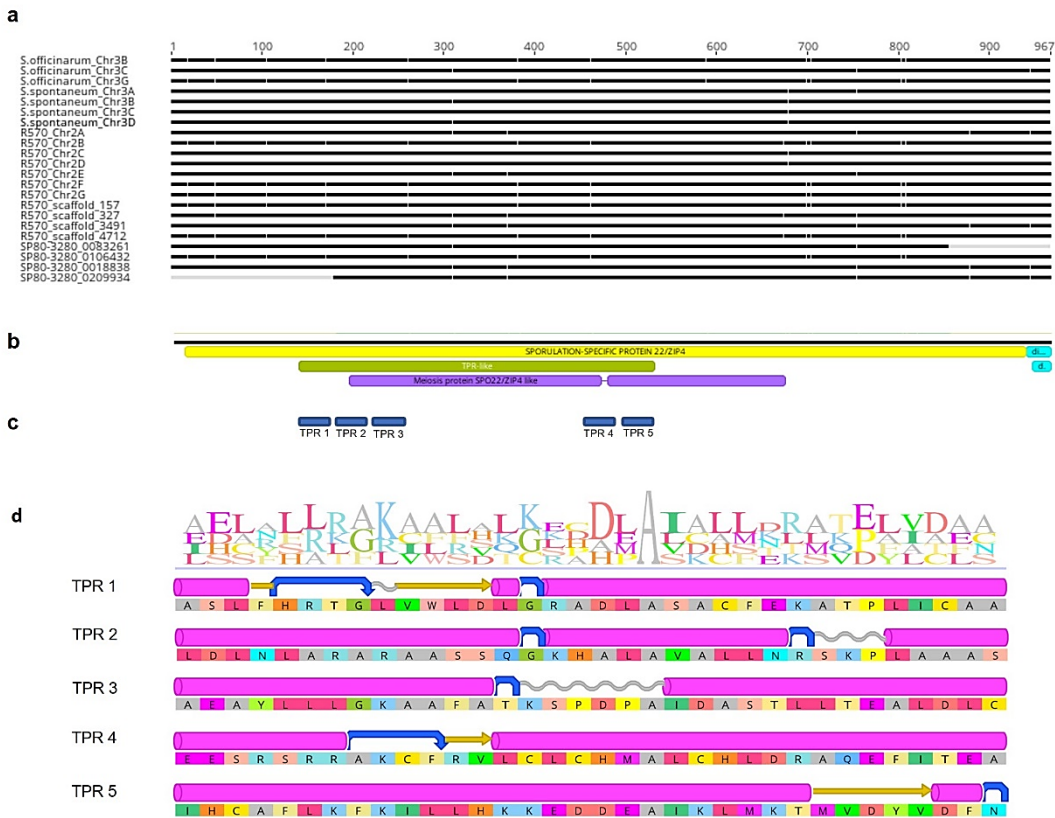


**Figure 5. ZIP4 protein alignment in *Saccharum*.** a) ZIP4 multiple amino acid sequence alignment. Regions with identical amino acid sequences across the proteins are in black, and polymorphism sites are in white vertical lines. b) Predicted functional domains (SPORULATION-SPECIFIC PROTEIN 22/ZIP4, TPR-like and Meiosis protein SPO22/ZIP4 like). c) Predicted TPRs. d) Graphical representation of the conserved residues in the aligned TPR sequences: A is the only conserved amino acid. Predicted secondary structure of the TPRs' copies (1–5). ‘Alpha Helix’ is represented by a pink cylindrical shape, ‘Beta Strand’ by the yellow arrow, ‘Coil’ is shown as a white wave and ‘Turn’ is represented by a blue arrow.

### 4.3.2. Comparison between *Saccharum* ZIP4 and TaZIP4 from wheat

The CDS alignment between *Saccharum* ZIP4 consensus sequence and TaZIP4-3A, TaZIP4-3B, TaZIP4-3D from wheat, has generated an identity of approximately 67% whilst to TaZIP4-B2, 63% (Figure 3a). Regarding multiple amino acid sequence alignments, a higher identity with the wheat copies located on chromosome 3 (3A, 3B, 3D), approximately 65%, was found in comparison with that copy located on 5B (B2), approximately 60% (Figure 3b, Supplementary 8).

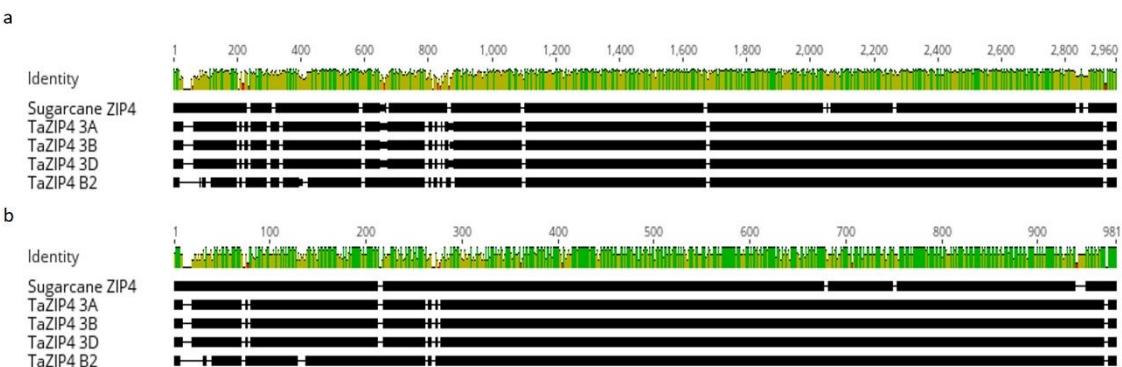


**Figure 6. ZIP4 sequence alignment in *Saccharum* and wheat (Ta).** a) Alignment of the *Saccharum* CDS nucleotide consensus sequence and the corresponding *TaZIP4* CDSs. b) Alignment of the *Saccharum* aminoacid consensus sequence and *TaZIP4* proteins. Identity bar with green, yellow, and red colors, representing high, medium and low identity among sequences. White spaces represent gaps created during the sequences alignments.

### 4.3.3. 3D protein structure prediction

A 3D protein prediction was performed using the ZIP4 protein and *TaZIP4*-3A, the wheat ZIP4 copy with higher identity with that of *Saccharum*, and *TaZIP4*-B2. Long coiled-coil proteins were identified (Figure 7). TM-scores of 0.88 and 0.77 were found between the sugarcane ZIP4 structure and *TaZIP4*-B2 and *TaZIP4*-3A structures, respectively. The TM-score is a metric for assessing the topological similarity of protein structures, it varies from 0 to 1, a perfect match between two structures equal to 1 (Xu & Zhang, 2010).

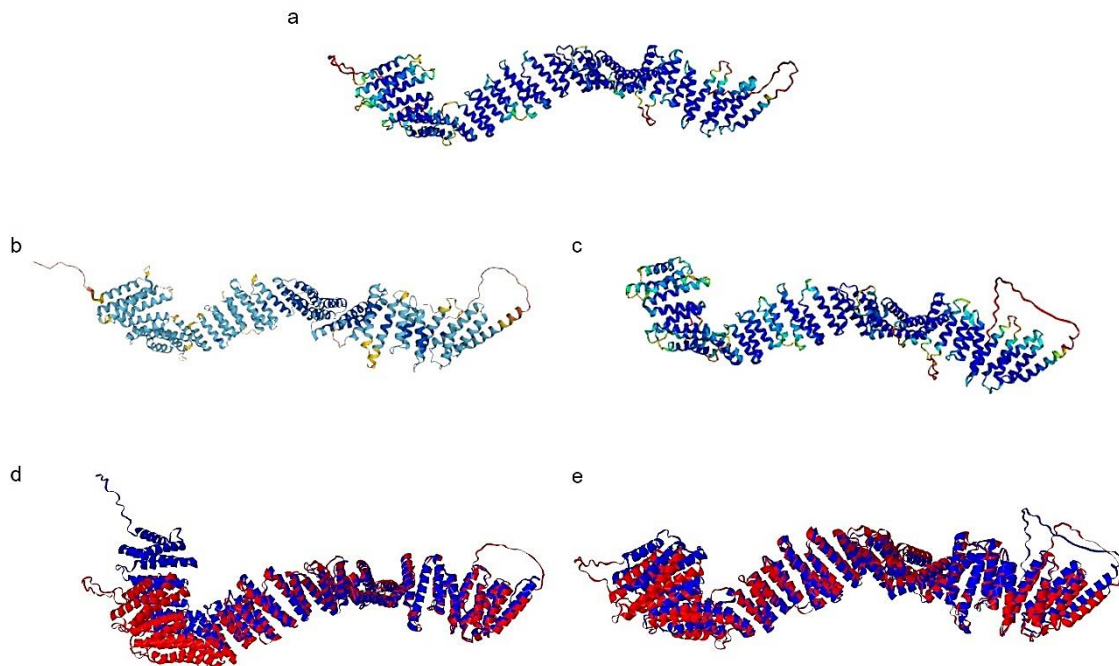


**Figure 7. ZIP4 3D protein prediction and structure alignments.** a) *Saccharum*. b) *TaZIP4* 3A. c) *TaZIP4* B2. Merged alignments: d) *Saccharum* ZIP4 and *TaZIP4* 3A. e) *Saccharum* ZIP4 and *TaZIP4* B2. *Saccharum* ZIP4 structure is in red and *TaZIP4* 3A and *TaZIP4* B2 are in blue. Protein prediction was done using AlphaFold2 and structure alignments with iCn3D.

### 4.3.4. ZIP4 gene expression

The analysis of the sugarcane *ZIP4* gene expression was performed in three different tissues: flowers (from the base of the inflorescence, where meiocytes are still at early meiotic phases), leaves and roots in the representatives of the parental species and SP80-3280. Remarkably, the *ZIP4* expression occurred in all tissues although much more expressed in

flowers, namely in *S. spontaneum* (SES205A), and SP80-3280, followed by roots and leaves (Figure 8).

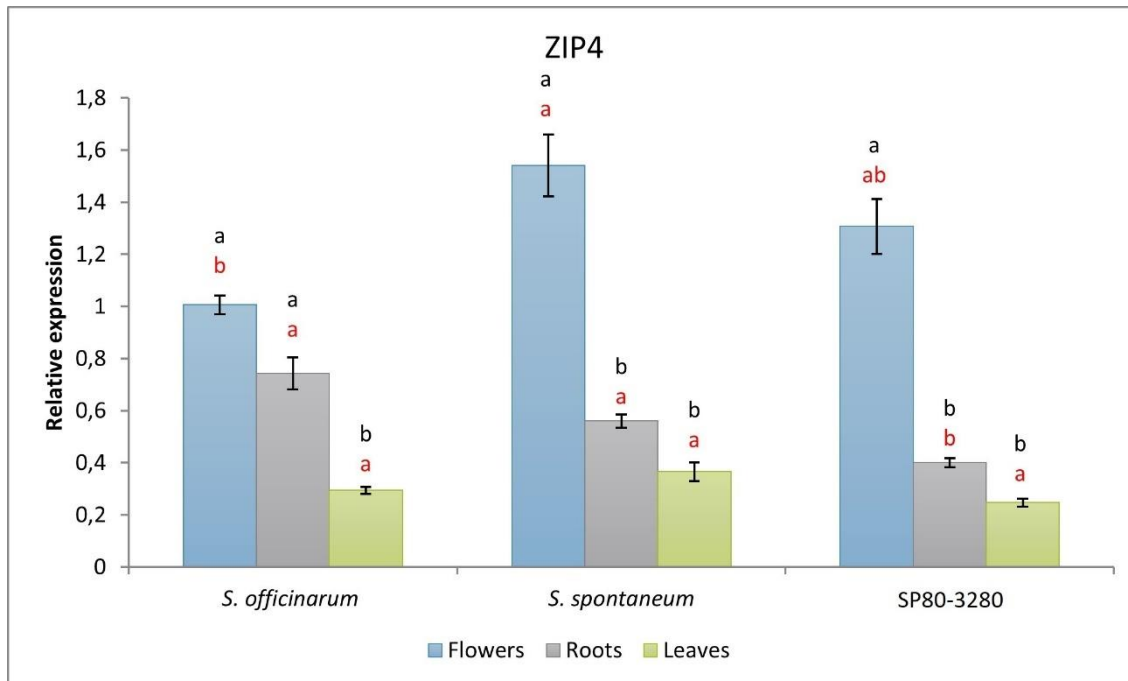


**Figure 8. Relative expression of the *ZIP4* gene in *S. officinarum*, *S. spontaneum* and SP80-3280 according to the Real Time-quantitative PCR results.** The relative gene expression in flower, roots and leaves are shown as blue, gray, and green bars, respectively. Graphing data expressed as fold changes between the *ZIP4* expression level with respect to that of reference genes. Different letters above the bars indicate expression levels significantly different ( $p < 0.05$ ) by one-way analysis of variance and Tukey's test. Black letters indicate comparisons across tissues from the same species, and red letters comparisons across species from the same tissue. Error bars correspond to the standard deviations of measurements performed in triplicate.

#### 4.3.5. Immunolocalization of the SC proteins, ZYP1 and ASY1

The ZYP1 and ASY1 proteins, which constitute the SC's TF and one of the components of the LE, respectively, were immunolocalized in 50 pachytene cells, for each parental species and cultivar SP80-3280. Pachytene stage cells were accessed by anther size correlation followed by DAPI staining, resulting in specific anthers sizes for each genotype, 0.55-1.0, 1.0-1.6 and 1.2-2.0 mm for *S. spontaneum*, *S. officinarum* and SP80-3280. According to our results, full synapsis can be achieved in *S. officinarum* only (Figure 9a). ZYP1 signals were observed on all chromosomes (Figure 9a) while ASY1 signals were detected as punctate foci distributed over the chromatin or as small stretches in all 50 cells analyzed (Figure 9a). In *S. spontaneum* and SP80-3280, ZYP1 was detected in most of the chromosomes (Figure 9b), and ASY1 was observed in a linear form and in larger amount than in *S. officinarum* (Figure 9a). ASY1 persistence during pachytene implies that the synapsis is not fully completed. In *S. spontaneum*, ASY1 presents as a single linear filament in 30 of the 50 analyzed cells or as a small coil (20 cells). In SP80-3280, the ASY1 filament appears to be coiled and dispersed in the cell nucleus in all analyzed cells (Figure 9c).

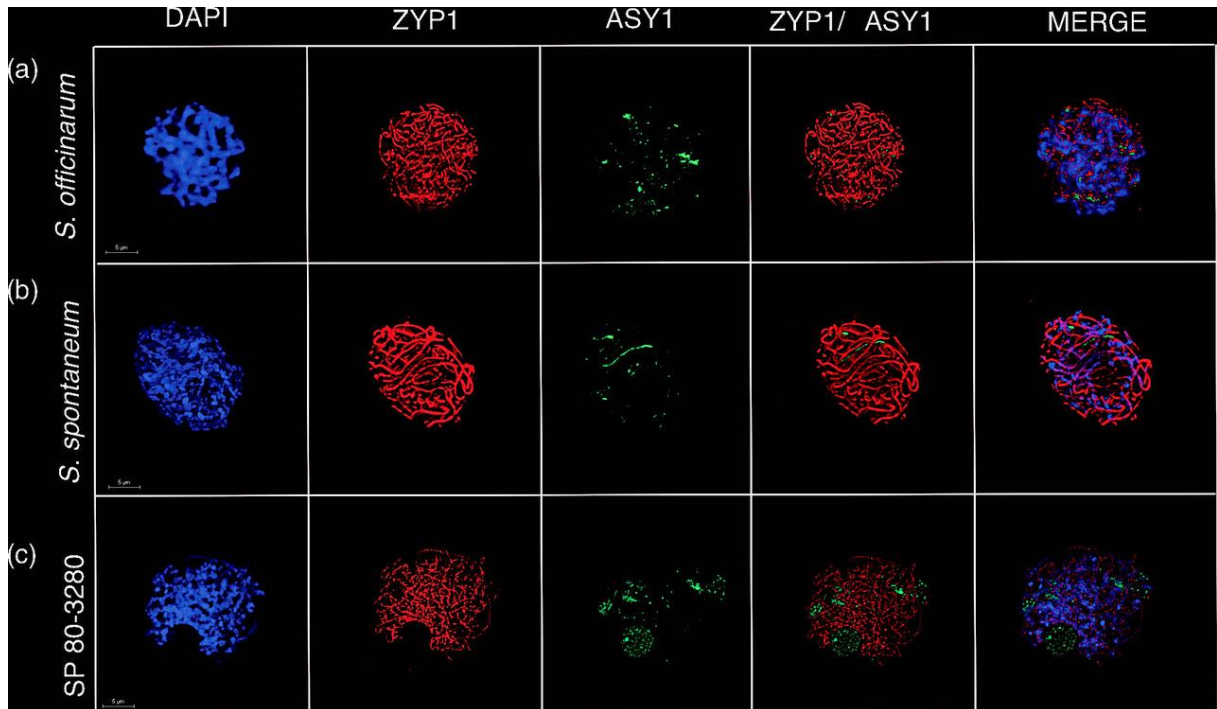


**Figure 9. Immunolocalization of synaptonemal complex proteins.** Immunolocalization of the ZYP1 and ASY1 proteins in *S. officinarum* (Caiana-Fita) (a), *S. spontaneum* (SES205) (b) and SP80-3280 (c), in late pachytene. Bar 5 µm.

The relative proportion of each protein during pachytene in the three genotypes was examined. By counting the pixels of a certain hue, we were able to determine the average proportion of ZYP1 and ASY1, in 50 cells for each genotype, allowing us to compare the percentage of asynapsis during pachytene. As expected, *S. officinarum* (Caiana Fita) presented the highest percentage of ZYP1 (96%) and the lowest of ASY1 (4%), in *S. spontaneum* (SES205) and SP80-3280 these figures were 94% of ZYP1 and 6% ASY1, and 88% of ZYP1 and 12% of ASY1, respectively (Figure 10).

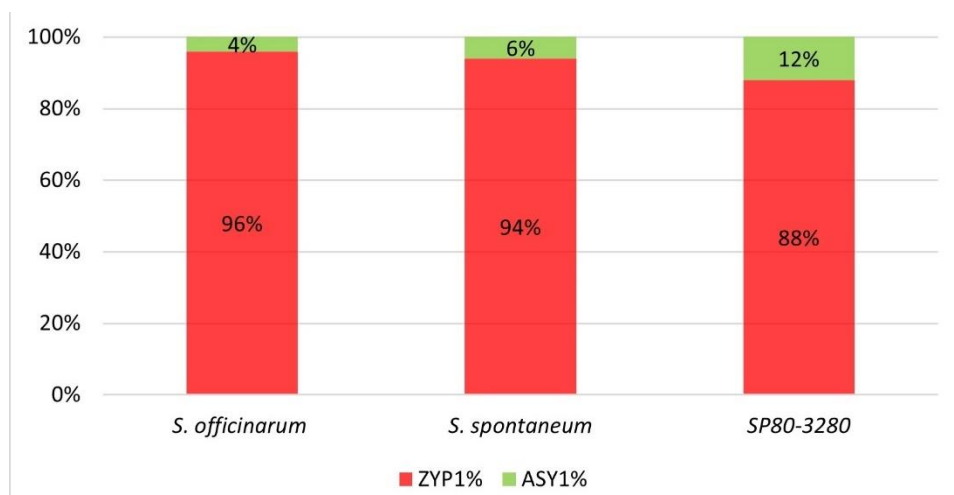


**Figure 10. Percentage of ZYP1 and ASY1 in sugarcane cells.** In red and green are the percentages of the ZYP1 and ASY1 proteins, respectively, in *S. officinarum*, *S. spontaneum* and SP80-3280.

#### 4.4. Discussion



#### 4.4.1. The sugarcane *ZIP4* gene and protein prediction

Sugarcane modern genotypes are man-made cultivars of interspecific origin, combining an overrepresentation of chromosomes originated from one parent (75–85%) with 15 up to 25% from the other parent, in addition to approximately 10% of recombinants, depending on the variety. Few generations after interspecific crossing, sugarcane was able to achieve meiosis regularity through a predominance of bivalents in the first division. Therefore, we propose that a genetically regulated strategy enforces bivalent formation.

The *ZIP4* gene has been widely studied in wheat with four copies located on chromosomes 3A, 3B, 3D and an extra copy on chromosome 5B, which emerged during polyploidization through a duplication of a 3A region and its insertion in 5B (Rey et al., 2017). This duplicated copy, *TaZIP4-B2*, is responsible for both promoting homologous synapsis and COs and restriction of homoeologous COs, and is involved in wheat improving synapsis efficiency, resulting in a regular meiosis with bivalent pairing. In the absence of the *TaZIP4-B2* there's the occurrence of multi and univalents (Martín et al., 2017; Rey et al., 2018).

The *ZIP4* meiotic gene is present in both parental species and in the sugarcane varieties. We were able to find four copies in *S. spontaneum* (AP85-441) and 11 copies in R570, both have the best assembled genomes. In *S. officinarum* (LA-purple), and SP80-3280, only a few copies were found, three and four, respectively, probably due to the inferior quality of their genome's assemblies. On the other hand, the CDS sequences are highly similar.

The protein sequence analysis revealed similar protein architecture found in wheat *TaZIP4-B2* (Alabdullah et al., 2021): SPORULATION-SPECIFIC PROTEIN 22/*ZIP4* (PTHR40375), TPR-like (SSF48452), and Meiosis protein Spo22/*ZIP4* like (PF08631). The TPR-like (SSF48452) domain contains TPRs, which are responsible for the scaffolding function of *ZIP4* during meiosis. In wheat, the number of TPRs per gene copy is much higher, ranging from nine to 12 (Alabdullah et al., 2021), compared to five in sugarcane; they also exhibit a continuous distribution along the TPR domain. On the other hand, in sugarcane, the TPRs' amino acid composition is more conserved within TPR copy and consequently a conserved secondary structure was found.

The 3D protein predictions revealed a long coiled-coil structure and the potential of these proteins to scaffold large macromolecular complexes have been extensively discussed (Truebestein & Leonard, 2016). *ZIP4* is essential for the formation of class I interference-sensitive CO and defines actual COs early in pre-recombination maturation (Lynn et al., 2007; Shen et al., 2012; Tsubouchi et al., 2006). *ZIP4* functions as a scaffold protein and may also act as a chaperone, and as a hub for multiple physical interactions between other ZMM proteins involved in CO, and components of the chromosome axis (De Muyt et al., 2018; Pyatnitskaya et al., 2019, 2022). Thus, *ZIP4* may provide a direct physical link between CO-designated recombination intermediates and SC assembly (De Muyt et al., 2018).

Some cultivars of sugarcane had their genome architecture (and karyotypes) recently decrypted by Piperides & D'Hont (2020) using chromosome-specific oligo probes. Herein, as in wheat, the sugarcane *ZIP4* gene was located on chromosome 2, with a higher identity between the respective copies concerning the coding and protein sequences. However, a higher similarity regarding the topological protein structure was found between the sugarcane *ZIP4* and *TaZIP4-B2*, revealing that the *ZIP4* protein function is directly correlated to its 3D structure, rather than aminoacid composition or TPR distribution.

The higher topological difference was at the N-terminal tail of the protein, and this may be interfering in sugarcane protein scaffolding function and consequently protein interaction. In *Saccharomyces cerevisiae*, it is well known that ZIP4 protein interacts with other proteins of the ZMM complex, SPO16, ZIP2, ZIP3 and MSH5, and the SC proteins, RED1 (LE) and ECM11 and GMC2 (CE). It encompasses 21 TPR motifs spanning the whole length of ZIP4. A 3D model of ZIP4, revealed an extensive surface featuring four distinct conserved patches likely to be involved in protein interactions, they are located at the N and C-terminal and two are distributed at the middle (Pyatnitskaya et al., 2019, 2022). We may speculate that the topology of the sugarcane protein could interfere in the scaffolding function and consequently in the correct progression of meiosis.

#### 4.4.2. Expression profile of the ZIP4 gene

The ZIP4 expression was high in flower tissues; however (although in lower levels), it was also expressed in roots and leaves. This expression profile is very similar of that of TaZIP4-B2. The copies TaZIP4-3A, 3B and 3D are only expressed in flowers (Martín et al., 2018). The different expression pattern of the ZIP4 gene in flower tissues may be linked to the meiotic behavior of each cane: the *S. officinarum* (Caiana Fita) exhibited the lowest level of ZIP4 expression. This species is a stable legitimate octoploid species with regular meiosis, and exclusive bivalent pairing (Vieira et al., 2018; Oliveira et al., 2023). The *S. spontaneum* (SES205A) exhibited the higher expression level. This species is very diverse, an establishing autopolyploid (Van Drunen et al., 2022), with several cytotypes and basic chromosome numbers ( $x$ ) equal to 10, 9 and 8 (Piperidis & D'Hont, 2020), being  $x = 8$  the most common. The analyzed clone has an irregular meiosis, approximately 52% of cells exhibiting abnormalities and up to 2 univalents are seen in diakinesis (Oliveira et al., 2023). Therefore, it is reasonable to speculate that meiotic cells require ZIP4 to be more expressed in order to achieve regular chromosome segregation. In SP80-3280, most of the meiotic cells (77%) exhibit abnormalities, and bivalents also prevail, but the number of univalents is higher than in *S. spontaneum* (SES205A), up to 4 (Oliveira et al., 2023). However, the higher ZIP4 expression in both *S. spontaneum* (SES205A) and in SP80-3280 is not enough to fully regulate meiotic pairing.

#### 4.4.3. Immunolocalization of SC proteins

The immunolocalization of the SC components, ZYP1 and ASY1, in pachytene cells, revealed that *S. officinarum* (Caiana Fita) is the only clones exhibiting a complete synapsis (96% of ZYP1 and 4% ASY1) corroborating previous results about its regular chromosome segregation and complete bivalent pairing (Oliveira et al., 2023). On the other hand, a higher amount of ASY1 was immunolocalized in *S. spontaneum* (SES205A) and SP80-3280 (6% and 12%, respectively), suggesting that synapsis was not completed.

In *S. spontaneum* (SES205A), although ZYP1 is loaded on mostly all the chromosomes, the presence of a long ASY1 filamentous strand, could indicate that two chromosomes are not synapsed, this would further result in two univalents, confirming the meiotic behavior exhibited by *S. spontaneum* (SES205A). In *S. spontaneum*, the presence of multivalents during pachytene have been reported by Zhang et al 2023, in autotetraploid (Np-X), autooctoploid (SES208), and autodecaploid (Yunnan 82–106) *S. spontaneum* clones, using (oligo)-based chromosome painting probes to identify individual chromosomes. During the early prophase I, multiple-chromosome alignments may be formed in polyploids, but these

associations are later resolved into bivalents, due either to the removal of SC sections or to the suppression of recombination during CO maturation, so that only bivalent associations are retained. Overall, the process of diploidization is a common evolutionary strategy adopted by a polyploid (see Soares et al., 2021).

In wheat, the immunolocalization of the SC components, AZY1 and ZYP1 revealed that during telomere bouquet stage (zygotene), only homologous synapsis occurs, while homoeologous synapsis starts later during telomere bouquet dispersal (pachytene) (Márton et al., 2017). SP80-3280, in turn, exhibited the higher amount of ASY1 whose filaments appear to be coiled. In SP80-3280, there are no multivalent associations but up to four univalents do occur (Oliveira et al., 2023). Notably, the constitution of non-synapsed chromosomes is unknown, whether from homoeologous associations between *S. officinarum*, *S. spontaneum* or recombinant chromosomes.

It seems clear that synapsis occurs mostly between homologous chromosomes in modern cultivars. A fundamental question that persists is how homeologues and recombinants behave during meiosis. Thus, decrypting this feature on sugarcane meiosis is of great importance for further understanding neoneopolyploids' meiotic behavior. Furthermore, our findings will have significant impact on sugarcane breeding, as well as genetic mapping and genomics studies, since this is a species of extreme commercial relevance, whose understanding of the inheritance of agronomic traits (Mendelian and quantitative) and genome organization still remains somewhat obscure.

## References

- Alabdullah, A. K., Moore, G., & Martín, A. C. (2021). A duplicated copy of the meiotic gene ZIP4 preserves up to 50% pollen viability and grain number in polyploid wheat. *Biology*, 10(4), 290. <https://doi.org/10.3390/biology10040290>
- Al-Kaff, N., Knight, E., Bertin, I., Foote, T., Hart, N., Griffiths, S., & Moore, G. (2008). Detailed dissection of the chromosomal region containing the Ph1 locus in wheat *Triticum aestivum*: with deletion mutants and expression profiling. *Annals of Botany*, 101(6), 863–872. <https://doi.org/10.1093/aob/mcm252>
- Armstrong, S. J., Caryl, A. P., Jones, G. H., & Franklin, F. C. H. (2002). Asy1, a protein required for meiotic chromosome synapsis, localizes to axis-associated chromatin in *Arabidopsis* and *Brassica*. *Journal of Cell Science*, 115(18), 3645–3655. <https://doi.org/10.1242/jcs.00048>
- Barreto, F. Z., Balsalobre, T. W. A., Chapola, R. G., Garcia, A. A. F., Souza, A. P., Hoffmann, H. P., Gazaffi, R., & Carneiro, M. S. (2021). Genetic variability, correlation among agronomic traits, and genetic progress in a sugarcane diversity panel. *Agriculture*, 11(6), 533. <https://doi.org/10.3390/agriculture11060533>
- Bielig, L. M., Mariani, A., & Berding, & N. (2003). Cytological studies of 2n male gamete formation in sugarcane, *Saccharum* L. In *Euphytica* (133), 117-124. <https://doi.org/doi.org/10.1023/A:1025628103101>
- Blum, M., Chang, H. Y., Chuguransky, S., Grego, T., Kandasamy, S., Mitchell, A., Nuka, G., Paysan-Lafosse, T., Qureshi, M., Raj, S., Richardson, L., Salazar, G. A., Williams, L., Bork, P., Bridge, A., Gough, J., Haft, D. H., Letunic, I., Marchler-Bauer, A., ... Finn, R. D. (2021). The InterPro protein families and domains database: 20 years on. *Nucleic Acids Research*, 49(1), 344–354. <https://doi.org/10.1093/NAR/GKAA977>
- Bremer, G. (1961). Problems in breeding and cytology of sugar cane - II. The sugar cane breeding from a cytological view-point. *Euphytica*, 10(2), 121–133. <https://doi.org/10.1007/BF00022203>
- Burner, D. M. (1991). Cytogenetic analyses of sugarcane relatives (Andropogoneae: Saccharinae). *Euphytica*, 54(1), 125–133. <https://doi.org/10.1007/BF00145639>
- Carver, T., Harris, S. R., Berriman, M., Parkhill, J. & McQuillan, J. A. (2011). Artemis: an integrated platform for visualization and analysis of high-throughput sequence-based experimental data. *Bioinformatics*, 28(4), 464-469. <https://doi.org/10.1093/bioinformatics/btr703>
- Castresana, J. (2000). Selection of conserved blocks from multiple alignments for their use in phylogenetic analysis. *Molecular Biology and Evolution*, 17(4), 540–552. <https://doi.org/10.1093/oxfordjournals.molbev.a026334>
- Capilla-Pérez, L., Durand, S., Hurel, A., Lian, Q., Chambon, A., Taochy, C., ... & Mercier, R. (2021). The synaptonemal complex imposes crossover interference and heterochiasmy in *Arabidopsis*. *Proceedings of the National Academy of Sciences*, 118(12), e2023613118. <https://doi.org/10.1073/pnas.2023613118>

- Cheavegatti-Gianotto, A., de Abreu, H. M. C., Arruda, P., Bespalkok Filho, J. C., Burnquist, W. L., Creste, S., di Ciero, L., Ferro, J. A., de Oliveira Figueira, A. V., de Sousa Filgueiras, T., Grossi-de-Sá, M. de F., Guzzo, E. C., Hoffmann, H. P., de Andrade Landell, M. G., Macedo, N., Matsuoka, S., de Castro Reinach, F., Romano, E., da Silva, W. J., ... César Ulian, E. (2011). Sugarcane (*Saccharum X officinarum*): A reference study for the regulation of genetically modified cultivars in Brazil. *Tropical Plant Biology*, 4(1), 62–89. <https://doi.org/10.1007/s12042-011-9068-3>
- Chelysheva, L., Gendrot, G., Vezon, D., Doutriaux, M.-P., Mercier, R., & Grelon, M. (2007). Zip4/Spo22 is required for Class I CO formation but not for synapsis completion in *Arabidopsis thaliana*. *PLoS Genetics*, 3(5), 83. <https://doi.org/10.1371/journal.pgen.0030083>
- Cuacos, M., Lambing, C., Pachon-Penalba, M., Osman, K., Armstrong, S. J., Henderson, I. R., Sanchez-Moran, E., Franklin, F. C. H., & Heckmann, S. (2021). Meiotic chromosome axis remodelling is critical for meiotic recombination in *Brassica rapa*. *Journal of Experimental Botany*, 72(8), 3012–3027. <https://doi.org/10.1093/jxb/erab035>
- Cuadrado, A. (2004). Genome remodeling in three modern *S. officinarum* x *S. spontaneum* sugarcane cultivars. *Journal of Experimental Botany*, 55(398), 847–854. <https://doi.org/10.1093/jxb/erh093>
- Cursi, D. E., Hoffmann, H. P., Barbosa, G. V. S., Bressiani, J. A., Gazaffi, R., Chapola, R. G., Fernandes Junior, A. R., Balsalobre, T. W. A., Diniz, C. A., Santos, J. M., & Carneiro, M. S. (2021). History and current status of sugarcane breeding, germplasm development and molecular genetics in Brazil. *Sugar Tech*, 24(1), 112-133. <https://doi.org/10.1007/s12355-021-00951-1>
- da Silva Santos, P. H., Manechini, J. R. V., Brito, M. S., Romanel, E., Vicentini, R., Scarpari, M., Jackson, S., & Pinto, L. R. (2021). Selection and validation of reference genes by RT-qPCR under photoperiodic induction of flowering in sugarcane (*Saccharum* spp.). *Scientific Reports*, 11(1), 1–10. <https://doi.org/10.1038/s41598-021-83918-2>
- de Muyt, A., Pyatnitskaya, A., Andréani, J., Ranjha, L., Ramus, C., Laureau, R., Fernandez-Vega, A., Holoch, D., Girard, E., Govin, J., Margueron, R., Couté, Y., Cejka, P., Guérois, R., & Borde, V. (2018). A meiotic XPF–ERCC1-like complex recognizes joint molecule recombination intermediates to promote crossover formation. *Genes & Development*, 32(3), 283–296. <https://doi.org/10.1101/GAD.308510.117>
- Denham, T. (2011). Early agriculture and plant domestication in New Guinea and Island Southeast Asia. *Current Anthropology*, 52(4), 379–395. <https://doi.org/10.1086/658682>
- D'Hont, A., Garsmeur, O. & Piperidis, N. (2023). Sugarcane genome architecture revealed by chromosome-specific probes, implication for chromosome nomenclature. *Proceedings of the International Society of Sugar Cane Technologists*, (31), 266–273.

- D'Hont, A., Grivet, L., Feldmann, P., Glaszmann, J. C., Rao, S., & Berding, N. (1996). Characterisation of the double genome structure of modern sugarcane cultivars (*Saccharum* spp.) by molecular cytogenetics. *Molecular and General Genetics MGG*, 250(4), 405–413. <https://doi.org/10.1007/BF02174028>
- France, M. G., Enderle, J., Röhrig, S., Puchta, H., Franklin, F. C. H., & Higgins, J. D. (2021). ZYP1 is required for obligate cross-over formation and cross-over interference in *Arabidopsis*. *Proceedings of the National Academy of Sciences*, 118(14), e2021671118. <https://doi.org/10.1073/pnas.2021671118>
- Gao, J., & Colaiácovo, M. P. (2018). Zipping and unzipping: protein modifications regulating synaptonemal complex dynamics. *Trends in Genetics*, 34(3), 232–245. <https://doi.org/10.1016/J.TIG.2017.12.001>
- Garsmeur, O., Droc, G., Antonise, R., Grimwood, J., Potier, B., Aitken, K., Jenkins, J., Martin, G., Charron, C., Hervouet, C., Costet, L., Yahiaoui, N., Healey, A., Sims, D., Cherukuri, Y., Sreedasyam, A., Kilian, A., Chan, A., Van Sluys, M.-A., ... D'Hont, A. (2018). A mosaic monoploid reference sequence for the highly complex genome of sugarcane. *Nature Communications*, 9(1), 2638. <https://doi.org/10.1038/s41467-018-05051-5>
- Gouy, M., Nibouche, S., Hoarau, J. Y., & Costet, L. (2013). Improvement of yield per se in sugarcane. In *Translational Genomics for Crop Breeding* (211–237). John Wiley & Sons. <https://doi.org/10.1002/9781118728482.ch13>
- Griffiths, S., Sharp, R., Foote, T. N., Bertin, I., Wanous, M., Reader, S., Colas, I., & Moore, G. (2006). Molecular characterization of Ph1 as a major chromosome pairing locus in polyploid wheat. *Nature*, 439(7077), 749–752. <https://doi.org/10.1038/nature04434>
- Grivet, L., Daniels, C., Glaszmann, J. C., & D'Hont, A. (2004). A review of recent molecular genetics evidence for sugarcane evolution and domestication. *Ethnobotany Research and Applications*, 2, 009. <https://doi.org/10.17348/era.2.0.9-17>
- Higgins, D. G., & Sharp, P. M. (1988). CLUSTAL: A package for performing multiple sequence alignment on a microcomputer. *Gene*, 73(1), 237–244. [https://doi.org/10.1016/0378-1119\(88\)90330-7](https://doi.org/10.1016/0378-1119(88)90330-7)
- Hurel, A., Phillips, D., Vrielynck, N., Mézard, C., Grelon, M., & Christophorou, N. (2018). A cytological approach to studying meiotic recombination and chromosome dynamics in *Arabidopsis thaliana* male meiocytes in three dimensions. *The Plant Journal*, 95(2), 385–396. <https://doi.org/10.1111/tpj.13942>
- International Wheat Genome Sequencing Consortium (IWGSC). (2018). Shifting the limits in wheat research and breeding using a fully annotated reference genome. *Science*, 361(6403). <https://doi.org/10.1126/science.aar7191>
- Jumper, J., Evans, R., Pritzel, A., Green, T., Figurnov, M., Ronneberger, O., Tunyasuvunakool, K., Bates, R., Žídek, A., Potapenko, A., Bridgland, A., Meyer, C., Kohl, S. A. A., Ballard, A. J., Cowie, A., Romera-Paredes, B.,

- Nikolov, S., Jain, R., Adler, J., ... Hassabis, D. (2021). Highly accurate protein structure prediction with AlphaFold. *Nature*, 596(7873), 583–589. <https://doi.org/10.1038/s41586-021-03819-2>
- Katoh, K., Rozewicki, J., & Yamada, K. D. (2019). MAFFT online service: multiple sequence alignment, interactive sequence choice and visualization. *Briefings in Bioinformatics*, 20(4), 1160–1166. <https://doi.org/10.1093/BIB/BBX108>
- Kline, K. L., Msangi, S., Dale, V. H., Woods, J., Souza, G. M., Osseweijer, P., Clancy, J. S., Hilbert, J. A., Johnson, F. X., McDonnell, P. C., & Muger, H. K. (2017). Reconciling food security and bioenergy: priorities for action. *GCB Bioenergy*, 9(3), 557–576. <https://doi.org/10.1111/gcbb.12366>
- Larkin, M. A., Blackshields, G., Brown, N. P., Chenna, R., McGettigan, P. A., McWilliam, H., Valentin, F., Wallace, I. M., Wilm, A., Lopez, R., Thompson, J. D., Gibson, T. J., & Higgins, D. G. (2007). Clustal W and Clustal X version 2.0. *Bioinformatics*, 23(21), 2947–2948. <https://doi.org/10.1093/bioinformatics/btm404>
- Lenormand, T., Engelstädter, J., Johnston, S. E., Wijnker, E., & Haag, C. R. (2016). Evolutionary mysteries in meiosis. *Philosophical Transactions of the Royal Society B: Biological Sciences*, 371(1706), 1–27. <https://doi.org/10.1098/rstb.2016.0001>
- Long, S. P., Karp, A., Buckeridge, M. S., Davis, S. C., Jaiswal, D., Moore, P. H., Moose, S. P., Murphy, D. J., Onwona-Agyeman, S., & Vonshak, A. (2015). Chapter 10: Feedstocks for biofuels and bioenergy. *Bioenergy & Sustainability: Bridging the Gaps*, 302–346.
- Lynn, A., Soucek, R., & Börner, G. V. (2007). ZMM proteins during meiosis: Crossover artists at work. *Chromosome Research*, 15(5), 591–605. <https://doi.org/10.1007/s10577-007-1150-1>
- Madeira, F., Pearce, M., Tivey, A. R. N., Basutkar, P., Lee, J., Edbali, O., Madhusoodanan, N., Kolesnikov, A., & Lopez, R. (2022). Search and sequence analysis tools services from EMBL-EBI in 2022. *Nucleic Acids Research*, 50(1), 276–279. <https://doi.org/10.1093/nar/gkac240>
- Maestra, B., De Jong, J. H., Shepherd, K., & Naranjo, T. (2002). Chromosome arrangement and behaviour of two rye homologous telomers at the onset of meiosis in disomic wheat-5RL addition lines with and without the Ph1 locus. *Chromosome Research*, 10(8), 655–667. <https://doi.org/10.1023/A:1021564327226>
- Martín, A. C., Alabdullah, A. K., & Moore, G. (2021). A separation-of-function ZIP4 wheat mutant allows crossover between related chromosomes and is meiotically stable. *Scientific Reports*, 11(1), 1–13. <https://doi.org/10.1038/s41598-021-01379-z>
- Martín, A. C., Borrill, P., Higgins, J., Alabdullah, A., Ramírez-gonzález, R. H., Swarbreck, D., Uauy, C., Shaw, P., & Moore, G. (2018). Genome-wide transcription during early wheat meiosis is independent of synapsis, ploidy level, and the Ph1 locus. *Frontiers in Plant Science*, 9, 1–19. <https://doi.org/10.3389/fpls.2018.01791>

- Martín, A. C., Rey, M. D., Shaw, P., Moore, G., & Moore, G. (2017). Dual effect of the wheat Ph1 locus on chromosome synapsis and crossover. *Chromosoma*, 126(6), 669–680. <https://doi.org/10.1007/s00412-017-0630-0>
- Martín, A. C., Shaw, P., Phillips, D., Reader, S., Moore, G., & Marti, A. C. (2014). Licensing MLH1 sites for crossover during meiosis. *Nature Communications*, 5, 1–5. <https://doi.org/10.1038/ncomms5580>
- McCormick, R. F., Truong, S. K., Sreedasyam, A., Jenkins, J., Shu, S., Sims, D., ... Mullet, J. E. (2017). The Sorghum bicolor reference genome: improved assembly, gene annotations, a transcriptome atlas, and signatures of genome organization. *The Plant Journal*, 93(2), 338–354. <https://doi.org/10.1111/tpj.13781>
- Nair, M. K. (1975). Cytogenetics of *Saccharum officinarum* L. and *S. spontaneum* L. IV. Chromosome number and meiosis in *S. officinarum* x *S. spontaneum* hybrids. *Caryologia*, 28(1), 1–14. <https://doi.org/10.1080/00087114.1975.10796591>
- Oliveira, G. K., Soares, N. R., Costa, Z. P., Almeida, C. B., Machado, R. M., Mesquita, A. T., Carneiro, M. S., Forni-Martins, E. R., Mondin, M., & Vieira, M. L. C. (2023). Meiotic abnormalities in sugarcane (*Saccharum* spp.) and parental species: Evidence for peri- and paracentric inversions. *Annals of Applied Biology*. <https://doi.org/10.1111/aab.12855>
- Pfaffl, M. W., Horgan, G. W., & Dempfle, L. (2002). Relative expression software tool (REST) for group-wise comparison and statistical analysis of relative expression results in real-time PCR. *Nucleic Acids Research*, 30(9). <https://doi.org/10.1093/NAR/30.9.E36>
- Piperidis, G., Piperidis, N., & D'Hont, A. (2010). Molecular cytogenetic investigation of chromosome composition and transmission in sugarcane. *Molecular Genetics and Genomics*, 284(1), 65–73. <https://doi.org/10.1007/s00438-010-0546-3>
- Piperidis, N., & D'Hont, A. (2020). Sugarcane genome architecture decrypted with chromosome-specific oligo probes. *The Plant Journal*, 103(6), 2039–2051. <https://doi.org/10.1111/tpj.14881>
- Price, S. (1961). Cytological studies in *Saccharum* and allied genera VII. Maternal chromosome transmission by *S. officinarum* in intra- and interspecific crosses. *Botanical Gazette*, 122(4), 298–305. <https://doi.org/10.1086/336118>
- Price, S. (1963a). Cytogenetics of modern sugar canes. *Economic Botany*, 17(2), 97–103. <https://www.jstor.org/stable/4252420>



- Price, S. (1963b). Cytological studies in *Saccharum* and allied genera. VIII. F2 and BC1 progenies from 112- and 136-chromosome *S. officinarum* x *S. spontaneum* hybrids. *Botanical Gazette*, 124(3), 186–190. <https://doi.org/10.1086/336190>
- Pyatnitskaya, A., Andreani, J., Guérois, R., De Muyt, A., & Borde, V. (2022). The Zip4 protein directly couples meiotic crossover formation to synaptonemal complex assembly. *Genes & Development*, 36(1–2), 53–69. <https://doi.org/10.1101/GAD.348973.121>
- Pyatnitskaya, A., Borde, V., & De Muyt, A. (2019). Crossing and zipping: molecular duties of the ZMM proteins in meiosis. *Chromosoma*, 128(3), 181–198. <https://doi.org/10.1007/s00412-019-00714-8>
- Ramakers, C., Ruijter, J. M., Lekanne Deprez, R. H., & Moorman, A. F. M. (2003). Assumption-free analysis of quantitative real-time polymerase chain reaction (PCR) data. *Neuroscience Letters*, 339(1), 62–66. [https://doi.org/10.1016/S0304-3940\(02\)01423-4](https://doi.org/10.1016/S0304-3940(02)01423-4)
- Rey, M. D., Martín, A. C., Higgins, J., Swarbreck, D., Uauy, C., Shaw, P., & Moore, G. (2017). Exploiting the ZIP4 homologue within the wheat Ph1 locus has identified two lines exhibiting homoeologous crossover in wheat-wild relative hybrids. *Molecular Breeding*, 37(8). <https://doi.org/10.1007/s11032-017-0700-2>
- Rey, M.-D., Martín, A. C., Smedley, M., Hayta, S., Harwood, W., Shaw, P., & Moore, G. (2018). Magnesium increases homoeologous crossover frequency during meiosis in ZIP4 (Ph1 gene) mutant wheat-wild relative hybrids. *Frontiers in Plant Science*, 9, 1–12. <https://doi.org/10.3389/fpls.2018.00509>
- Rice, P., Longden, L., & Bleasby, A. (2000). EMBOSS: The European Molecular Biology Open Software Suite. *Trends in Genetics*, 16(6), 276–277. [https://doi.org/10.1016/S0168-9525\(00\)02024-2](https://doi.org/10.1016/S0168-9525(00)02024-2)
- Riley, R., & Chapman, V. (1958). Genetic control of the cytologically diploid behaviour of hexaploid wheat. *Nature*, 182(4637), 713–715. <https://doi.org/10.1038/182713a0>
- Sears, E. R. (1976). genetic control of chromosome pairing in wheat. *Annual Review of Genetics*, 10(1), 31–51. <https://doi.org/10.1146/annurev.ge.10.120176.000335>
- Sepsi, A., Higgins, J. D., Heslop-Harrison, J. S. (Pat), & Schwarzacher, T. (2017). CENH3 morphogenesis reveals dynamic centromere associations during synaptonemal complex formation and the progression through male meiosis in hexaploid wheat. *The Plant Journal*, 89(2), 235–249. <https://doi.org/10.1111/tpj.13379>
- Sforça, D. A., Vautrin, S., Cardoso-Silva, C. B., Mancini, M. C., Romero-da Cruz, M. V., Pereira, G. da S., Conte, M., Bellec, A., Dahmer, N., Fourment, J., Rodde, N., Van Sluys, M. A., Vicentini, R., Garcia, A. A. F., Forni-Martins, E. R., Carneiro, M. S., Hoffmann, H. P., Pinto, L. R., Landell, M. G. de A., ... de Souza, A. P. (2019). Gene duplication in the sugarcane genome: A case study of allele interactions and evolutionary patterns in two genic regions. *Frontiers in Plant Science*, 10(May). <https://doi.org/10.3389/fpls.2019.00553>

- Shen, Y., Tang, D., Wang, K., Wang, M., Huang, J., Luo, W., Luo, Q., Hong, L., Li, M., & Cheng, Z. (2012). ZIP4 in homologous chromosome synapsis and crossover formation in rice meiosis. *Journal of Cell Science*, 125(11), 2581–2591. <https://doi.org/10.1242/jcs.090993>
- Simmonds, N. W. (1975). Sugar canes. In *Evolution of Crop Plants* (104–108). Longman.
- Soares, N. R., Mollinari, M., Oliveira, G. K., Pereira, G. S., & Vieira, M. L. C. (2021). Meiosis in polyploids and implications for genetic mapping: a review. *Genes*, 12(10), 1517. <https://doi.org/10.3390/genes12101517>
- Souza, G. M., Van Sluys, M. A., Lembke, C. G., Lee, H., Margarido, G. R. A., Hotta, C. T., Gaiarsa, J. W., Diniz, A. L., Oliveira, M. de M., Ferreira, S. D. S., Nishiyama, M. Y., Ten-Caten, F., Ragagnin, G. T., Andrade, P. de M., De Souza, R. F., Nicastro, G. G., Pandya, R., Kim, C., Guo, H., ... Heckerman, D. (2019). Assembly of the 373k gene space of the polyploid sugarcane genome reveals reservoirs of functional diversity in the world's leading biomass crop. *GigaScience*, 8(12), 1–18. <https://doi.org/10.1093/gigascience/giz129>
- Suzuki, E. (1941). Cytological Studies of Sugar Cane. *Cytologia*, 11(4), 507-514. <https://doi.org/10.1508/cytologia.11.507>
- Truebestein, L., & Leonard, T. A. (2016). Coiled-coils: The long and short of it. *BioEssays*, 38(9), 903–916. <https://doi.org/10.1002/bies.201600062>
- Tsubouchi, T., Zhao, H., & Roeder, G. S. (2006). The meiosis-specific ZIP4 protein regulates crossover distribution by promoting synaptonemal complex formation together with ZIP2. *Developmental Cell*, 10(6), 809–819. <https://doi.org/10.1016/j.devcel.2006.04.003>
- Van Drunen, W., Friedman, J. (2022). Autopolyploid establishment depends on life-history strategy and the mating outcomes of clonal architecture. *Evolution*, 76(9), 1953- 1970. <https://doi.org/10.1111/evo.14582>
- Vieira, M. L. C., Almeida, C. B., Oliveira, C. A., Tacuatiá, L. O., Munhoz, C. F., Cauz-Santos, L. A., Pinto, L. R., Monteiro-Vitorello, C. B., Xavier, M. A., & Forni-Martins, E. R. (2018). Revisiting meiosis in sugarcane: chromosomal irregularities and the prevalence of bivalent configurations. *Frontiers in Genetics*, 9, 1–12. <https://doi.org/10.3389/fgene.2018.00213>
- Wang, J., Youkharibache, P., Zhang, D., Lanczycki, C. J., Geer, R. C., Madej, T., Phan, L., Ward, M., Lu, S., Marchler, G. H., Wang, Y., Bryant, S. H., Geer, L. Y., & Marchler-Bauer, A. (2020). iCn3D, a web-based 3D viewer for sharing 1D/2D/3D representations of biomolecular structures. *Bioinformatics*, 36(1), 131–135. <https://doi.org/10.1093/bioinformatics/btz502>
- Wang, Y., Van Rengs, W. M. J., Zaidan, M. W. A. M., & Underwood, C. J. (2021). Meiosis in crops: From genes to genomes. In *Journal of Experimental Botany*, 72(18), 6091–6109. <https://doi.org/10.1093/jxb/erab217>

- Wheeler, T. J., Clements, J., & Finn, R. D. (2014). Skylin: A tool for creating informative, interactive logos representing sequence alignments and profile hidden Markov models. *BMC Bioinformatics*, 15(1), 1–9. <https://doi.org/10.1186/1471-2105-15-7>
- Xu, J., & Zhang, Y. (2010). How significant is a protein structure similarity with TM-score = 0.5? *Bioinformatics*, 26(7), 889–895. <https://doi.org/10.1093/bioinformatics/btq066>
- Zhang, J., Zhang, X., Tang, H., Zhang, Q., Hua, X., Ma, X., Zhu, F., Jones, T., Zhu, X., Bowers, J., Wai, C. M., Zheng, C., Shi, Y., Chen, S., Xu, X., Yue, J., Nelson, D. R., Huang, L., Li, Z., ... Ming, R. (2018). Allele-defined genome of the autopolyploid sugarcane *Saccharum spontaneum* L. *Nature Genetics*, 50(11), 1565–1573. <https://doi.org/10.1038/s41588-018-0237-2>
- Zhang, X., Meng, Z., Han, J., Khurshid, H., Esh, A., Hasterok, R., & Wang, K. (2023). Characterization of meiotic chromosome behavior in the autopolyploid *Saccharum spontaneum* reveals preferential chromosome pairing without distinct DNA sequence variation. *The Crop Journal*. <https://doi.org/10.1016/j.cj.2023.02.008>
- Zickler, D. (2006). From early homologue recognition to synaptonemal complex formation. *Chromosoma*, 115(3), 158–174. <https://doi.org/10.1007/s00412-006-0048-6>
- Zimmermann, L., Stephens, A., Nam, S. Z., Rau, D., Kübler, J., Lozajic, M., Gabler, F., Söding, J., Lupas, A. N., & Alva, V. (2018). A completely reimplemented MPI bioinformatics toolkit with a new HHpred server at its core. *Journal of Molecular Biology*, 430(15), 2237–2243. <https://doi.org/10.1016/J.JMB.2017.12.007>







	1110	1120	1130	1140	1150	1160	1170	1180	1190	1200
Consensus	GTACCTAGCCAGTGC...GAGGGTGTG									
S.officinatum_Chr3B	GTACCTAGCCAGTGC...GAGGGTGTG									
S.officinatum_Chr3C	GTACCTAGCCAGTGC...GAGGGTGTG									
S.officinatum_Chr3G	GTACCTAGCCAGTGC...GAGGGTGTG									
S.spontaneum_Chr3A	GTACCTAGCCAGTGC...GAGGGTGTG									
S.spontaneum_Chr3B	GTACCTAGCCAGTGC...GAGGGTGTG									
S.spontaneum_Chr3C	GTACCTAGCCAGTGC...GAGGGTGTG									
S.spontaneum_Chr3D	GTACCTAGCCAGTGC...GAGGGTGTG									
R570_Chr2A	GTACCTAGCCAGTGC...GAGGGTGTG									
R570_Chr2B	GTACCTAGCCAGTGC...GAGGGTGTG									
R570_Chr2C	GTACCTAGCCAGTGC...GAGGGTGTG									
R570_Chr2D	GTACCTAGCCAGTGC...GAGGGTGTG									
R570_Chr2E	GTACCTAGCCAGTGC...GAGGGTGTG									
R570_Chr2F	GTACCTAGCCAGTGC...GAGGGTGTG									
R570_Chr2G	GTACCTAGCCAGTGC...GAGGGTGTG									
R570_scaffold_157	GTACCTAGCCAGTGC...GAGGGTGTG									
R570_scaffold_327	GTACCTAGCCAGTGC...GAGGGTGTG									
R570_scaffold_3491	GTACCTAGCCAGTGC...GAGGGTGTG									
R570_scaffold_4712	GTACCTAGCCAGTGC...GAGGGTGTG									
SP80-3280_0083261	GTACCTAGCCAGTGC...GAGGGTGTG									
SP80-3280_0106432	GTACCTAGCCAGTGC...GAGGGTGTG									
SP80-3280_0018838	GTACCTAGCCAGTGC...GAGGGTGTG									
SP80-3280_0209934	GTACCTAGCCAGTGC...GAGGGTGTG									

	1210	1220	1230	1240	1250	1260	1270	1280	1290	1300
Consensus	AAAAACGGTGGTT...GAGGGTGTG									
S.officinatum_Chr3B	AAAAACGGTGGTT...GAGGGTGTG									
S.officinatum_Chr3C	AAAAACGGTGGTT...GAGGGTGTG									
S.officinatum_Chr3G	AAAAACGGTGGTT...GAGGGTGTG									
S.spontaneum_Chr3A	AAAAACGGTGGTT...GAGGGTGTG									
S.spontaneum_Chr3B	AAAAACGGTGGTT...GAGGGTGTG									
S.spontaneum_Chr3C	AAAAACGGTGGTT...GAGGGTGTG									
S.spontaneum_Chr3D	AAAAACGGTGGTT...GAGGGTGTG									
R570_Chr2A	AAAAACGGTGGTT...GAGGGTGTG									
R570_Chr2B	AAAAACGGTGGTT...GAGGGTGTG									
R570_Chr2C	AAAAACGGTGGTT...GAGGGTGTG									
R570_Chr2D	AAAAACGGTGGTT...GAGGGTGTG									
R570_Chr2E	AAAAACGGTGGTT...GAGGGTGTG									
R570_Chr2F	AAAAACGGTGGTT...GAGGGTGTG									
R570_Chr2G	AAAAACGGTGGTT...GAGGGTGTG									
R570_scaffold_157	AAAAACGGTGGTT...GAGGGTGTG									
R570_scaffold_327	AAAAACGGTGGTT...GAGGGTGTG									
R570_scaffold_3491	AAAAACGGTGGTT...GAGGGTGTG									
R570_scaffold_4712	AAAAACGGTGGTT...GAGGGTGTG									
SP80-3280_0083261	AAAAACGGTGGTT...GAGGGTGTG									
SP80-3280_0106432	AAAAACGGTGGTT...GAGGGTGTG									
SP80-3280_0018838	AAAAACGGTGGTT...GAGGGTGTG									
SP80-3280_0209934	AAAAACGGTGGTT...GAGGGTGTG									

	1310	1320	1330	1340	1350	1360	1370	1380	1390	1400
Consensus	CTAACACCCATGAG...GAGGGTGTG									
S.officinatum_Chr3B	CTAACACCCATGAG...GAGGGTGTG									
S.officinatum_Chr3C	CTAACACCCATGAG...GAGGGTGTG									
S.officinatum_Chr3G	CTAACACCCATGAG...GAGGGTGTG									
S.spontaneum_Chr3A	CTAACACCCATGAG...GAGGGTGTG									
S.spontaneum_Chr3B	CTAACACCCATGAG...GAGGGTGTG									
S.spontaneum_Chr3C	CTAACACCCATGAG...GAGGGTGTG									
S.spontaneum_Chr3D	CTAACACCCATGAG...GAGGGTGTG									
R570_Chr2A	CTAACACCCATGAG...GAGGGTGTG									
R570_Chr2B	CTAACACCCATGAG...GAGGGTGTG									
R570_Chr2C	CTAACACCCATGAG...GAGGGTGTG									
R570_Chr2D	CTAACACCCATGAG...GAGGGTGTG									
R570_Chr2E	CTAACACCCATGAG...GAGGGTGTG									
R570_Chr2F	CTAACACCCATGAG...GAGGGTGTG									
R570_Chr2G	CTAACACCCATGAG...GAGGGTGTG									
R570_scaffold_157	CTAACACCCATGAG...GAGGGTGTG									
R570_scaffold_327	CTAACACCCATGAG...GAGGGTGTG									
R570_scaffold_3491	CTAACACCCATGAG...GAGGGTGTG									
R570_scaffold_4712	CTAACACCCATGAG...GAGGGTGTG									
SP80-3280_0083261	CTAACACCCATGAG...GAGGGTGTG									
SP80-3280_0106432	CTAACACCCATGAG...GAGGGTGTG									
SP80-3280_0018838	CTAACACCCATGAG...GAGGGTGTG									
SP80-3280_0209934	CTAACACCCATGAG...GAGGGTGTG									

	1410	1420	1430	1440	1450	1460	1470	1480	1490	1500
Consensus	GAGGTCAGTGC...GAGGGTGTG									
S.officinatum_Chr3B	GAGGTCAGTGC...GAGGGTGTG									
S.officinatum_Chr3C	GAGGTCAGTGC...GAGGGTGTG									
S.officinatum_Chr3G	GAGGTCAGTGC...GAGGGTGTG									
S.spontaneum_Chr3A	GAGGTCAGTGC...GAGGGTGTG									
S.spontaneum_Chr3B	GAGGTCAGTGC...GAGGGTGTG									
S.spontaneum_Chr3C	GAGGTCAGTGC...GAGGGTGTG									
S.spontaneum_Chr3D	GAGGTCAGTGC...GAGGGTGTG									
R570_Chr2A	GAGGTCAGTGC...GAGGGTGTG									
R570_Chr2B	GAGGTCAGTGC...GAGGGTGTG									
R570_Chr2C	GAGGTCAGTGC...GAGGGTGTG									
R570_Chr2D	GAGGTCAGTGC...GAGGGTGTG									
R570_Chr2E	GAGGTCAGTGC...GAGGGTGTG									
R570_Chr2F	GAGGTCAGTGC...GAGGGTGTG									
R570_Chr2G	GAGGTCAGTGC...GAGGGTGTG									
R570_scaffold_157	GAGGTCAGTGC...GAGGGTGTG									
R570_scaffold_327	GAGGTCAGTGC...GAGGGTGTG									
R570_scaffold_3491	GAGGTCAGTGC...GAGGGTGTG									











S.spontaneum_Chr3A	G
S.spontaneum_Chr3B	G
S.spontaneum_Chr3C	G
S.spontaneum_Chr3D	G
R570_Chr2A	G
R570_Chr2B	G
R570_Chr2C	G
R570_Chr2D	G
R570_Chr2E	G
R570_Chr2F	G
R570_Chr2G	G
R570_scaffold_157	G
R570_scaffold_327	G
R570_scaffold_3491	G
R570_scaffold_4712	G
SP80-3280_0083261	-
SP80-3280_0106432	G
SP80-3280_0018838	G
SP80-3280_0209934	G

officinarium_Chr3B	99.07%	100%	99.07%	R570_Ch...	99.35%	99.24%	100%	100%	R570_Ch...	100%	100%	R570_sca...	99.31%	99.07%	100%	99.03%	SP80-32...	100%	99.07%	SP80-32...	99.15%
officinarium_Chr3C	99.07%	99.07%	99.69%	99.31%	99.66%	99.83%	99.07%	99.07%	99.07%	99.07%	99.07%	99.07%	99.76%	99.07%	100%	99.03%	100%	99.07%	100%	99.07%	100%
officinarium_Chr3G	100%	99.28%	99.31%	99.35%	99.35%	99.24%	100%	100%	99.07%	99.07%	99.07%	100%	99.31%	99.07%	100%	99.03%	99.07%	99.07%	100%	99.07%	99.15%
spontaneum_Chr2A	99.28%	99.28%	99.83%	99.28%	99.86%	99.83%	99.28%	99.28%	99.28%	99.28%	99.28%	99.28%	99.76%	99.28%	99.77%	99.28%	99.31%	99.28%	99.28%	99.69%	99.70%
spontaneum_Chr3B	99.31%	99.69%	99.28%	99.90%	99.90%	99.86%	99.31%	99.31%	99.31%	99.31%	99.31%	99.31%	99.79%	99.31%	99.73%	99.31%	99.31%	99.31%	99.31%	99.62%	99.58%
spontaneum_Chr2C	99.38%	99.62%	99.38%	99.97%	99.97%	99.79%	99.38%	99.38%	99.38%	99.38%	99.38%	99.38%	99.72%	99.38%	99.65%	99.38%	99.38%	99.38%	99.38%	99.62%	99.58%
spontaneum_Chr2D	99.31%	99.69%	99.31%	99.93%	99.93%	99.86%	99.31%	99.31%	99.31%	99.31%	99.31%	99.31%	99.79%	99.31%	99.73%	99.31%	99.31%	99.31%	99.31%	99.69%	99.66%
570_Chr2A	99.07%	100%	99.07%	99.69%	99.69%	99.83%	99.07%	99.07%	99.07%	99.07%	99.07%	99.07%	99.76%	99.07%	100%	99.03%	99.07%	100%	99.07%	100%	100%
570_Chr2B	100%	99.07%	100%	99.31%	99.31%	99.24%	99.07%	100%	100%	100%	100%	100%	99.31%	99.07%	99.03%	99.03%	100%	100%	99.07%	100%	99.15%
570_Chr2C	99.41%	99.59%	99.90%	99.90%	99.93%	99.76%	99.41%	99.41%	99.41%	99.41%	99.41%	99.41%	99.76%	99.41%	99.61%	99.41%	99.41%	99.41%	99.41%	99.59%	99.58%
570_Chr2D	99.35%	99.66%	99.90%	99.90%	99.93%	99.76%	99.35%	99.35%	99.35%	99.35%	99.35%	99.35%	99.69%	99.35%	99.69%	99.35%	99.35%	99.35%	99.35%	99.66%	99.58%
570_Chr2E	99.24%	99.83%	99.86%	99.86%	99.86%	99.76%	99.24%	99.24%	99.24%	99.24%	99.24%	99.24%	99.93%	99.24%	99.88%	99.24%	99.24%	99.24%	99.24%	99.83%	99.83%
570_Chr2F	100%	99.07%	99.31%	99.38%	99.38%	99.31%	99.07%	100%	100%	100%	100%	99.31%	99.31%	99.07%	100%	99.03%	100%	99.07%	100%	99.07%	99.15%
570_Chr2G	100%	99.07%	99.31%	99.38%	99.38%	99.31%	99.07%	100%	100%	100%	100%	99.31%	99.31%	99.07%	100%	99.03%	100%	99.07%	100%	99.07%	99.15%
570_scaffold_157	100%	99.07%	99.28%	99.28%	99.28%	99.28%	99.07%	100%	100%	100%	100%	99.31%	99.31%	99.07%	100%	99.03%	100%	99.07%	100%	99.07%	99.15%
570_scaffold_327	99.31%	99.76%	99.28%	99.79%	99.79%	99.83%	99.31%	99.31%	99.31%	99.31%	99.31%	99.31%	99.31%	99.07%	99.81%	99.31%	99.31%	99.31%	99.31%	99.76%	99.83%
570_scaffold_3491	99.07%	100%	99.72%	99.69%	100%	99.83%	99.07%	100%	99.07%	99.07%	99.07%	99.07%	99.76%	99.07%	100%	99.07%	99.07%	99.07%	99.07%	100%	100%
570_scaffold_4712	100%	99.07%	99.31%	99.31%	99.07%	99.24%	100%	100%	100%	100%	100%	99.31%	99.31%	99.07%	99.03%	99.03%	100%	99.07%	100%	99.07%	99.15%
P80-3280_0083261	99.03%	100%	99.77%	99.73%	100%	99.69%	99.03%	99.03%	99.03%	99.03%	99.03%	99.03%	99.81%	99.03%	99.03%	99.03%	99.03%	99.03%	99.03%	100%	100%
P80-3280_0106432	100%	99.07%	99.28%	99.31%	99.07%	99.31%	99.07%	100%	100%	100%	100%	99.31%	99.31%	99.07%	99.03%	99.03%	99.03%	99.03%	99.07%	99.07%	99.15%
P80-3280_0018838	99.07%	100%	99.72%	99.69%	100%	99.66%	99.07%	99.07%	99.07%	99.07%	99.07%	99.07%	99.76%	99.07%	100%	99.07%	99.07%	99.07%	99.07%	99.07%	99.15%
P80-3280_0209934	99.15%	100%	99.70%	99.66%	100%	99.58%	99.15%	99.15%	99.15%	99.15%	99.15%	99.15%	99.83%	99.15%	100%	99.15%	99.15%	99.15%	99.15%	99.15%	100%





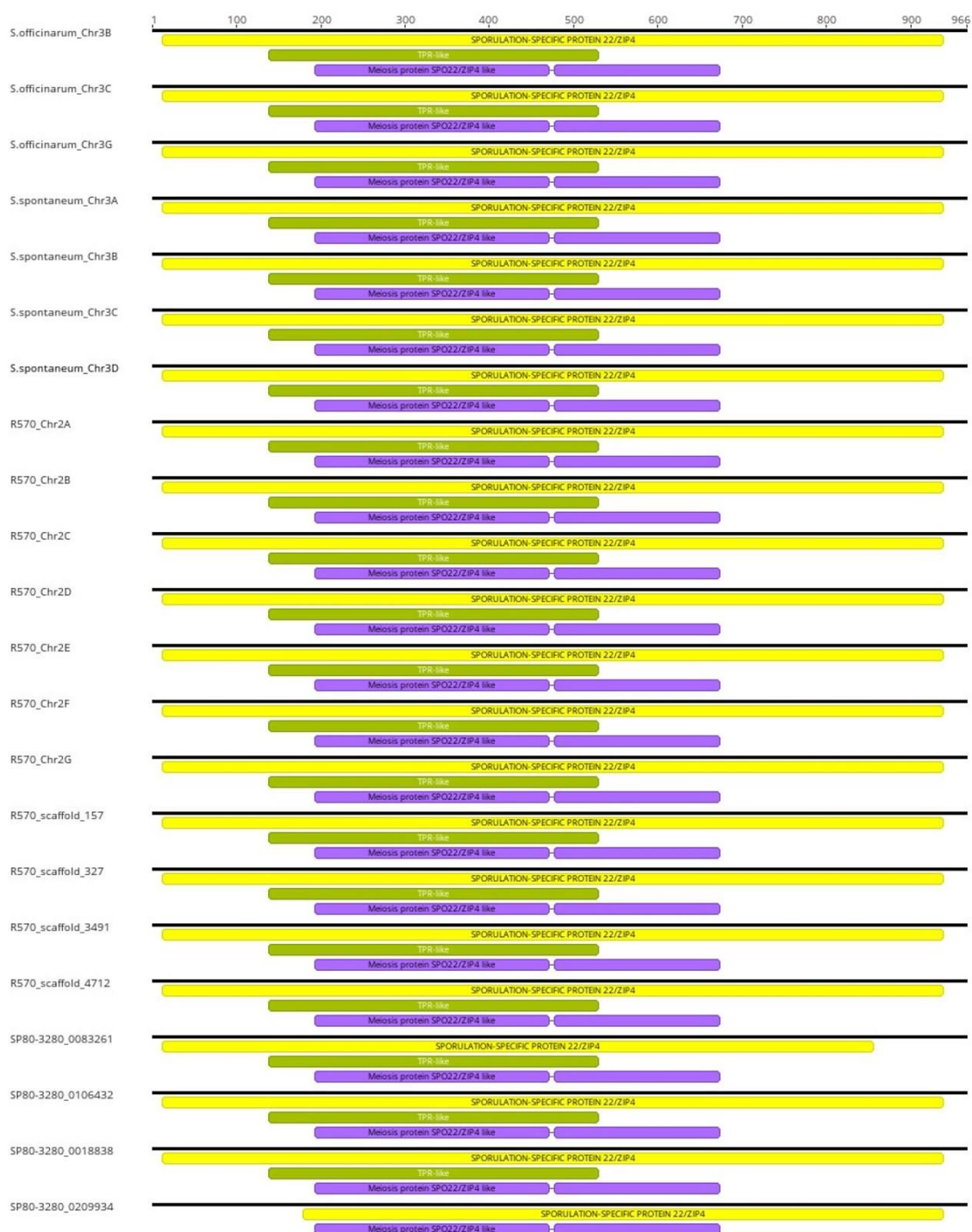
S.spontaneum\_Chrc3C AQPNLQVAEFLKASISTALASRSPNYGVI SAALRKLVLCSGLQDFSGSMSDAAYDVFPQAYQIVVGLRDGEYPFEEGRWLAITAWNKSYPGRLGQHSV 900  
S.spontaneum\_Chrc3D AQPNLQVAEFLKASISTALASRSPNYGVI SAALRKLVLCSGLQDFSGSMSDAAYDVFPQAYQIVVGLRDGEYPFEEGRWLAITAWNKSYPGRLGQHSV 900  
R570\_Chrc2A AQPNLQVAEFLKASISTALASRSPNYGVI SAALRKLVLCSGLQDFSGSMSDAAYDVFPQAYQIVVGLRDGEYPFEEGRWLAITAWNKSYPGRLGQHSV 900  
R570\_Chrc2B AQPNLQVAEFLKASISTALASRSPNYGVI SAALRKLVLCSGLQDFSGSMSDAAYDVFPQAYQIVVGLRDGEYPFEEGRWLAITAWNKSYPGRLGQHSV 900  
R570\_Chrc2C AQPNLQVAEFLKASISTALASRSPNYGVI SAALRKLVLCSGLQDFSGSMSDAAYDVFPQAYQIVVGLRDGEYPFEEGRWLAITAWNKSYPGRLGQHSV 900  
R570\_Chrc2D AQPNLQVAEFLKASISTALASRSPNYGVI SAALRKLVLCSGLQDFSGSMSDAAYDVFPQAYQIVVGLRDGEYPFEEGRWLAITAWNKSYPGRLGQHSV 900  
R570\_Chrc2E AQPNLQVAEFLKASISTALASRSPNYGVI SAALRKLVLCSGLQDFSGSMSDAAYDVFPQAYQIVVGLRDGEYPFEEGRWLAITAWNKSYPGRLGQHSV 900  
R570\_Chrc2F AQPNLQVAEFLKASISTALASRSPNYGVI SAALRKLVLCSGLQDFSGSMSDAAYDVFPQAYQIVVGLRDGEYPFEEGRWLAITAWNKSYPGRLGQHSV 900  
R570\_Chrc2G AQPNLQVAEFLKASISTALASRSPNYGVI SAALRKLVLCSGLQDFSGSMSDAAYDVFPQAYQIVVGLRDGEYPFEEGRWLAITAWNKSYPGRLGQHSV 900  
R570\_scaffold\_157 AQPNLQVAEFLKASISTALASRSPNYGVI SAALRKLVLCSGLQDFSGSMSDAAYDVFPQAYQIVVGLRDGEYPFEEGRWLAITAWNKSYPGRLGQHSV 900  
R570\_scaffold\_327 AQPNLQVAEFLKASISTALASRSPNYGVI SAALRKLVLCSGLQDFSGSMSDAAYDVFPQAYQIVVGLRDGEYPFEEGRWLAITAWNKSYPGRLGQHSV 900  
R570\_scaffold\_3491 AQPNLQVAEFLKASISTALASRSPNYGVI SAALRKLVLCSGLQDFSGSMSDAAYDVFPQAYQIVVGLRDGEYPFEEGRWLAITAWNKSYPGRLGQHSV 900  
R570\_scaffold\_4712 AQPNLQVAEFLKASISTALASRSPNYGVI SAALRKLVLCSGLQDFSGSMSDAAYDVFPQAYQIVVGLRDGEYPFEEGRWLAITAWNKSYPGRLGQHSV 900  
SP80-3280\_0083261 AQPNLQVAEFLKASISTALASRSPNYGVI SAALRKLVLCSGLQDFSGSMSDAAYXX 900  
SP80-3280\_0106432 AQPNLQVAEFLKASISTALASRSPNYGVI SAALRKLVLCSGLQDFSGSMSDAAYDVFPQAYQIVVGLRDGEYPFEEGRWLAITAWNKSYPGRLGQHSV 900  
SP80-3280\_0018838 AQPNLQVAEFLKASISTALASRSPNYGVI SAALRKLVLCSGLQDFSGSMSDAAYDVFPQAYQIVVGLRDGEYPFEEGRWLAITAWNKSYPGRLGQHSV 900  
SP80-3280\_0209934 AQPNLQVAEFLKASISTALASRSPNYGVI SAALRKLVLCSGLQDFSGSMSDAAYDVFPQAYQIVVGLRDGEYPFEEGRWLAITAWNKSYPGRLGQHSV 900

Consensus AKKWMKMGDLARHFDrmklyIPGMEECFEFKQKLSGKEPDECSQDGEpSTSMsGTGSMSQPVLV\* 967  
S.officinatum\_Chrc3B AKKWMKMGDLARHFDrmklyIPGMEECFEFKQKLSGKEPDECSQDGEpSTSMsGTGSMSQPVLV- 966  
S.officinatum\_Chrc3C AKKWMKMGDLARHFDrmklyIPGMEECFEFKQKLSGKEPDECSHQDGEpSTSMsGTGSMSQPVLV- 966  
S.officinatum\_Chrc3G AKKWMKMGDLARHFDrmklyIPGMEECFEFKQKLSGKEPDECSQDGEpSTSMsGTGSMSQPVLV- 966  
S.spontaneum\_Chrc3A AKKWMKMGDLARHFDrmklyIPGMEECFEFKQKLSGKEPDECSQDGEpSTSMsGTGSMSQPVLV- 966  
S.spontaneum\_Chrc3B AKKWMKMGDLARHFDrmklyIPGMEECFEFKQKLSGKEPDECSQDGEpSTSMsGTGSMSQPVLV- 966  
S.spontaneum\_Chrc3C AKKWMKMGDLARHFDrmklyIPGMEECFEFKQKLSGKEPDECSQDGEpSTSMsGTGSMSQPVLV\* 966  
S.spontaneum\_Chrc3D AKKWMKMGDLARHFDrmklyIPGMEECFEFKQKLSGKEPDECSQDGEpSTSMsGTGSMSQPVLV- 966  
R570\_Chrc2A AKKWMKMGDLARHFDrmklyIPGMEECFEFKQKLSGKEPDECSHQDGEpSTSMsGTGSMSQPVLV\* 967  
R570\_Chrc2B AKKWMKMGDLARHFDrmklyIPGMEECFEFKQKLSGKEPDECSQDGEpSTSMsGTGSMSQPVLV\* 967  
R570\_Chrc2C AKKWMKMGDLARHFDrmklyIPGMEECFEFKQKLSGKEPDECSQDGEpSTSMsGTGSMSQPVLV\* 967  
R570\_Chrc2D AKKWMKMGDLARHFDrmklyIPGMEECFEFKQKLSGKEPDECSQDGEpSTSMsGTGSMSQPVLV\* 967  
R570\_Chrc2E AKKWMKMGDLARHFDrmklyIPGMEECFEFKQKLSGKEPDECSQDGEpSTSMsGTGSMSQPVLV\* 967  
R570\_Chrc2F AKKWMKMGDLARHFDrmklyIPGMEECFEFKQKLSGKEPDECSQDGEpSTSMsGTGSMSQPVLV\* 967  
R570\_Chrc2G AKKWMKMGDLARHFDrmklyIPGMEECFEFKQKLSGKEPDECSQDGEpSTSMsGTGSMSQPVLV\* 967  
R570\_scaffold\_157 AKKWMKMGDLARHFDrmklyIPGMEECFEFKQKLSGKEPDECSQDGEpSTSMsGTGSMSQPVLV\* 967  
R570\_scaffold\_327 AKKWMKMGDLARHFDrmklyIPGMEECFEFKQKLSGKEPDECSQDGEpSTSMsGTGSMSQPVLV\* 967  
R570\_scaffold\_3491 AKKWMKMGDLARHFDrmklyIPGMEECFEFKQKLSGKEPDECSHQDGEpSTSMsGTGSMSQPVLV\* 967  
R570\_scaffold\_4712 AKKWMKMGDLARHFDrmklyIPGMEECFEFKQKLSGKEPDECSQDGEpSTSMsGTGSMSQPVLV\* 967  
SP80-3280\_0083261 XXX 966  
SP80-3280\_0106432 AKKWMKMGDLARHFDrmklyIPGMEECFEFKQKLSGKEPDECSQDGEpSTSMsGTGSMSQPVLV\* 967  
SP80-3280\_0018838 AKKWMKMGDLARHFDrmklyIPGMEECFEFKQKLSGKEPDECSHQDGEpSTSMsGTGSMSQPVLV\* 967  
SP80-3280\_0209934 AKKWMKMGDLARHFDrmklyIPGMEECFEFKQKLSGKEPDECSHQDGEpSTSMsGTGSMSQPVLV\* 967





### Supplementary 3. Domains in the ZIP4 protein in sugarcane



APÊNDICE C.

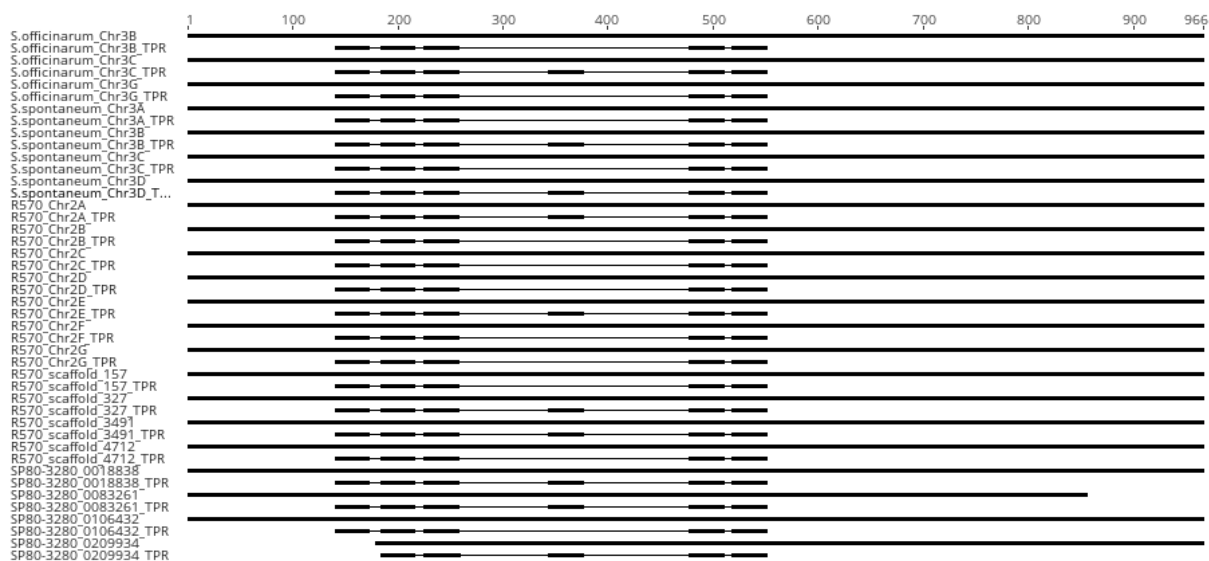
## APÊNDICE D.

Supplementary 4. The predicted Tetratricopeptide Repeats (TPRs) in the ZIP4 proteins.								
prediction was performed using the TPRpred program (version 11.0; Magis et al., 2014; Zimmermann et al., 2018).								
Gene	Per-protein P-value for being TPR	Probability for being TPR	TPR number	Repeat	Begin	Alignment	End	P-value
Officinarum_Chr3B	1.3E-09	93.97%	1	TPR	141	--ASLFHRTGLVWLDLGRADLASACFEKATPLICAA--	174	2.4e-06
Officinarum_Chr3B	1.3E-09	93.97%	2	TPR	184	--LDLNLARARAASSQGKHALAVALLNRSKPLAAS--	217	4.6e-04
Officinarum_Chr3B	1.3E-09	93.97%	3	TPR	225	--AEAYLLGKAAFATKSPDPAIDASTLLTEALDLC--	258	3.5e-04
Officinarum_Chr3B	1.3E-09	93.97%	4	TPR	477	--EESRRAKCFRVLCLCHMALCHLDRAQEFITEA--	510	2.5e-03
Officinarum_Chr3B	1.3E-09	93.97%	5	TPR	517	--IHCAFLKFKILLHKKEDDEAIKLMKTMVDYVDFN--	550	6.9e-04
Officinarum_Chr3C	9.4E-10	95.15%	1	TPR	141	--ASLFHRTGLVWLDLGRADLASACFEKATPLVCAA--	174	1.5e-06
Officinarum_Chr3C	9.4E-10	95.15%	2	TPR	184	--LDLNLARARAASSQGKHALAVALLNRSKPLAAS--	217	4.6e-04
Officinarum_Chr3C	9.4E-10	95.15%	3	TPR	225	--AEAYLLGKAAFATKSPDPAIDASTLLTEALDLC--	258	3.5e-04
Officinarum_Chr3C	9.4E-10	95.15%	4	TPR	477	--EESRRAKCFRVLCLCHMALCHLDRAQEFITEA--	510	2.5e-03
Officinarum_Chr3C	9.4E-10	95.15%	5	TPR	517	--IHCAFLKFKILLHKKEDDEAIKLMKTMVDYVDFN--	550	6.9e-04
Officinarum_Chr3G	1.3E-09	93.97%	1	TPR	141	--ASLFHRTGLVWLDLGRADLASACFEKATPLICAA--	174	2.4e-06
Officinarum_Chr3G	1.3E-09	93.97%	2	TPR	184	--LDLNLARARAASSQGKHALAVALLNRSKPLAAS--	217	4.6e-04
Officinarum_Chr3G	1.3E-09	93.97%	3	TPR	225	--AEAYLLGKAAFATKSPDPAIDASTLLTEALDLC--	258	3.5e-04
Officinarum_Chr3G	1.3E-09	93.97%	4	TPR	477	--EESRRAKCFRVLCLCHMALCHLDRAQEFITEA--	510	2.5e-03
Officinarum_Chr3G	1.3E-09	93.97%	5	TPR	517	--IHCAFLKFKILLHKKEDDEAIKLMKTMVDYVDFN--	550	6.9e-04
Spontaneum_Chr3A	8.2E-10	95.58%	1	TPR	141	--ASLFHRTGLVWLDLGRADLASACFEKATPLVCAA--	174	1.5e-06
Spontaneum_Chr3A	8.2E-10	95.58%	2	TPR	184	--LDLNLARARAASSQGKHALAVALLNRSKPLAAS--	217	4.6e-04
Spontaneum_Chr3A	8.2E-10	95.58%	3	TPR	225	--AEAYLLGKAAFATKSPDPAIDASTLLTEALDLC--	258	3.5e-04
Spontaneum_Chr3A	8.2E-10	95.58%	4	TPR	477	--EESRRAKCFRVLCLCHMALCHLDRAQEFITEA--	510	2.5e-03
Spontaneum_Chr3A	8.2E-10	95.58%	5	TPR	517	--IHCAFLKFKILLHKKEDDEAIKLMKTMVDYVDFN--	550	6.9e-04
Spontaneum_Chr3B	8.2E-10	95.58%	1	TPR	141	--ASLFHRTGLVWLDLGRADLASACFEKATPLVCAA--	174	1.5e-06
Spontaneum_Chr3B	8.2E-10	95.58%	2	TPR	184	--LDLNLARARAASSQGKHALAVALLNRSKPLAAS--	217	4.6e-04
Spontaneum_Chr3B	8.2E-10	95.58%	3	TPR	225	--AEAYLLGKAAFATKSPDPAIDASTLLTEALDLC--	258	3.5e-04
Spontaneum_Chr3B	8.2E-10	95.58%	4	TPR	477	--EESRRAKCFRVLCLCHMALCHLDRAQEFITEA--	510	2.5e-03
Spontaneum_Chr3B	8.2E-10	95.58%	5	TPR	517	--IHCAFLKFKILLHKKEDDEAIKLMKTMVDYVDFN--	550	6.9e-04
Spontaneum_Chr3C	8.2E-10	95.58%	1	TPR	141	--ASLFHRTGLVWLDLGRADLASACFEKATPLVCAA--	174	1.5e-06
Spontaneum_Chr3C	8.2E-10	95.58%	2	TPR	184	--LDLNLARARAASSQGKHALAVALLNRSKPLAAS--	217	4.6e-04
Spontaneum_Chr3C	8.2E-10	95.58%	3	TPR	225	--AEAYLLGKAAFATKSPDPAIDASTLLTEALDLC--	258	3.5e-04
Spontaneum_Chr3C	8.2E-10	95.58%	4	TPR	477	--EESRRAKCFRVLCLCHMALCHLDRAQEFITEA--	510	2.5e-03
Spontaneum_Chr3C	8.2E-10	95.58%	5	TPR	517	--IHCAFLKFKILLHKKEDDEAIKLMKTMVDYVDFN--	550	6.9e-04
Spontaneum_Chr3D	8.2E-10	95.58%	1	TPR	141	--ASLFHRTGLVWLDLGRADLASACFEKATPLVCAA--	174	1.5e-06

Spontaneum_Chr3D	8.2E-10	95.58%	2	TPR	184	--LDLNLARARAASSQGHALAVALLNRSKPLAAAS--	217	4.6e-04
Spontaneum_Chr3D	8.2E-10	95.58%	3	TPR	225	--AEAYLLLGKAAFATKSPDPAIDASTLLTEALDLC--	258	3.5e-04
Spontaneum_Chr3D	8.2E-10	95.58%	4	TPR	477	--EESRSRAKCFRVLCLCHMALCHLDRAQEFITEA--	510	2.5e-03
Spontaneum_Chr3D	8.2E-10	95.58%	5	TPR	517	--IHCAFLKFILLHKKEDDEAIKLMKTMVDYVDFN--	550	6.9e-04
R570_Chr2A	9.4E-10	95.15%	1	TPR	141	--ASLFHRTGLVWLDLGRADLASACFEKATPLVCAA--	174	1.5e-06
R570_Chr2A	9.4E-10	95.15%	2	TPR	184	--LDLNLARARAASSQGHALAVALLNRSKPLAAAS--	217	4.6e-04
R570_Chr2A	9.4E-10	95.15%	3	TPR	225	--AEAYLLLGKAAFATKSPDPAIDASTLLTEALDLC--	258	3.5e-04
R570_Chr2A	9.4E-10	95.15%	4	TPR	477	--EESRSRAKCFRVLCLCHMALCHLDRAQEFITEA--	510	2.5e-03
R570_Chr2A	9.4E-10	95.15%	5	TPR	517	--IHCAFLKFILLHKKEDDEAIKLMKTMVDYVDFN--	550	6.9e-04
R570_Chr2B	1.3E-09	93.97%	1	TPR	141	--ASLFHRTGLVWLDLGRADLASACFEKATPLICAA--	174	2.4e-06
R570_Chr2B	1.3E-09	93.97%	2	TPR	184	--LDLNLARARAASSQGHALAVALLNRSKPLAAAS--	217	4.6e-04
R570_Chr2B	1.3E-09	93.97%	3	TPR	225	--AEAYLLLGKAAFATKSPDPAIDASTLLTEALDLC--	258	3.5e-04
R570_Chr2B	1.3E-09	93.97%	4	TPR	477	--EESRSRAKCFRVLCLCHMALCHLDRAQEFITEA--	510	2.5e-03
R570_Chr2B	1.3E-09	93.97%	5	TPR	517	--IHCAFLKFILLHKKEDDEAIKLMKTMVDYVDFN--	550	6.9e-04
R570_Chr2C	8.2E-10	95.58%	1	TPR	141	--ASLFHRTGLVWLDLGRADLASACFEKATPLVCAA--	174	1.5e-06
R570_Chr2C	8.2E-10	95.58%	2	TPR	184	--LDLNLARARAASSQGHALAVALLNRSKPLAAAS--	217	4.6e-04
R570_Chr2C	8.2E-10	95.58%	3	TPR	225	--AEAYLLLGKAAFATKSPDPAIDASTLLTEALDLC--	258	3.5e-04
R570_Chr2C	8.2E-10	95.58%	4	TPR	477	--EESRSRAKCFRVLCLCHMALCHLDRAQEFITEA--	510	2.5e-03
R570_Chr2C	8.2E-10	95.58%	5	TPR	517	--IHCAFLKFILLHKKEDDEAIKLMKTMVDYVDFN--	550	6.9e-04
R570_Chr2D	8.2E-10	95.58%	1	TPR	141	--ASLFHRTGLVWLDLGRADLASACFEKATPLVCAA--	174	1.5e-06
R570_Chr2D	8.2E-10	95.58%	2	TPR	184	--LDLNLARARAASSQGHALAVALLNRSKPLAAAS--	217	4.6e-04
R570_Chr2D	8.2E-10	95.58%	3	TPR	225	--AEAYLLLGKAAFATKSPDPAIDASTLLTEALDLC--	258	3.5e-04
R570_Chr2D	8.2E-10	95.58%	4	TPR	477	--EESRSRAKCFRVLCLCHMALCHLDRAQEFITEA--	510	2.5e-03
R570_Chr2D	8.2E-10	95.58%	5	TPR	517	--IHCAFLKFILLHKKEDDEAIKLMKTMVDYVDFN--	550	6.9e-04
R570_Chr2E	9.4E-10	95.15%		TPR	141	--ASLFHRTGLVWLDLGRADLASACFEKATPLVCAA--	174	1.5e-06
R570_Chr2E	9.4E-10	95.15%		TPR	184	--LDLNLARARAASSQGHALAVALLNRSKPLAAAS--	217	4.6e-04
R570_Chr2E	9.4E-10	95.15%		TPR	225	--AEAYLLLGKAAFATKSPDPAIDASTLLTEALDLC--	258	3.5e-04
R570_Chr2E	9.4E-10	95.15%		TPR	477	--EESRSRAKCFRVLCLCHMALCHLDRAQEFITEA--	510	2.5e-03
R570_Chr2E	9.4E-10	95.15%		TPR	517	--IHCAFLKFILLHKKEDDEAIKLMKTMVDYVDFN--	550	6.9e-04
R570_Chr2F	1.3E-09	93.97%	1	TPR	141	--ASLFHRTGLVWLDLGRADLASACFEKATPLICAA--	174	2.4e-06
R570_Chr2F	1.3E-09	93.97%	2	TPR	184	--LDLNLARARAASSQGHALAVALLNRSKPLAAAS--	217	4.6e-04
R570_Chr2F	1.3E-09	93.97%	3	TPR	225	--AEAYLLLGKAAFATKSPDPAIDASTLLTEALDLC--	258	3.5e-04
R570_Chr2F	1.3E-09	93.97%	4	TPR	477	--EESRSRAKCFRVLCLCHMALCHLDRAQEFITEA--	510	2.5e-03
R570_Chr2F	1.3E-09	93.97%	5	TPR	517	--IHCAFLKFILLHKKEDDEAIKLMKTMVDYVDFN--	550	6.9e-04
R570_Chr2G	1.3E-09	93.97%	1	TPR	141	--ASLFHRTGLVWLDLGRADLASACFEKATPLICAA--	174	2.4e-06
R570_Chr2G	1.3E-09	93.97%	2	TPR	184	--LDLNLARARAASSQGHALAVALLNRSKPLAAAS--	217	4.6e-04
R570_Chr2G	1.3E-09	93.97%	3	TPR	225	--AEAYLLLGKAAFATKSPDPAIDASTLLTEALDLC--	258	3.5e-04

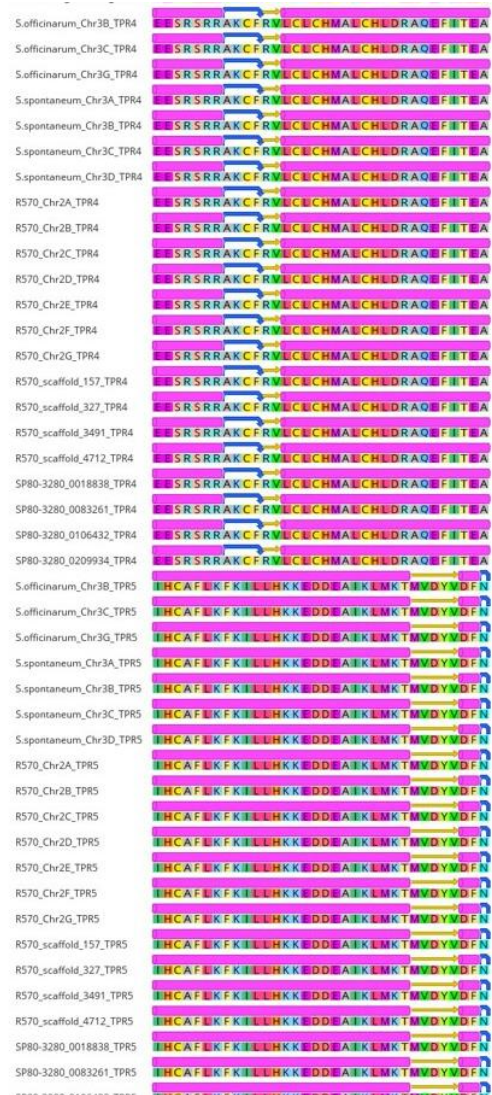
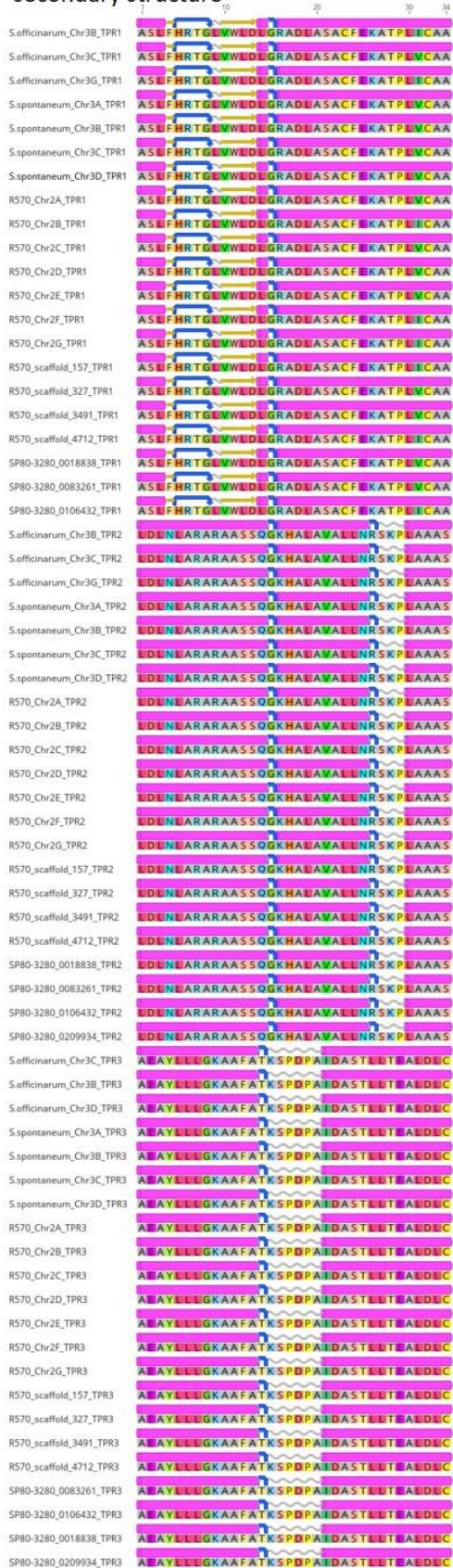
R570_Ch2G	<b>1.3E-09</b>	<b>93.97%</b>	4	TPR	477	--EESRRAKCFRVLCLCHMALCHLDRAQEFITEA--	510	2.5e-03
R570_Ch2G	<b>1.3E-09</b>	<b>93.97%</b>	5	TPR	517	--IHCAFLKFILLHKKEDDEAIKLMKTMVDYVDFN--	550	6.9e-04
R570_scaffold_157	<b>1.3E-09</b>	<b>93.97%</b>	1	TPR	141	--ASLFHRTGLVWLDLGRADLASACFEKATPLVCAA--	174	2.4e-06
R570_scaffold_157	<b>1.3E-09</b>	<b>93.97%</b>	2	TPR	184	--LDLNLARARAASSQGKHALAVALLNRSKPLAAAS--	217	4.6e-04
R570_scaffold_157	<b>1.3E-09</b>	<b>93.97%</b>	3	TPR	225	--AEAYLLLKKAATKSPDPIDASTLLTEALDLC--	258	3.5e-04
R570_scaffold_157	<b>1.3E-09</b>	<b>93.97%</b>	4	TPR	477	--EESRRAKCFRVLCLCHMALCHLDRAQEFITEA--	510	2.5e-03
R570_scaffold_157	<b>1.3E-09</b>	<b>93.97%</b>	5	TPR	517	--IHCAFLKFILLHKKEDDEAIKLMKTMVDYVDFN--	550	6.9e-04
R570_scaffold_327	<b>9.4E-10</b>	<b>95.15%</b>		TPR	141	--ASLFHRTGLVWLDLGRADLASACFEKATPLVCAA--	174	1.5e-06
R570_scaffold_327	<b>9.4E-10</b>	<b>95.15%</b>		TPR	184	--LDLNLARARAASSQGKHALAVALLNRSKPLAAAS--	217	4.6e-04
R570_scaffold_327	<b>9.4E-10</b>	<b>95.15%</b>		TPR	225	--AEAYLLLKKAATKSPDPIDASTLLTEALDLC--	258	3.5e-04
R570_scaffold_327	<b>9.4E-10</b>	<b>95.15%</b>		TPR	477	--EESRRAKCFRVLCLCHMALCHLDRAQEFITEA--	510	2.5e-03
R570_scaffold_327	<b>9.4E-10</b>	<b>95.15%</b>		TPR	517	--IHCAFLKFILLHKKEDDEAIKLMKTMVDYVDFN--	550	6.9e-04
R570_scaffold_3491	<b>9.4E-10</b>	<b>95.15%</b>		TPR	141	--ASLFHRTGLVWLDLGRADLASACFEKATPLVCAA--	174	1.5e-06
R570_scaffold_3491	<b>9.4E-10</b>	<b>95.15%</b>		TPR	184	--LDLNLARARAASSQGKHALAVALLNRSKPLAAAS--	217	4.6e-04
R570_scaffold_3491	<b>9.4E-10</b>	<b>95.15%</b>		TPR	225	--AEAYLLLKKAATKSPDPIDASTLLTEALDLC--	258	3.5e-04
R570_scaffold_3491	<b>9.4E-10</b>	<b>95.15%</b>		TPR	477	--EESRRAKCFRVLCLCHMALCHLDRAQEFITEA--	510	2.5e-03
R570_scaffold_3491	<b>9.4E-10</b>	<b>95.15%</b>		TPR	517	--IHCAFLKFILLHKKEDDEAIKLMKTMVDYVDFN--	550	6.9e-04
R570_scaffold_4712	<b>1.3E-09</b>	<b>93.97%</b>	1	TPR	141	--ASLFHRTGLVWLDLGRADLASACFEKATPLVCAA--	174	2.4e-06
R570_scaffold_4712	<b>1.3E-09</b>	<b>93.97%</b>	2	TPR	184	--LDLNLARARAASSQGKHALAVALLNRSKPLAAAS--	217	4.6e-04
R570_scaffold_4712	<b>1.3E-09</b>	<b>93.97%</b>	3	TPR	225	--AEAYLLLKKAATKSPDPIDASTLLTEALDLC--	258	3.5e-04
R570_scaffold_4712	<b>1.3E-09</b>	<b>93.97%</b>	4	TPR	477	--EESRRAKCFRVLCLCHMALCHLDRAQEFITEA--	510	2.5e-03
R570_scaffold_4712	<b>1.3E-09</b>	<b>93.97%</b>	5	TPR	517	--IHCAFLKFILLHKKEDDEAIKLMKTMVDYVDFN--	550	6.9e-04
SP80-3280_0018838	<b>9.4E-10</b>	<b>95.15%</b>		TPR	141	--ASLFHRTGLVWLDLGRADLASACFEKATPLVCAA--	174	1.5e-06
SP80-3280_0018838	<b>9.4E-10</b>	<b>95.15%</b>		TPR	184	--LDLNLARARAASSQGKHALAVALLNRSKPLAAAS--	217	4.6e-04
SP80-3280_0018838	<b>9.4E-10</b>	<b>95.15%</b>		TPR	225	--AEAYLLLKKAATKSPDPIDASTLLTEALDLC--	258	3.5e-04
SP80-3280_0018838	<b>9.4E-10</b>	<b>95.15%</b>		TPR	477	--EESRRAKCFRVLCLCHMALCHLDRAQEFITEA--	510	2.5e-03
SP80-3280_0018838	<b>9.4E-10</b>	<b>95.15%</b>		TPR	517	--IHCAFLKFILLHKKEDDEAIKLMKTMVDYVDFN--	550	6.9e-04
SP80-3280_0083261	<b>4.1E-10</b>	<b>97.22%</b>		TPR	141	--ASLFHRTGLVWLDLGRADLASACFEKATPLVCAA--	174	1.5e-06
SP80-3280_0083261	<b>4.1E-10</b>	<b>97.22%</b>		TPR	184	--LDLNLARARAASSQGKHALAVALLNRSKPLAAAS--	217	4.6e-04
SP80-3280_0083261	<b>4.1E-10</b>	<b>97.22%</b>		TPR	225	--AEAYLLLKKAATKSPDPIDASTLLTEALDLC--	258	3.5e-04
SP80-3280_0083261	<b>4.1E-10</b>	<b>97.22%</b>		TPR	477	--EESRRAKCFRVLCLCHMALCHLDRAQEFITEA--	510	2.5e-03
SP80-3280_0083261	<b>4.1E-10</b>	<b>97.22%</b>		TPR	517	--IHCAFLKFILLHKKEDDEAIKLMKTMVDYVDFN--	550	6.9e-04
SP80-3280_0106432	<b>1.3E-09</b>	<b>93.97%</b>	1	TPR	141	--ASLFHRTGLVWLDLGRADLASACFEKATPLVCAA--	174	2.4e-06
SP80-3280_0106432	<b>1.3E-09</b>	<b>93.97%</b>	2	TPR	184	--LDLNLARARAASSQGKHALAVALLNRSKPLAAAS--	217	4.6e-04
SP80-3280_0106432	<b>1.3E-09</b>	<b>93.97%</b>	3	TPR	225	--AEAYLLLKKAATKSPDPIDASTLLTEALDLC--	258	3.5e-04
SP80-3280_0106432	<b>1.3E-09</b>	<b>93.97%</b>	4	TPR	477	--EESRRAKCFRVLCLCHMALCHLDRAQEFITEA--	510	2.5e-03

SP80-3280_0106432	1.3E-09	93.97%	5	TPR	517	--IHCAFLKFKILLHKKEDDEAIKLMKTMVDYVDFN--	550	6.9e-04
SP80-3280_0209934	2.7E-06	6.39%		TPR	5	--LDLNLARARAASSQGKHALAVALLNRSKPLAAS--	38	4.6e-04
SP80-3280_0209934	2.7E-06	6.39%		TPR	46	--AEAYLLLGKAAFATKSPDPAIDASTLLTEALDLC--	79	3.5e-04
SP80-3280_0209934	2.7E-06	6.39%		TPR	298	--EESRSRAKCFRVLCLCHMALCHLDRAQEFITEA--	331	2.5e-03
SP80-3280_0209934	2.7E-06	6.39%		TPR	338	--IHCAFLKFKILLHKKEDDEAIKLMKTMVDYVDFN--	371	6.9e-04

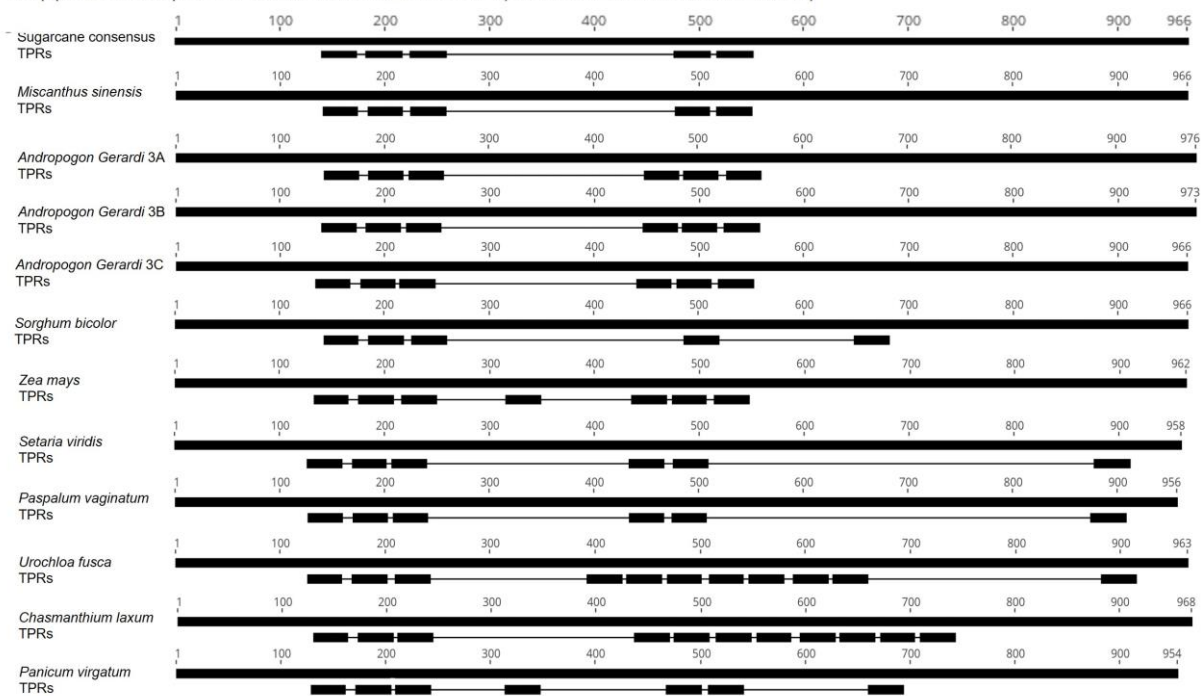


## APÊNDICE E.

### Supplementary 6. Sugarcane's TPR secondary structure



## APÊNDICE G.

Supplementary 7. TPR distribution in some species of the *Poaceae* family



## APÊNDICE H.

### Supplementary 8. Similarity matrices

#### a Sugarcane and Wheat ZIP4 CDS alignment

	Sugarcane ...	TaZIP4 3A	TaZIP4 3B	TaZIP4 3D	TaZIP4 B2
Sugarcane ZIP4		67.26%	66.91%	67.33%	63.63%
TaZIP4 3A	67.26%		96.72%	97.43%	90.98%
TaZIP4 3B	66.91%	96.72%		97.03%	92.95%
TaZIP4 3D	67.33%	97.43%	97.03%		91.54%
TaZIP4 B2	63.63%	90.98%	92.95%	91.54%	

#### b Sugarcane and Wheat ZIP4 protein alignment

	Sugarcane ...	TaZIP4 3A	TaZIP4 3B	TaZIP4 3D	TaZIP4 B2
Sugarcane ZIP4		65.07%	64.66%	64.96%	59.78%
TaZIP4 3A	65.07%		94.89%	96.34%	86.00%
TaZIP4 3B	64.66%	94.89%		94.89%	88.80%
TaZIP4 3D	64.96%	96.34%	94.89%		86.20%
TaZIP4 B2	59.78%	86.00%	88.80%	86.20%	